

**Regional Climate and Hydrologic Change in the
Northern US Rockies and Pacific Northwest:
Internally Consistent Projections of Future Climate
for Resource Management**

Jeremy S. Littell
Marketa McGuire Elsner
Guillaume Mauger

with

Eric Lutz
Alan F. Hamlet
Eric Salathé

17 April 2011



Climate Impacts Group
University of Washington
College of the Environment

Suggested citation:

Littell, J.S., M.M. Elsner, G. S. Mauger, E. Lutz, A.F. Hamlet, and E. Salathé. 2011. Regional Climate and Hydrologic Change in the Northern US Rockies and Pacific Northwest: Internally Consistent Projections of Future Climate for Resource Management. Project report: April 17, 2011. Latest version online at: http://ces.washington.edu/picea/USFS/pub/Littell_etal_2010/

Planned updates:

- 1) Citations list is currently incomplete, particularly for HCN and VIC sections.
- 2) There will eventually be a table with the % numbers of basins that transition from categorical snow/transient dominant to transient/rain to complement figure 4.5
- 3) Soil moisture and runoff maps will be expressed in %ile rather than %
- 4) Trend maps for HCN historical climate data are preliminary
- 5) There will eventually be maps comparing RCM deltas with GCM deltas directly.

Location of this document for updates:

http://ces.washington.edu/picea/USFS/pub/Littell_etal_2010/

For data, products, and publications using the dataset, see the R1/R6 project website:

<http://ces.washington.edu/data/r1r6.shtml>

Table of Contents

Introduction and Overview	5
1.1 Funding	5
1.2 Rationale	5
1.3 Project Objectives.....	6
1.4 Products.....	6
1.5 Data locations (see Appendix 1 for further details):	7
2. Historical and future climate in the in the Columbia, upper Missouri, and upper Colorado River basins of the western U.S.	8
2.1 Study domain and baseline regional climate for GCM comparisons.....	8
2.2 Historical trends in temperature and precipitation in the Columbia, upper Missouri, and upper Colorado River basins of the western U.S.....	10
2.2.1 Climate trends from 1950 - 2006.....	10
2.2.2 Climate trends from 1970 - 2006.....	13
2.3 Greenhouse gas emissions scenarios	16
2.4 Analysis of future regional climate projections.....	17
2.5 Bias analysis and selection of global climate models: comparing GCMs with 20th century climate, trends, and seasonal cycles	27
2.5.1 Observed temperature trend	28
2.5.2 Observed climatology.....	31
2.5.3 Seasonal cycle of precipitation.....	31
2.5.4 Fidelity to north Pacific / north America pressure patterns	34
2.6 An ensemble of best - performing models.....	34
2.6.1 Selection of ensemble members.....	34
2.6.2 Performance of Ensemble A1B sub-sample	37
3. Downscaling from regional projections to 6km projections: delta method and modified delta downscaling approaches	48
3.1 Advantages and Limitations of the Modified Delta Method	49
3.2 Applications of the Modified Delta Method	50
3.3 Modified Delta Method Runs for the Columbia, Colorado and Upper Missouri Watersheds.....	51
4. Using modified delta method downscaled climate projections as inputs for hydrologic modeling in the Variable Infiltration Capacity model.....	53
4.1 Primary Macro-Scale Hydrologic Products.....	53
4.2 VIC model implementation	53
4.2.1 General VIC implementation.....	55
4.2.2 Development of historical gridded climate forcing for VIC	56
4.3 Projections of future hydrologic conditions	57
5. Regional climate modeling	65
5.1 Regional climate modeling and models used in this study	65
5.2 Regional climate modeling: historical modeling.....	68
5.3 Regional climate modeling: future projections.....	71
6. Acknowledgements	79
7. References	79
Appendix 1: Key climatic and hydrologic products for USFS Regions 1 and 6	83

Appendix 2: Gridded Regional Datasets..... 91

Introduction and Overview

1.1 Funding

This project was funded by a consortium of federal agencies that required new regional and summary data on projected climate changes for planning purposes and impacts studies. Funding was provided by the United States Forest Service (USFS) Region 1, United States Fish and Wildlife Services (USFWS), USFS Rocky Mountain Research Station Boise Aquatic Sciences Lab, and USFS Region 6. The project builds on the considerable research effort and funding already devoted to similar goals in the Climate Impacts Group's Washington Climate Change Impacts Assessment (WACCIA, <http://ces.washington.edu/cig/res/ia/waccia.shtml>) and The Columbia Basin Climate Change Scenarios Project (2860, <http://www.hydro.washington.edu/2860/>), and would not have been possible without the resources and personnel associated with those projects.

1.2 Rationale

Planning for the effects of climate change on natural resources often requires detailed projections of future climate at scales consistent with the processes managers typically consider. While it is numerically possible to produce downscaled climate at very fine scales (<5km), both the absence of a sufficiently dense network of long term climate observations and the presence of local contingencies such as topography and land surface feedbacks from vegetation and snowpack make accurate estimation at these scales difficult and less tractable without very detailed local information. For such purposes as developing adaptation strategies, vulnerability assessments, climate impacts assessments, and specific resource modeling at landscape scales, downscaled projections can be developed that maximize translation of climatic information from the coarser scales of global climate models (GCMs) to more local scales. This project was designed to provide climate information that meets those needs and creates a basis for more detailed work or for a more comprehensive approach to downscaling and regional climate modeling.

1.3 Project Objectives

The goal of this project was to (1) develop consistent historical and future downscaled climate and hydrologic data and projections using the same methodology for several major river basins in the western United States (Columbia, upper Missouri, upper Colorado, and Great Basins) and (2) summarize that information in forms consistent with the needs of the funding agencies. This report describes where to get the information developed as well as the methods, results obtained, uses of and uncertainties associated with the data and projections.

1.4 Products

First, we analyzed GCMs available from the IPCC AR4 assessment to better understand the projected future regional climate, individual model sensitivities and regional differences in models used for downscaling. We then developed an ensemble of climate models that have the best capability in the basins in this project and use them to project sub-regional future climate based on an ensemble delta method. We also developed historical (1916-2006) and future (2030-2059, “2040s”; 2070-2099, “2080s”) 1/16th degree (~6km) hydrologic output from the historical and future climate to estimate variables more useful for impacts assessment (e.g., snow water equivalent, soil moisture, potential evapotranspiration, runoff). The result is a consistent set of downscaled climate and hydrologic projections at 6km for the entire Columbia, upper Missouri, and upper Colorado basins and 12km for the Great and lower Colorado basins. The data are summarized at monthly time scales for Bailey’s Ecoregions, Omernik Level III Ecoregions, and 8-digit Hydrologic Unit Code (HUC 4) basins but are available in raw form on a grid-cell basis at daily time steps and in ascii grid (ArcGIS) format for observed and future climatologies of selected variables. For the ratio of April 1 SWE to cool season snowpack, a variable useful for categorizing watershed snowpack vulnerability to climate change, we have summarized data at 10 digit HUC basins.

1.5 Data locations (see Appendix 1 for further details):

1. Trend maps (graphics) and station tables for Historical Climate Network climate trends:

<http://cses.washington.edu/picea/USFS/pub/HCN/>

These maps and the associated tables show trends at HCN stations for maximum and minimum temperature as well as precipitation for three time periods: 1915-2006, 1950-2006, and 1970-2006. The maps are by basin (CO = Colorado, GB = Great Basin, MB = Missouri Basin, PNW = Columbia),

2. Bias analysis of all available GCMs (scenarios B1, A1B, A2) by region:

http://cses.washington.edu/picea/USFS/pub/GCM_plots/

3. Data, graphics, future projections, summarized by:

- Bailey ecosections
- 8 digit HUCs
- Omernik ecoregions

http://cses.washington.edu/picea/USFS/pub/subrgn_summaries/

4. Western US ascii grids of 23 climatic and hydrologic variables, monthly climatologies:

- Historical (1916-2006)
- A1B 2030 – 2059 ensemble, miroc 3.2, and pcm1
- A1B 2070 – 2099 ensemble, miroc 3.2, and pcm1

<http://cses.washington.edu/picea/USFS/pub/summaries/>

5. Ratios of April 1 SWE to cool season snowpack, by 10 digit HUCs

http://cses.washington.edu/picea/USFS/pub/summary_tables/HUC5_apr01swe_to_ONDJFMprecip_ratio_wus.dat

6. Variable Infiltration Capacity hydrologic model output for historical period and future scenarios (tar.gz bulk download):

<http://cses.washington.edu/picea/USFS/pub/summaries/>

7. Regional climate modeling: WRF projections from CCSM3 and ECHAM5 GCMs

http://www.atmos.washington.edu/~salathe/reg_climate_mod/WRF_West/data_ascii/

2. Historical and future climate in the in the Columbia, upper Missouri, and upper Colorado River basins of the western U.S.

In this section, we use methods similar to those described in Mote and Salathé (2010) and Hamlet et al. (2010) to develop projections of future climate, fidelity of global climate models (GCMs) to regional climate, and use subsets of the GCMs to project future climate for several major river basins in the western United States (Columbia, upper Missouri, upper Colorado, and Great Basins). The basis of this downscaling are the GCMs also used for the Intergovernmental Panel on Climate Change (IPCC)'s fourth assessment (AR4) (e.g., Meehl et al. 2007a,b). The GCM future projection and historical datasets used to generate the core regional climate datasets in this report can be obtained from the Coupled Model Intercomparison Project (CMIP3) website and are archived online by the Program for Climate Model Diagnosis and Intercomparison (PCMDI). The downscaling and hydrologic modeling described below were possible because of a decade or more investment in such capability at the University of Washington's Climate Impacts Group.

2.1 Study domain and baseline regional climate for GCM comparisons

The domain of this study is primarily focused on three regions: Pacific Northwest, upper Missouri Basin, and upper Colorado Basin (Figure 2.1), but related projects also required data from the lower Colorado and Great Basins. In this section, we evaluate the recent (1950-2006) trends in observed temperature and precipitation, evaluate the fidelity of a pool of 19 available GCMs to observed, regionally averaged climatologies and climatic trends. For each region, we followed Mote and Salathé (2010) and area-averaged historical (1900-1999 for GCM trend analysis, 1970-1999 for monthly analyses of GCM bias) 0.5° - 0.5° (latitude-longitude) gridded data of the University of East Anglia Climatic Research Unit (CRU) version 2.02 (Mitchell et al. 2004). We then compared each GCM's responses during these same periods to develop an objective ranking of model bias and a basis for selecting a "least biased" subset of the available GCMs.



Figure 2.1. This study focuses on the Columbia River and Upper Missouri River Basins, but similar data was produced in the Great Basin and Colorado River Basin. Map: Robert Norheim

The capability of global climate models relative to each other or some benchmark depends greatly on the study objectives, and the result of any such ranking exercise will therefore vary – no “best” subset of climate models exists. Moreover, fidelity to the observed record does not guarantee that a model or multi-model ensemble has the greatest possible skill for future projection. Frequently, impacts assessments approach the pool of available GCMs by averaging all available projections (e.g., Elsner et al. 2010). Alternatively, models are sometimes ranked to reduce the size of the ensemble by rejecting models that do not perform as well (e.g., Overland and Wang, 2007). In this study, we developed a process to select 10 GCMs that perform similarly well in the PNW / Columbia Basin, the Northern Rockies / Upper Missouri Basin, and the Central Rockies / Upper Colorado Basin. The result is an internally consistent set of projections, downscaled to ~6km, and run through a hydrologic model to develop plausible estimates of climate and hydroclimate variables in the future over much of the western U.S.

2.2 *Historical trends in temperature and precipitation in the Columbia, upper Missouri, and upper Colorado River basins of the western U.S.*

Historical trends in regional climate provide a necessary empirical basis for interpreting future climate projections and climate impacts. In this section, we use the US Historical Climate Network (USHCN, Easterling et al. 1996, Menne et al. 2009) data to assess trends by station in regional temperature and precipitation. We analyzed trends for the periods 1915-2006, 1950-2006, and 1970-2006 and present the latter two here.

We used ordinary least squares regression to estimate the slope of the trend in temperature and precipitation at each HCN station. We estimated the total change (trend) by multiplying the annual increment (slope) by the number of years in the observation period. Because annual precipitation varies by an order of magnitude or more in different parts of the study region, we then benchmarked the precipitation trend in mm to the average annual precipitation taken across the observation period, 1916-2006. This differs from the approach taken by Mote (2003) for the Pacific Northwest, which compares the total change to the first year of the observation period.

2.2.1 *Climate trends from 1950 - 2006*

Temperature trends were similar in magnitude for maximum and minimum temperatures across basins for the 1950-2006 period, around 0.18 °C / decade (~1.0 °C total, Table 2.1, Figure 2.2).

Table 2.1. 1950-2006 Historical Climate Network trend and station ranges for minimum temperature, maximum temperature, and precipitation, by basin. Trend is the average total change across stations within the basin for the observation period (57 yr).

Basin	Tmin Trend (C°)	Tmax Trend (C°)	Precip Trend (mm)
Columbia	+1.0 (-0.7 - +2.6) ^a	+1.0 (0.9 - +2.5) ^b	-3.6 (-40 - +14) ^c
Missouri	+1.1(-1.8 - +3.5) ^d	+0.9 (-0.9 - 2.9) ^d	+4.5 (-19 - +28) ^e
Colorado	+1.1 (-0.8 - +3.1) ^f	+0.8 (-2.3 - +2.7) ^g	+3.0 (-12 - +16) ^h

^a= 153 stations, ^b = 154 stations, ^c = 77 stations; ^d= 247 stations; ^e = 153 stations; ^f= 100 stations, ^g = 98 stations, ^h = 29 stations

In the Columbia Basin, 84% (81%) of stations showed an increase in minimum (maximum) temperature of +0.5 °C or greater over the period 1950-2006, and only 1% (3%) station(s) showed a decrease of more than -0.5°C. At least 80% of the stations had minimum temperature increases statistically significantly different from zero (5% confidence interval for slope of regression greater than 0), while at least 71% had maximum temperature increases that were statistically significantly different from zero. At all stations with decreases in minimum temperature, the trend could not be statistically distinguished from zero change. Precipitation trends were mixed, with ~21% of stations showing declines in annual precipitation of -1cm or greater and 4% showing increases in annual precipitation of +1cm or greater. About 12% of stations had significant increasing trends, and about 6% had significantly decreasing trends, indicating strong spatial variability in the nature of precipitation trends. Most of the increases were west of the Cascades, and most decreases east of the Cascades and in Idaho and western Montana (Figure 2.3).

In the Missouri Basin, 65% (54%) of stations showed an increase in minimum (maximum) temperature of +0.5 °C or greater over the period 1950-2006, and < 1% (1%) of stations showed a decrease of more than -0.5°C. At least 71% of the stations had minimum temperature increases statistically significantly different from zero (5% confidence interval for slope of regression greater than 0), while at least 48% had maximum temperature increases that were statistically significantly different from zero. At about 1% of all stations, decreases in minimum (maximum) temperature could be statistically distinguished from zero change. Precipitation trends were mixed, with ~2% of stations showing declines in annual precipitation of -1cm or greater and 23% showing increases in annual precipitation of +1cm or greater. About 16% of stations had significant increasing trends, and about 2% had significantly decreasing trends.

In the Colorado Basin, 68% (46%) of stations showed an increase in minimum (maximum) temperature of +0.5 °C or greater over the period 1950-2006, and 1% (3%) station(s) showed a decrease of more than -0.5°C. At least 74% of the stations had minimum temperature increases statistically significantly different from zero (5%

confidence interval for slope of regression greater than 0), while at least 52% had maximum temperature increases that were statistically significantly different from zero. At about 3% (3%) of all stations, the trend in decreases in minimum (maximum) temperature could be statistically distinguished from zero change. Precipitation trends were mixed, with ~3% of stations showing declines in annual precipitation of -1cm or greater and 14% showing increases in annual precipitation of +1cm or greater. About 24% of stations had significant increasing trends, and about 3% had significantly decreasing trends.



Figure 2.2. Tmin and Tmax trends 1950-2006. Blue dots indicate increases, red dots decreases. The size of the dot is roughly proportional to the magnitude of the change over the period of measurement. NOTE: This is a draft graphic.

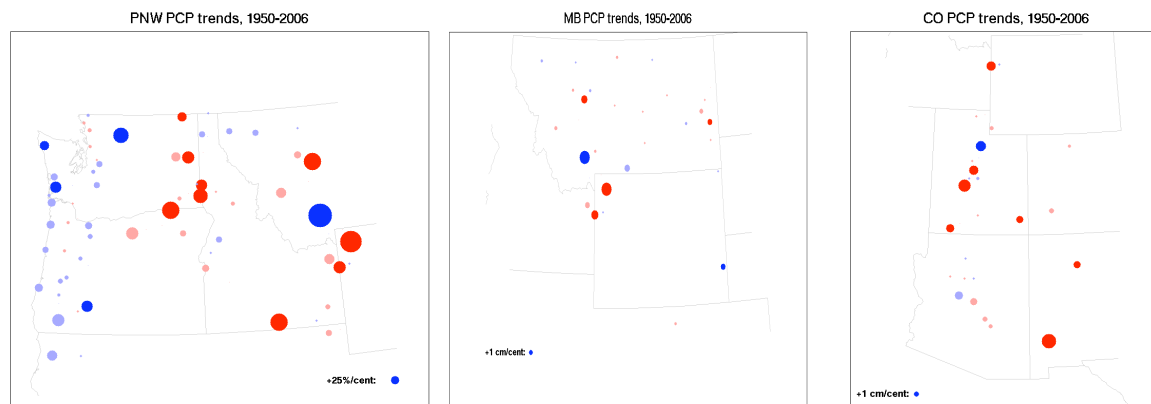


Figure 2.3. Precip trends 1950-2006. Blue dots indicate increases, red dots decreases. The size of the dot is roughly proportional to the magnitude of the change over the period of measurement. NOTE: This is a draft graphic.

2.2.2 Climate trends from 1970 - 2006

Temperature trends were slightly greater for maximum compared to minimum temperatures for the 1970-2006 period. Basin average minimum temperature trends were $0.26\text{ }^{\circ}\text{C} / \text{decade}$ ($\sim 1.0\text{ }^{\circ}\text{C}$ total, Table 2.2) in the Columbia and Missouri basins and $0.38\text{ }^{\circ}\text{C} / \text{decade}$ ($\sim 1.4\text{ }^{\circ}\text{C}$ total, Table 2.2) in the Colorado. Basin average maximum temperature trends were $0.34\text{ }^{\circ}\text{C} / \text{decade}$ ($\sim 1.0\text{ }^{\circ}\text{C}$ total, Table 2.2) in the Columbia and Missouri basins and $0.40\text{ }^{\circ}\text{C} / \text{decade}$ ($\sim 1.4\text{ }^{\circ}\text{C}$ total, Table 2.2) in the Colorado.

Table 2.2. 1970-2006 Historical Climate Network trend and ranges for minimum temperature, maximum temperature, and precipitation, by basin. Trend is the average total change across stations within the basin for the observation period (37 yr).

Basin	Tmin Trend ($^{\circ}\text{C}$)	Tmax Trend ($^{\circ}\text{C}$)	Precip Trend (mm)
Columbia	$+1.0$ (-1.4 - $+2.8$) ^a	$+1.3$ (-0.7 - $+2.6$) ^b	-2.6 (-24 - $+18$) ^c
Missouri	$+1.0$ (-1.6 - $+3.3$) ^d	$+1.2$ (-0.5 - $+3.6$) ^d	-0.7 (-22 - $+23$) ^e
Colorado	$+1.4$ (-1.3 - $+3.3$) ^f	$+1.5$ (-0.6 - $+3.5$) ^f	-1.1 (-12 - $+8$) ^g

^a= 153 stations, ^b = 154 stations, ^c = 77 stations; ^d= 247 stations; ^e = 153 stations; ^e= 101 stations, ^g = 31 stations

In the Columbia Basin, 86% (89%) of stations showed an increase in minimum (maximum) temperature of $+0.5\text{ }^{\circ}\text{C}$ or greater over the period 1970-2006, and only 3% (1%) of stations showed a decrease of more than $-0.5\text{ }^{\circ}\text{C}$ (Figure 2.4). At least 75% of the stations had minimum temperature increases statistically significantly different from zero

(5% confidence interval for slope of regression greater than 0), while at least 77% had maximum temperature increases that were statistically significantly different from zero. One station (<1%) had a decline in minimum temperature that was statistically significantly different from zero trend, while no stations had significant declines in maximum temperature. Precipitation trends were mixed (Figure 2.5), with ~17% of stations showing declines in annual precipitation of -1cm or greater and 3% showing increases in annual precipitation of +1cm or greater. No stations had significant increasing trends, and about 2% had significantly decreasing trends.

In the Missouri Basin, 83% (87%) of stations showed an increase in minimum (maximum) temperature of +0.5 °C or greater over the period 1970-2006, and only 2% (0%) of stations showed a decrease of more than -0.5°C. At least 58% of the stations had minimum temperature increases statistically significantly different from zero (5% confidence interval for slope of regression greater than 0), while at least 58% had maximum temperature increases that were statistically significantly different from zero. At about 1% (0%) of all stations, decreases in minimum (maximum) temperature could be statistically distinguished from zero change. Precipitation trends were mixed, with ~8% of stations showing declines in annual precipitation of -1cm or greater and 7% showing increases in annual precipitation of +1cm or greater. About 2% of stations had significant increasing trends, and about 4% had significantly decreasing trends.

In the Colorado Basin, 88% (91%) of stations showed an increase in minimum (maximum) temperature of +0.5 °C or greater over the period 1970-2006, and 2% (1%) of stations showed a decrease of more than -0.5°C. At least 78% of the stations had minimum temperature increases statistically significantly different from zero (5% confidence interval for slope of regression greater than 0), while at least 81% had maximum temperature increases that were statistically significantly different from zero. At about 1% (0%) of all stations, the trend in decreases in minimum (maximum) temperature could be statistically distinguished from zero change. Precipitation trends were mixed, with ~16% of stations showing declines in annual precipitation of -1cm or

greater and no stations showing increases in annual precipitation of +1cm or greater. No stations had significant trends over this period.



Figure 2.4. Tmin (top) and Tmax (bottom) trends 1970-2006. Blue dots indicate increases, red dots decreases. The size of the dot is roughly proportional to the magnitude of the change over the period of measurement. NOTE: This is a draft graphic.

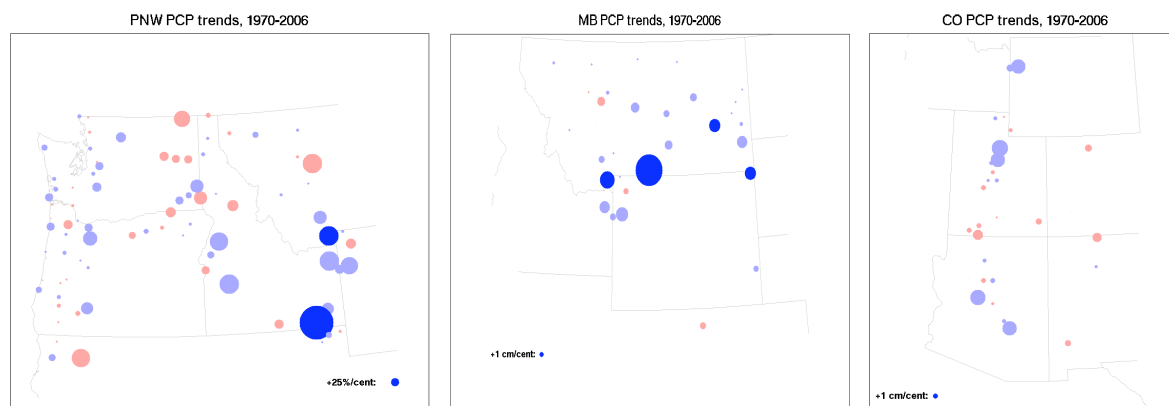


Figure 2.5. Precip trends 1970-2006. Blue dots indicate increases, red dots decreases. The size of the dot is roughly proportional to the magnitude of the change over the period of measurement. NOTE: This is a draft graphic.

2.3 Greenhouse gas emissions scenarios

In order to develop projections of 21st century, it is necessary to estimate the concentrations of compounds that affect radiative forcing in the atmosphere, including future greenhouse gas emissions and sulfate aerosols. Multiple emissions scenarios were produced under the auspices of the IPCC (Special Report on Emissions Scenarios, or SRES, Nakicenovic et al. 2000), and incorporate a wide range of possible future socioeconomic changes. Three SRES scenarios were most commonly chosen by independent climate modeling groups as GCM forcings: B1, A1B, and A2, each of which results in different levels of surface warming by the late 21st century (Figure 2.6). A2 produces the highest climate forcing by the end of the century, but before mid-century, none of the scenarios is consistently the highest. All three scenarios are analyzed here in terms of the future regional scale projections expected from the available IPCC AR4 models. More modeling groups ran A1B, recent emissions have been closer to the upper end trajectory than B1 (Raupach et al. 2007), and the focus for many impacts studies and planning efforts is on mid-century change, so for this study, we chose scenario A1B as the basis for downscaling and hydrologic modeling. The Washington Climate Change Impacts Assessment (WACCIA) chose A1B as the higher emissions scenario and B1 as the low emissions scenario for our analysis of 21st Century PNW climate. One goal of this project was to provide projections most relevant for vulnerability assessment and scenario planning exercises, and to that end we elected to focus on the A1B

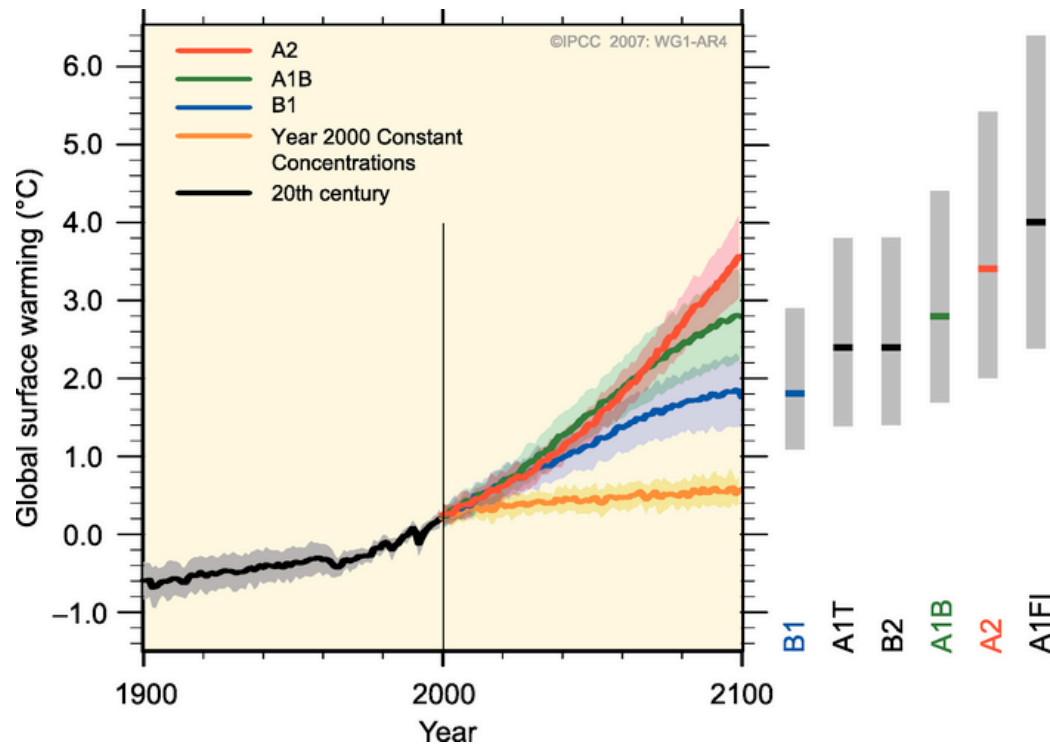


Figure 2.6 (after IPCC AR4 SPM.5). Solid lines are multi-model global averages of surface warming (relative to 1980–1999) for the scenarios A2, A1B and B1, shown as continuations of the 20th century simulations. Shading denotes the ± 1 standard deviation range of individual model annual averages. The orange line is for the experiment where concentrations were held constant at year 2000 values. The grey bars at right indicate the best estimate (solid line within each bar) and the likely range assessed for the six SRES marker scenarios. The assessment of the best estimate and likely ranges in the grey bars includes the AOGCMs in the left part of the figure, as well as results from a hierarchy of independent models and observational constraints.

2.4 Analysis of future regional climate projections

We first analyzed the regional climate projected by 19 GCMs used in IPCC AR4 for different SRES emissions scenarios. We averaged the GCM grid cell deltas across the regional domains in Figure 2.7 to produce annual and three month seasonal (winter – “DJF”, spring – “MAM”, summer - “JJA”, and fall – “SON”) future average deltas by model and time period.

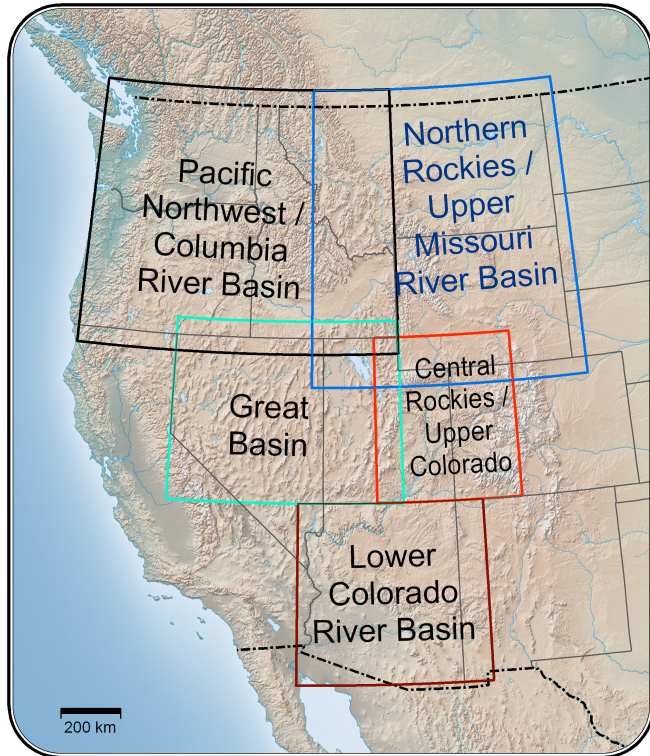


Figure 2.7. Domains for regional GCM bias comparisons:

Pacific Northwest / Columbia Basin
(41.5 – 49.5N, -124.0 – -111.0W),

Northern Rockies / Upper Missouri Basin
(40.5 – 49.5N, -114.5 – 103.5W),

Central Rockies / Upper Colorado Basin
(37.0 – 42.0N, -106.5 – -112.0W),

Great Basin
(37.0 – 42.5N, -120.0 – -111.0),

Lower Colorado Basin
(31.5 – 37.0N, -115.0 – -108.0W).

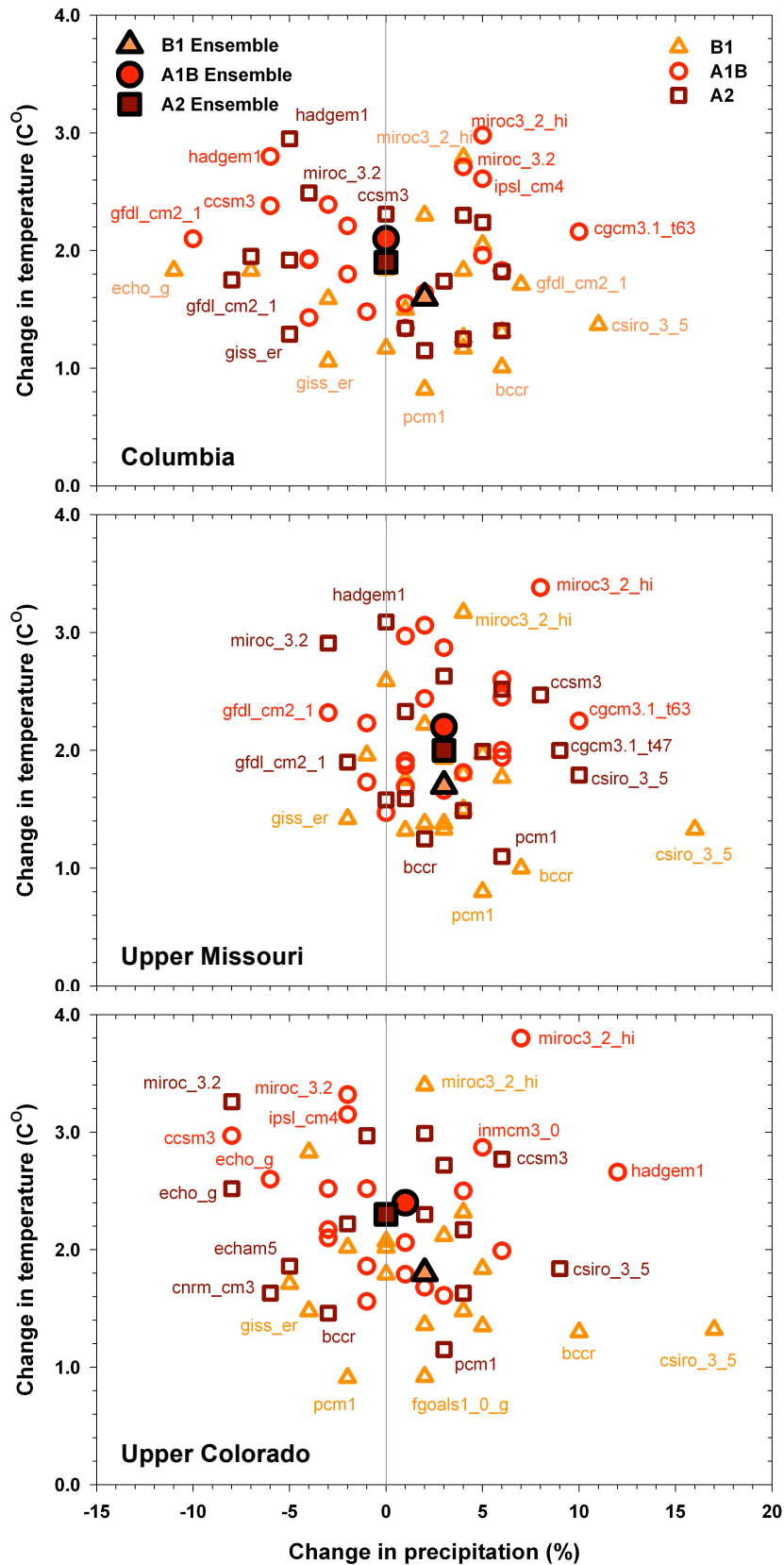


Figure 2.8. Scatterplots of annual temperature and precipitation deltas for different GCMs and regional ensemble means for the 2040s (2030-2059). Ensemble deltas are for all GCMs by SRES scenario. Ensemble averages differ from Mote and Salathé (2010) because ensembles were not weighted in this analysis.

There are small differences among regions in the regionally averaged annual deltas expected over all models (Table 2.3), but important differences among models. Some models (e.g., bccr, pcm1, csiro_3_5) are cooler than the ensemble for all three regions, while others (e.g., miroc_3_2, miroc_3_2_hi, hadgem) tend to be warmer. Csiro_3_5 is also wet for all three regions, but models vary substantially across the three regions in terms of models projecting drier annual climate (Figure 2.8).

Table 2.3. Future deltas (annual) for subregions by scenario and time period

SRES Scenario	No. GCMS		Temperature change (C)			Precipitation change (%)		
			Columbia	Missouri	Colorado	Columbia	Missouri	Colorado
B1	18	2040s	1.6	1.7	1.8	2	3	2
		2080s	2.5	2.7	2.8	1	4	3
A1B	19	2040s	2.1	2.2	2.4	0	3	1
		2080s	3.5	3.8	4.0	2	7	2
A2	15	2040s	1.9	2.0	2.3	0	3	0
		2080s	4.5	4.3	4.7	1	7	1
Ensemble* A1B	10	2040s	2.1	2.3	2.4	0	3	2
		2080s	3.8	4.1	4.3	2	7	5
MIROC_3.2	1	2040s	2.7	3.1	3.3	4	2	-2
		2080s	4.6	5.3	5.7	0	-1	-7
PCM1	1	2040s	1.8	1.7	1.7	-2	3	2
		2080s	2.7	2.6	2.6	-5	5	7

* See section 4. **An ensemble of best – performing models** for details. Ensemble A1B is the subset of 10 best performing models from a multi-variate ranking described below.

Seasonal changes in temperature and precipitation can be much more important for impacts analysis and vulnerability assessment than annual changes, which can average out important seasonal differences that may have larger effects than the annual changes alone would imply. Figures 2.9 through 2.14 show 2040s and 2080s seasonal changes in temperature and precipitation for the Columbia, upper Missouri, and upper Colorado basins for SRES scenarios B1, A1B, and A2.

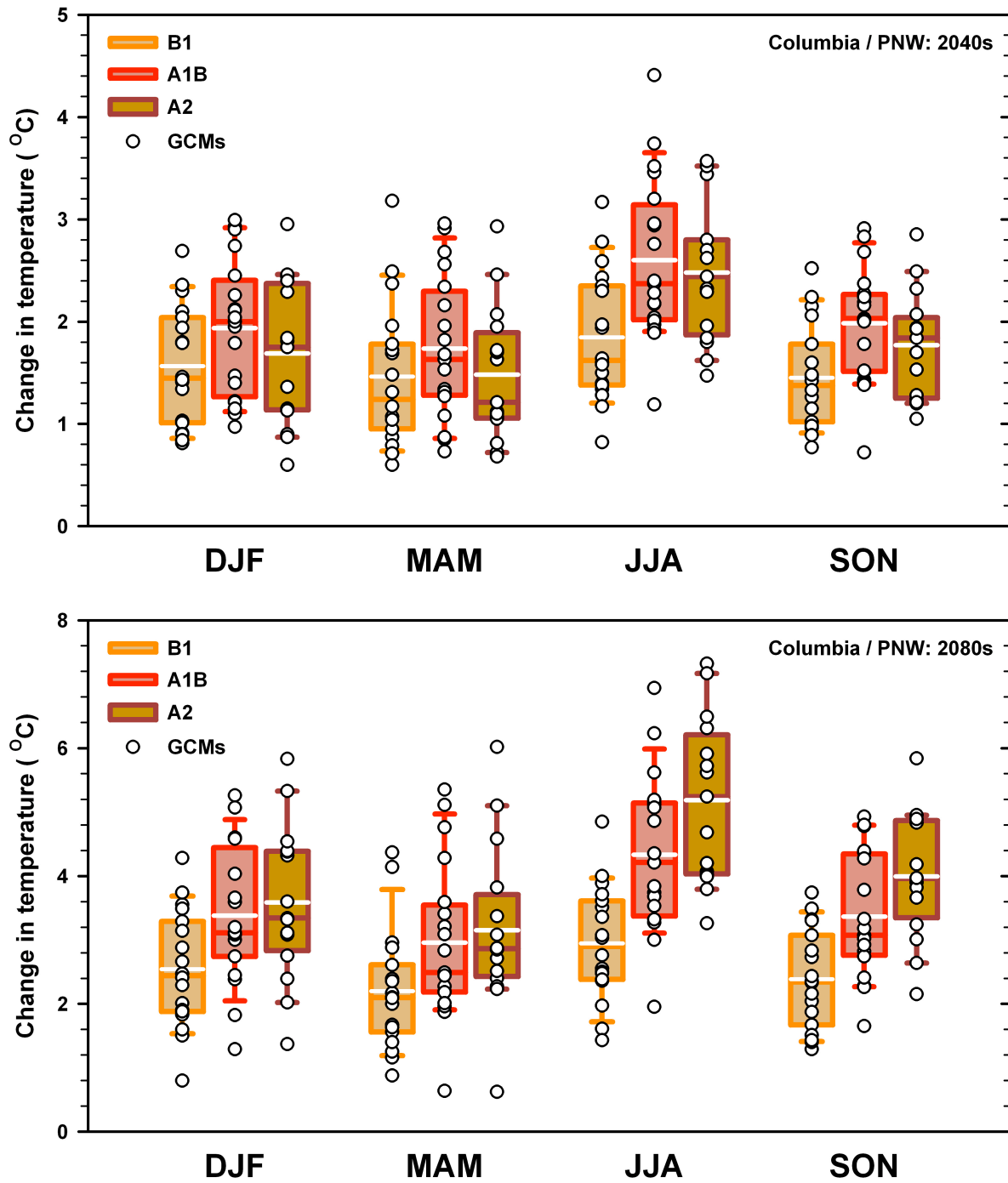


Figure 2.9. Range of projected changes in temperature (relative to 1970-1999) for the Columbia Basin / PNW for the 2040s (top) and 2080s (bottom) for each season (DJF = winter etc.). In each box-and-whiskers trio, the left most is for SRES scenario B1, the center for A1B, and the right for A2; circles are individual model values. Box and whiskers plots indicated 10th and 90th percentiles (whiskers) and 75th percentiles (box ends) and median (solid middle bar) for each season and scenario. White bars indicate mean of GCM deltas.

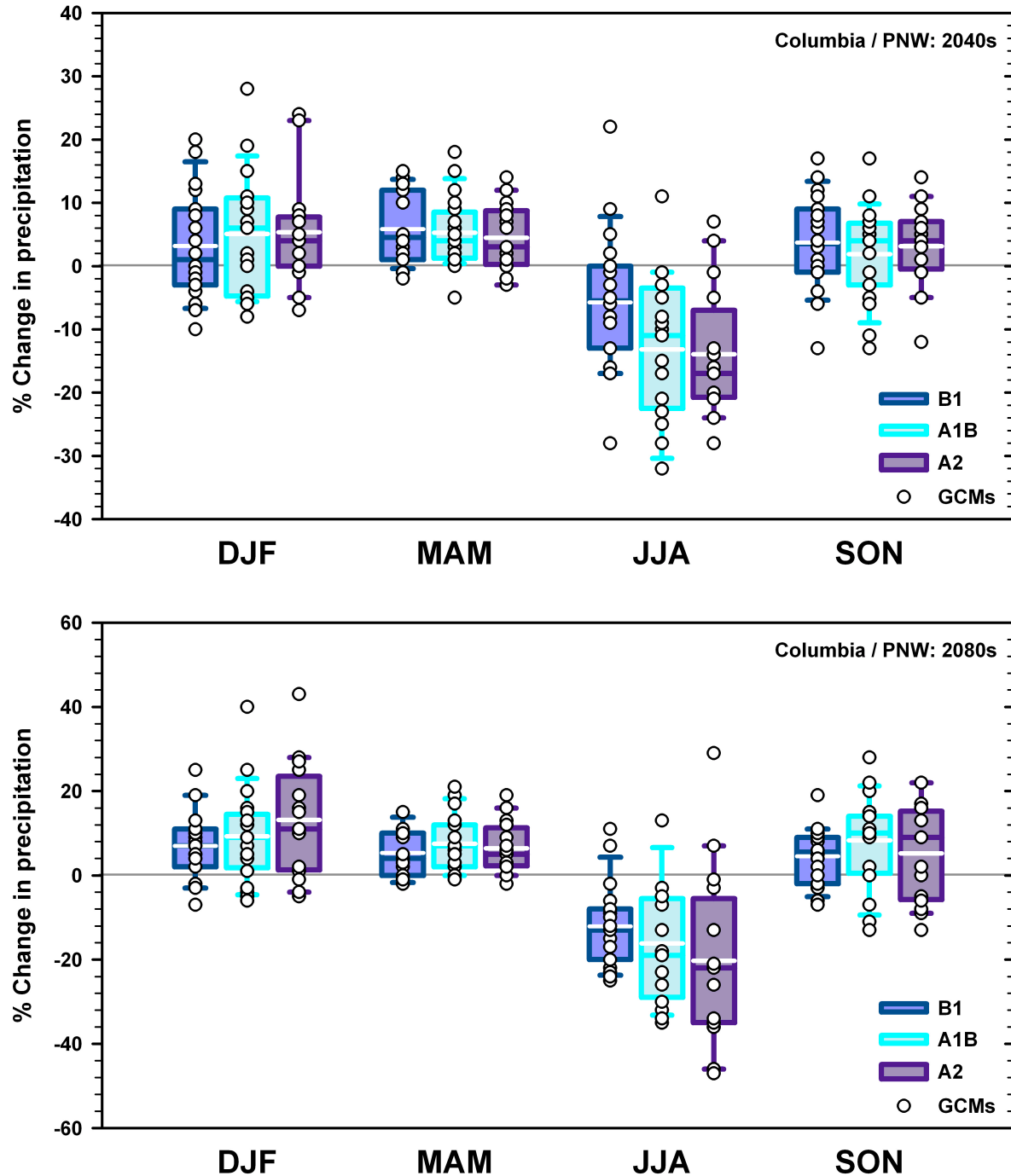


Figure 2.10. Range of projected changes in precipitation (relative to 1970-1999) for the Columbia Basin / PNW for the 2040s (top) and 2080s (bottom) for each season (DJF = winter etc.). In each box-and-whiskers trio, the left most is for SRES scenario B1, the center for A1B, and the right for A2; circles are individual model values. Box and whiskers plots indicated 10th and 90th percentiles (whiskers) and 75th percentiles (box ends) and median (solid middle bar) for each season and scenario. White bars indicate mean of GCM deltas.

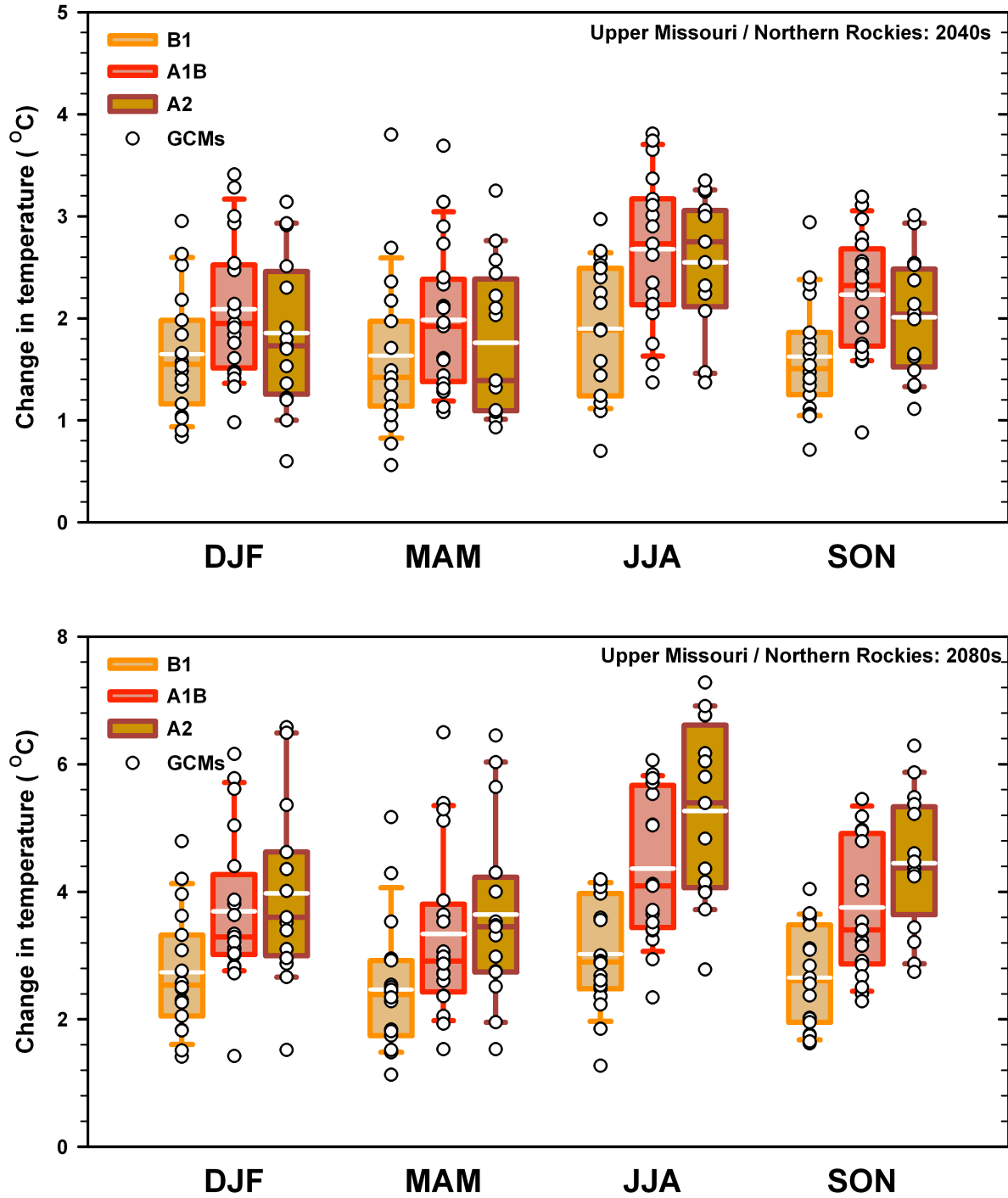


Figure 2.11. Range of projected changes in temperature (relative to 1970-1999) for the upper Missouri Basin / Northern Rockies for the 2040s (top) and 2080s (bottom) for each season (DJF = winter etc.). In each box-and-whiskers trio, the left most is for SRES scenario B1, the center for A1B, and the right for A2; circles are individual model values. Box and whiskers plots indicated 10th and 90th percentiles (whiskers) and 75th percentiles (box ends) and median (solid middle bar) for each season and scenario. White bars indicate mean of GCM deltas.

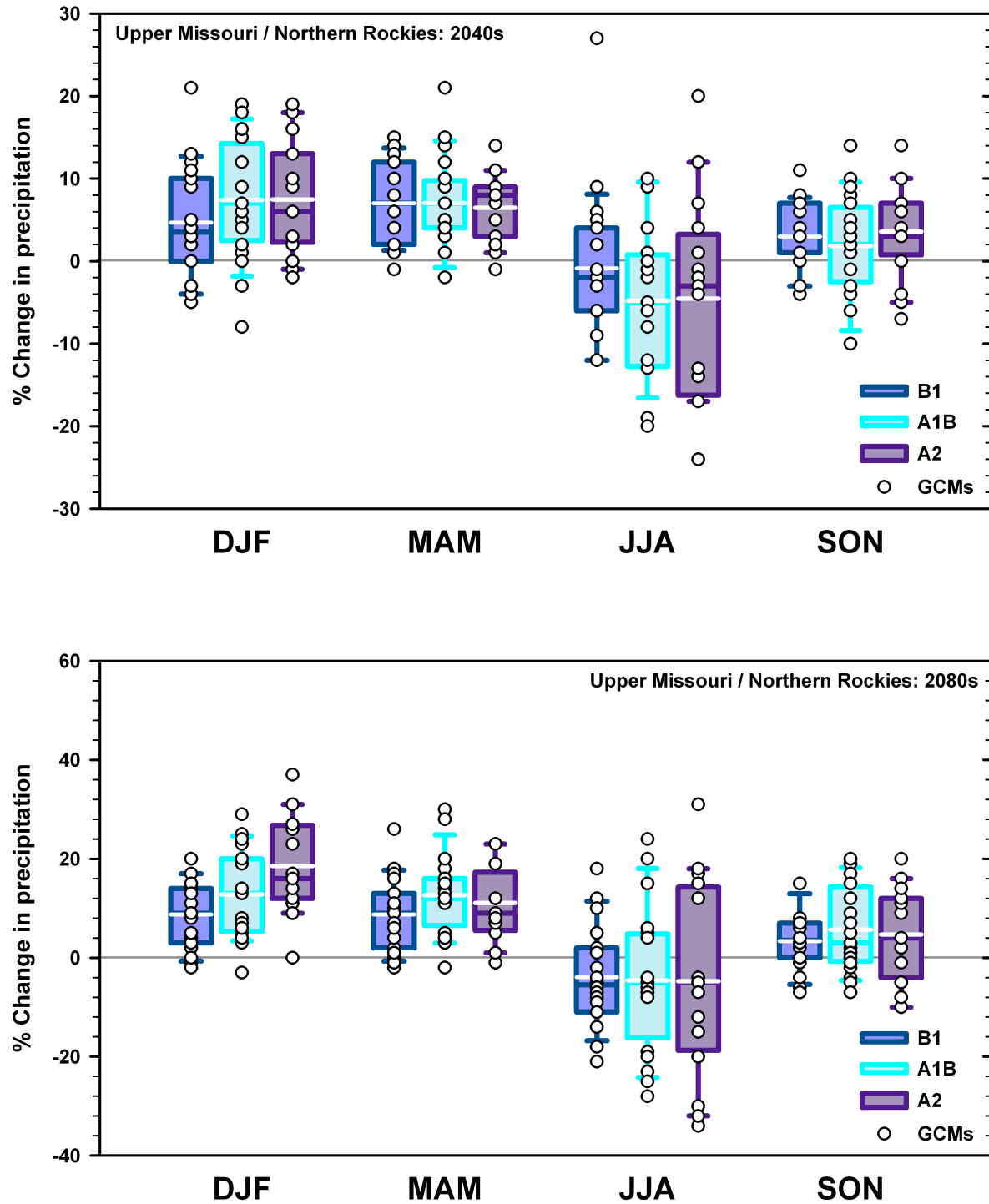


Figure 2.12. Range of projected changes in precipitation (relative to 1970-1999) for the upper Missouri Basin / Northern Rockies for the 2040s (top) and 2080s (bottom) for each season (DJF = winter etc.). In each box-and-whiskers trio, the left most is for SRES scenario B1, the center for A1B, and the right for A2; circles are individual model values. Box and whiskers plots indicated 10th and 90th percentiles (whiskers) and 75th percentiles (box ends) and median (solid middle bar) for each season and scenario. White bars indicate mean of GCM deltas.

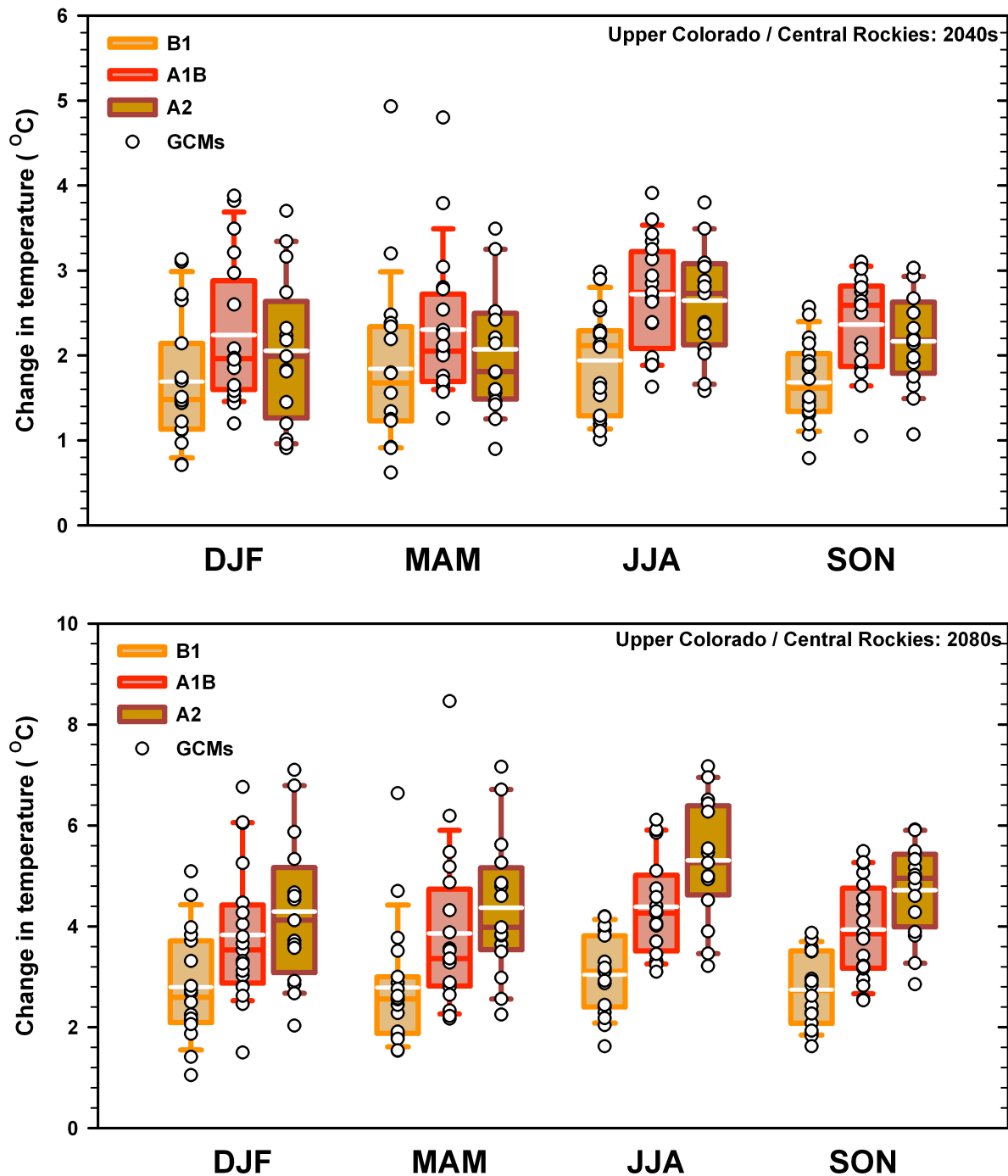


Figure 2.13. Range of projected changes in temperature (relative to 1970-1999) for the upper Colorado Basin / central Rockies for the 2040s (top) and 2080s (bottom) for each season (DJF = winter etc.). In each box-and-whiskers trio, the left most is for SRES scenario B1, the center for A1B, and the right for A2; circles are individual model values. Box and whiskers plots indicated 10th and 90th percentiles (whiskers) and 75th percentiles (box ends) and median (solid middle bar) for each season and scenario. White bars indicate mean of GCM deltas.

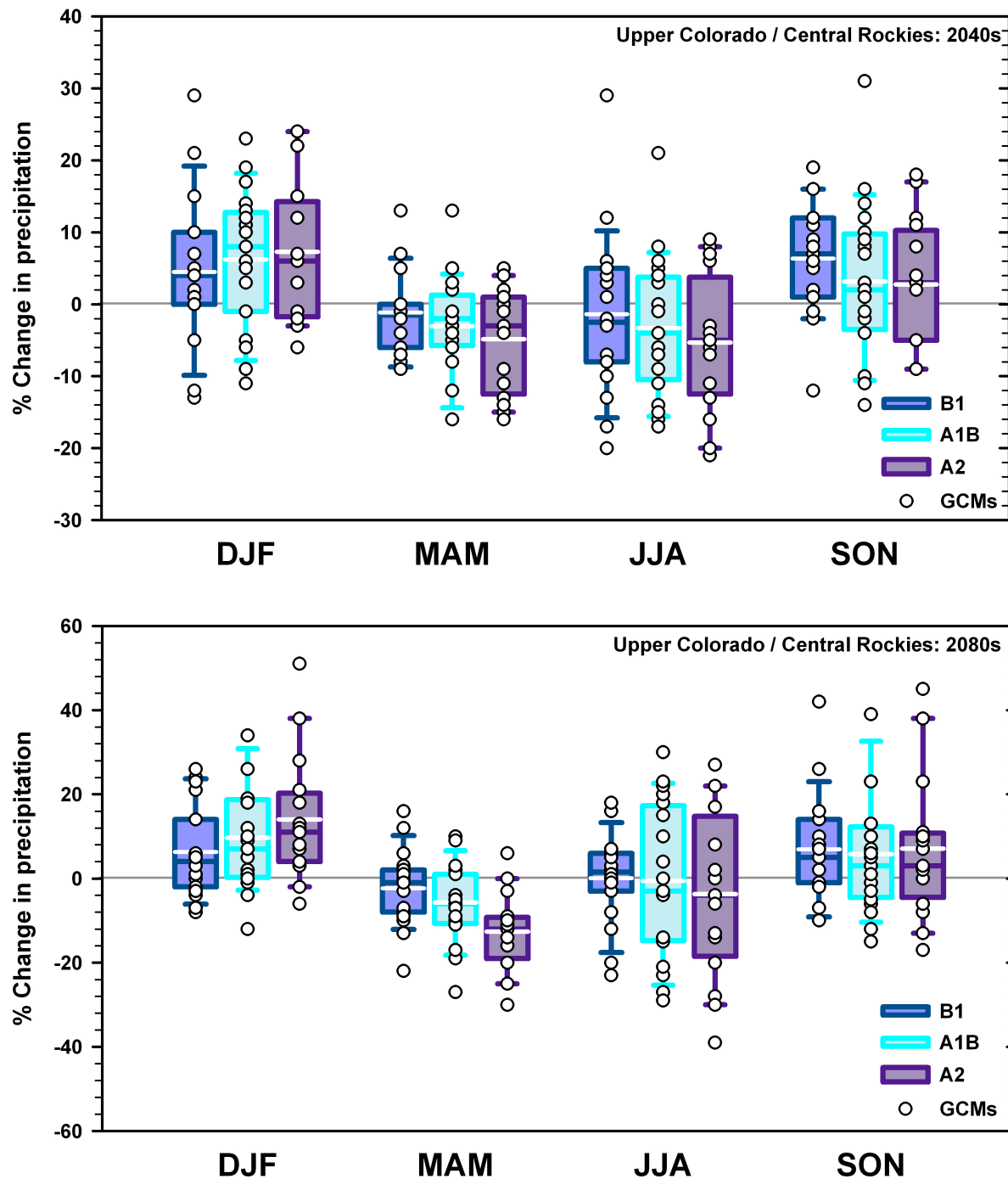


Figure 2.14. Range of projected changes in precipitation (relative to 1970-1999) for the upper Colorado Basin / central Rockies for the 2040s (top) and 2080s (bottom) for each season (DJF = winter etc.). In each box-and-whiskers trio, the left most is for SRES scenario B1, the center for A1B, and the right for A2; circles are individual model values. Box and whiskers plots indicated 10th and 90th percentiles (whiskers) and 75th percentiles (box ends) and median (solid middle bar) for each season and scenario. White bars indicate mean of GCM deltas.

There is considerable variation in individual GCM performance, with ranges of several degrees in the increase in annual temperature projected by each GCM within a season and SRES scenario (Table 2.3, Figures 2.9, 2.11, 2.13). Note that the increases in temperature projected for the 2040s are marginally (0.1 – 0.2 C) greater for A1B than A2 (Table 2.3), consistent with the lower emissions of A2 until the mid 21st century (Figure 2.6). The seasonality and sign of precipitation changes varies with region (Figures 2.10, 2.12, 2.14). Slight increases (on average) are projected in the PNW in all seasons (+4% winter, +5% spring, +3% autumn in the 2040s averaged across all scenarios) except summer that suggest a decrease (-11% 2040s). Similar seasonal changes are projected for the Upper Missouri, with a slightly greater increase in winter (+7%) and similar values for spring (+3%), and autumn (+3%) with a smaller decrease in precipitation in summer (-3%) compared to the PNW. In the upper Colorado, the seasonality of changes in precipitation is more like the southwest than the northwest, with decreases in precipitation projected for spring and summer (-3% for both in the 2040s), and slight increases in the winter and fall (+6% and +4% respectively). It is worth noting that the **range** of precipitation projections is quite large among models, less so among scenarios (Figures 2.10, 2.12, 2.14) and that therefore the **mean** taken across all scenarios and models is often a middle value with a very wide range. Given the ecological impacts of some of these changes, scenario planning can be a worthwhile exercise.

2.5 Bias analysis and selection of global climate models: comparing GCMs with 20th century climate, trends, and seasonal cycles

An open question in regional impacts assessment is, “Is there a subset of available GCMs that performs better in a region of interest than an ensemble composed of all GCMs?”. The answer to this question depends a great deal on the intended use of the ensemble in question, the methods used to select the subset of models that are included, and the performance metric of greatest interest. It is worth noting that the narrowing of the pool of GCMs (which are themselves a narrowing of the physically possible futures, both within and among models) is in some ways a narrowing of uncertainty; the models in the ensemble have been shown to perform well against chosen metrics. But it also affects the decision environment in which products are eventually used by narrowing the range of plausible futures considered – no ensemble should

be considered the most likely single future scenario. Instead, the ensemble constructed below should be considered a robust scenario within the range of likely scenarios derived from multiple models. It is therefore a good basis for assessment, planning, and impacts studies.

In the following section, we use a variety of performance metrics to evaluate the performance of GCMs in the three regions of interest and select from those GCMs a subset of 10 to be used in an ensemble applied consistently across all regions in Figure 2.1. We compare the models based on (1) observed temperature trend from 1900-1999, (2) observed temperature and precipitation climatology (average) from 1970 – 1999, (3) seasonal cycle of precipitation, and (4) fidelity to north Pacific / north America pressure patterns (after Mote and Salathé 2010).

2.5.1 Observed temperature trend

One metric that can be used to evaluate the performance of GCMs in a region is the ability of each GCM (and the ensemble) to capture the observed trends in temperature and precipitation. For this analysis, we used an area-weighted average to develop GCM means over the regions of interest (Figure 2.1). In the Washington Climate Change Impacts Assessment, Mote and Salathé (2010) evaluated model trends against the US Historical Climate Network (USHCN) dataset and found good correspondence between the observed PNW trend and the ensemble trend. Here, we use a different dataset (CRU 2.02, Mitchell et al. 2004) for the trend analyses. While the HCN station density is potentially useful for this approach in the PNW, it is not as appropriate in regions where stations are more sparsely distributed and topography has the capacity to exert a greater influence on the difference between regional station means and expected regional climate averaged over all locations. We present the precipitation trends here as well, though these were not used as metrics of performance. Figure 2.15 (temperature) and Figure 2.16 (precipitation) show the regional CRU climate trends for each basin and the GCM projections averaged over the same region for the period 1900-1999. Most models are warmer than the CRU trend, with ensembles ~ 0.2 to 0.4 C warmer than CRU regional estimates of +0.5 C/century (Columbia), +0.6 C/century (Upper Missouri), and +0.4 C/century (Upper Colorado). The giss_aom model has trends very cool relative to the observed in all three basins, and several models are warmer than CRU in all three basins. Precipitation projections do not generally capture the positive trends in precipitation in the three basins, with about half the models projecting declining trends in annual precipitation and half projecting increases.

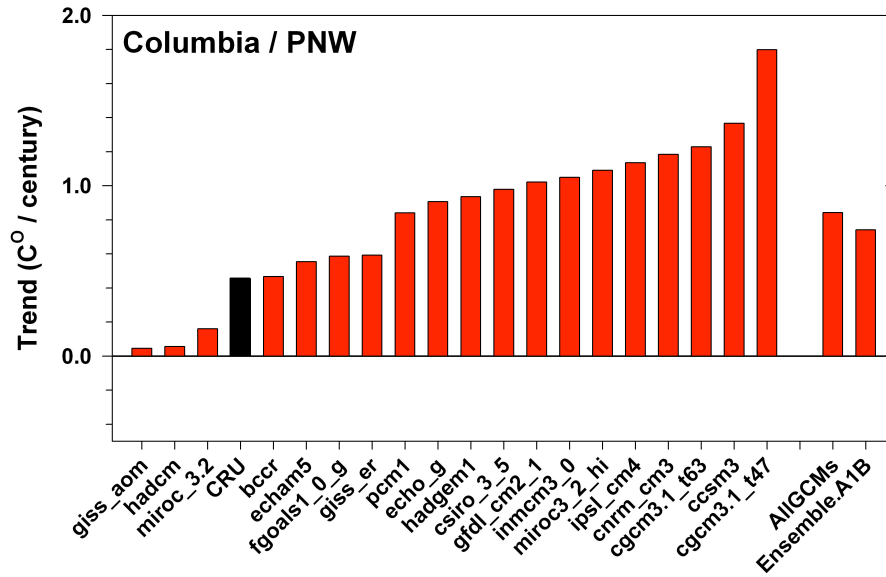
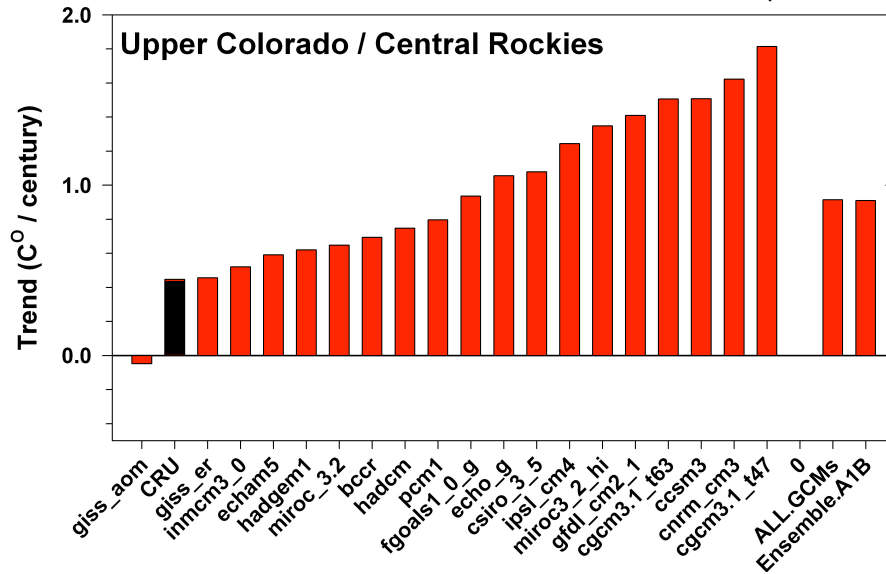
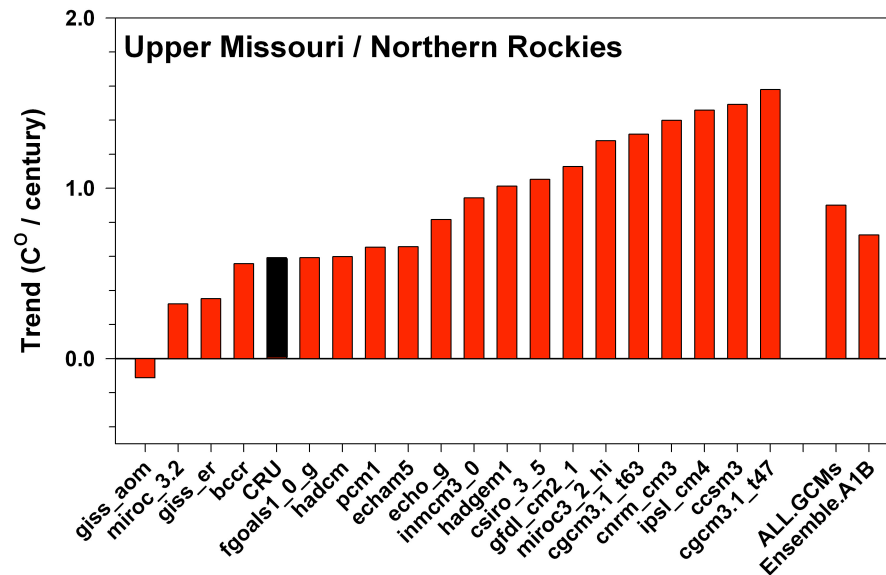


Figure 2.15. Temperature trend bias analysis of 19 GCMs against 1900-1999 regionally averaged CRU 2.02 historical temperatures. The black bar indicates the CRU regional average, and the right-most red bars indicate the ensemble mean for all GCMs and the ensemble mean for the subset of GCMs used to project A1B future temperatures for this project.



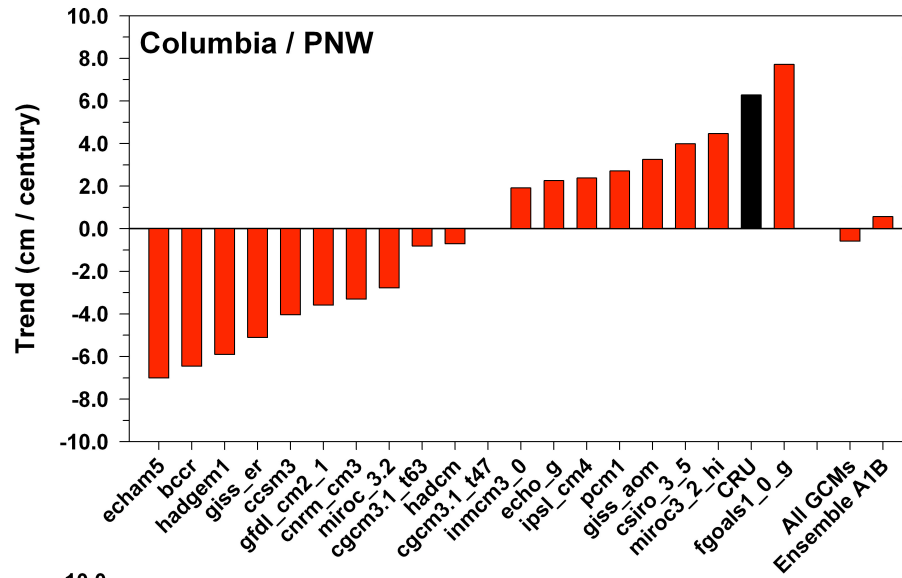
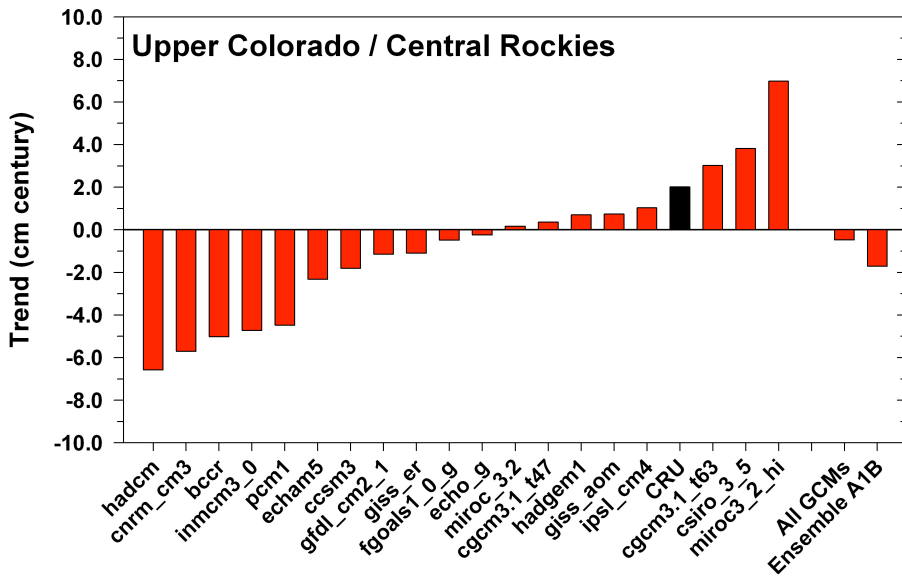
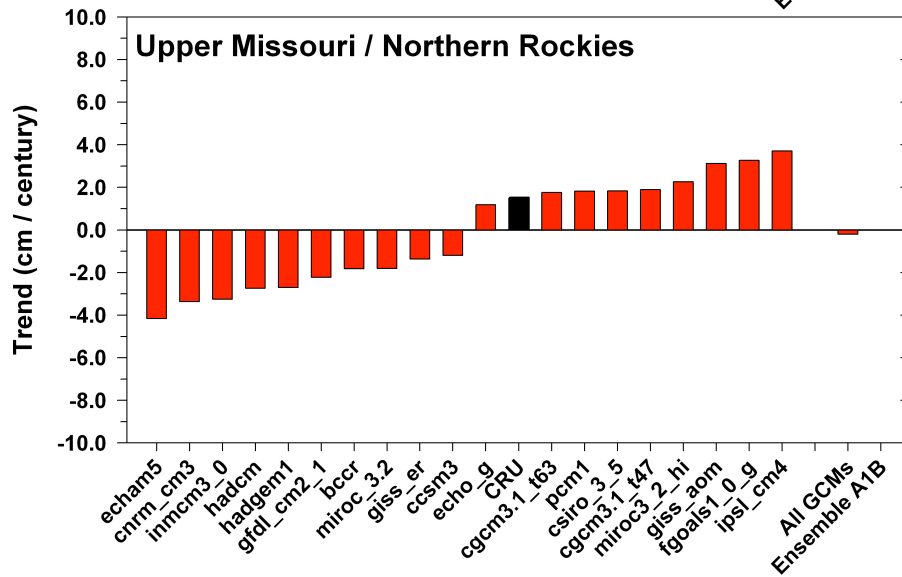


Figure 2.16. Precipitation trend bias analysis of 19 GCMs against 1900-1999 regionally averaged CRU 2.02 historical temperatures. The black bar indicates the CRU regional average, and the right-most red bars indicate the ensemble mean for all GCMs and the ensemble mean for the subset of GCMs used to project A1B future precipitation for this project.



Models are not always similarly biased in the different basins, indicating the potential for geographically specific subsets to perform better when historical conditions are used to test model trend. It is worth noting that the both the ensemble of all GCMs and the ensemble A1B (10 GCMs in this study) approach CRU for temperature, but are biased toward lower or opposite sign (drier) trends in precipitation.

2.5.2 *Observed climatology*

A second metric of comparison between GCMs and the observed record is the bias of each GCM compared to a mean climate value, or climatology. In this study, we compared GCMs and observed climate (1970-1999) by examining both the annual bias in annual average temperature and annual total precipitation. There is a considerable range evident in the bias associated with different GCMs. For precipitation, nearly all models rank too wet (Figure 2.17), with the ensemble mean annual total bias across all models about 32 cm (PNW), 30cm (Upper Missouri), and 23cm (Upper Colorado) total. Similarly, most models are too cold (Figure 2.17), with ensemble means across all models ~ -1.8 C (PNW), -1.3 C (Upper Missouri), and -0.5 (Upper Colorado). There are regional differences in the ranking of the models, but giss_aom and fgoals_1_0_g appear to be much too wet in all three basins. Cgcm3.1_t63 is too cold in all three regions, and csiro_3_5 is too warm in all three regions, though the absolute value of the bias is greater in the former.

2.5.3 *Seasonal cycle of precipitation*

A third metric of comparison between GCMs is the seasonal cycle of precipitation, which is also a key determinant of ecological response to climate change due to the timing of water supply and demand and how it relates to energy demand for water (Littell et al. 2010). For each GCM, we calculated the ratio of months of maximum precipitation to months of minimum precipitation for each region: November to January/July to September - PNW; June to September / November to February - upper CO; May-June / October to January - upper Missouri. This ratio was then compared to the historical ratio. In the PNW, most GCMs roughly have the seasonal cycle indicated by the observed record, although the magnitude of precipitation associated with winter peak and summer low precipitation is often considerably

off (Figure 2.18). Most models have reasonable (if amplified) seasonal cycles in terms of the timing of peak precipitation (winter in the PNW, late spring in the upper Missouri).

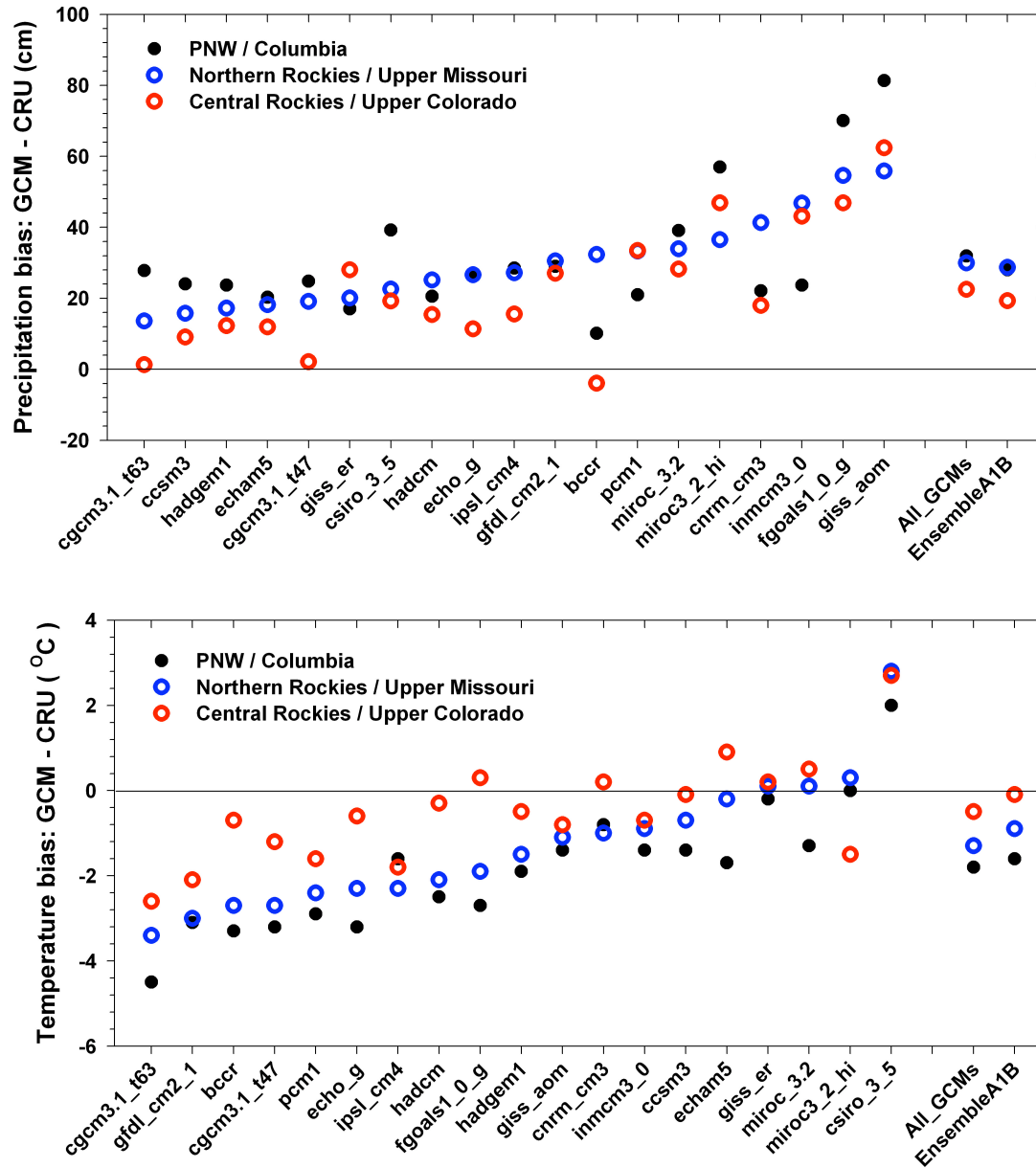


Figure 2.17. Annual total precipitation (top) and annual average temperature (bottom) bias (compared to 1970-1999 CRU data) among GCMs, averaged across all available GCMs, and averaged across just the ensemble members selected for this work. Order of GCMs is ranking for Northern Rockies.

The seasonal variation in precipitation in the upper Colorado is more difficult to define in the first place, with the most common feature the decline in precipitation from May to June. We did not use seasonal cycle of temperature as a performance metric for evaluating GCMs, but we present results here (Figure 2.18).

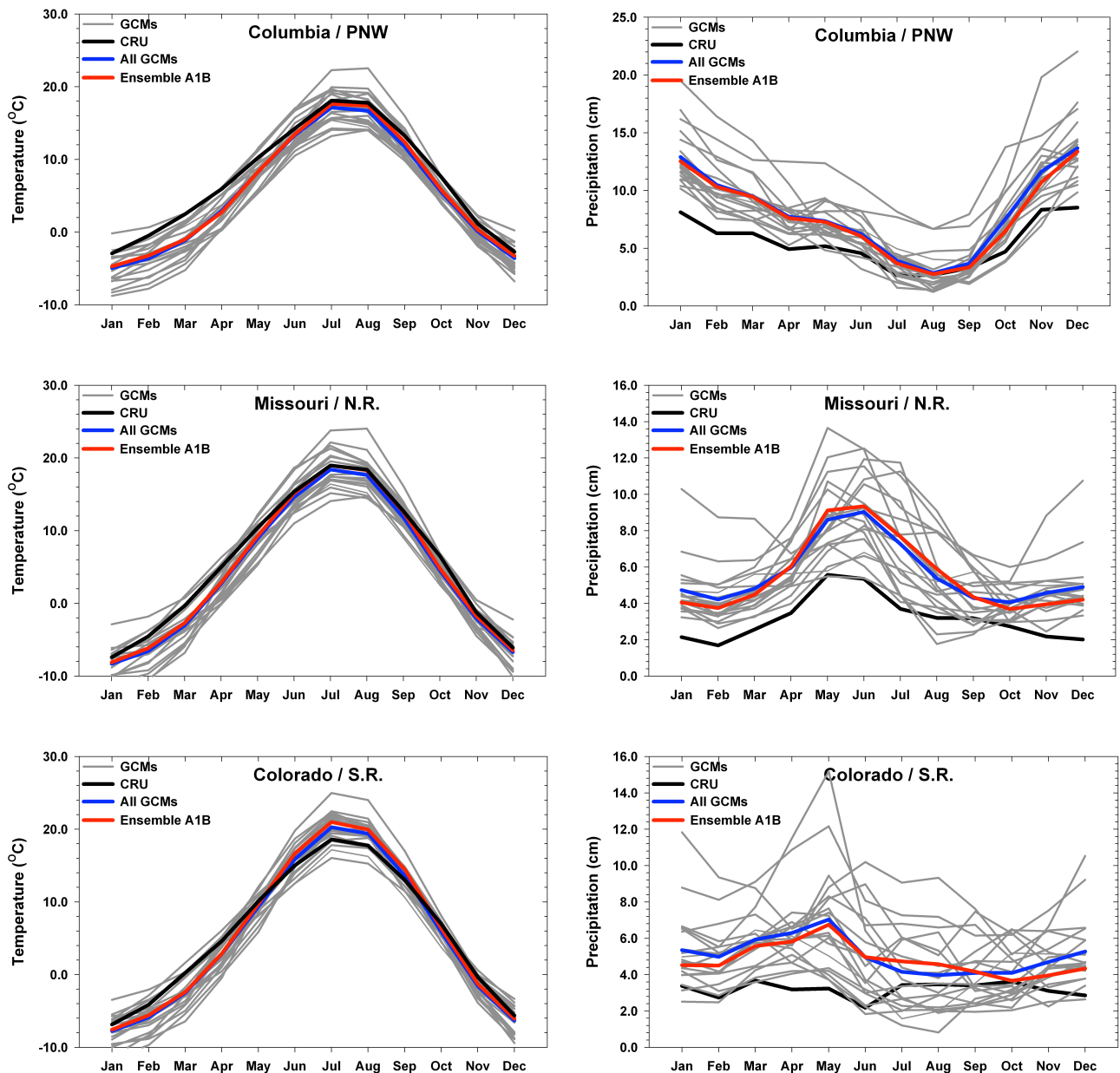


Figure 2.18. Monthly average temperature (left column) and monthly total precipitation (right column) bias among GCMs by basin (compared to 1970-1999 CRU data).

Models vary in their skill at capturing the regional differences in seasonal temperature (Figure 2.18), but the differences are more evident in precipitation than temperature. Most GCMs (and the ensemble mean) are too cold between January and April in all three basins, and too warm in July and August in the Colorado basin.

2.5.4 Fidelity to north Pacific / north America pressure patterns

Mote and Salathé (2010) note that the moisture flux provided by the GCM into a particular region is an important component determining the amount and distribution of precipitation. They evaluated the GCMs in the WACCIA study based on a comparison of precipitation, sea level pressure, and temperature from GCMs compared to the NCEP / NCAR reanalysis (Kalnay et al. 1996) for 1950-1999 over the domain of the north Pacific and north America. In this comparison, temperature is best simulated, followed by sea level pressure, and precipitation. An exception is the giss_er model, which positions the Aleutian Low too far to the west (Mote and Salathé 2010). We used the rankings provided by Mote and Salathé (2010) in this analysis because they apply to all three focus regions.

2.6 An ensemble of best – performing models

2.6.1 Selection of ensemble members

We set out to develop future climatologies for each of the focus regions based on monthly GCM projections, from deltas calculated for a baseline climatology of 1970-1999 (CRU 2.02, Mitchell et al. 2004). Based on the results of analyses above, we selected a subset of 10 GCMs that ranked among the best in the Northern Rockies / Upper Missouri and the Central Rockies / Upper Colorado for five variables: 20th century temperature trend, average annual temperature, average annual precipitation, proportion of seasonal precipitation, and North Pacific conditions (after Mote and Salathé 2010). These rankings are in Table 2.4 We explored several methods for developing an ensemble that could be applied in all three regions, including average rankings, bias Z-scores, and elimination of the worst ranking model(s) in each category. None of these approaches appeared more robust or objective than any other. In all three approaches

and for all three regions, 6 models are the same: echam5, bccr, hadcm, miroc_3.2, hadgem1, echo_g. After that the choice of the “best” GCMs to include in the ensemble varies with region and method.

To develop an ensemble, we chose to eliminate the lowest ranking models by variable (see Table 2.4) for the upper Missouri because robust modeling has been done for more GCMs in the PNW. The models retained include: bccr, cnrm_cm3, csiro_3_5, echam5, echo_g, hadcm, hadgem1, miroc_3.2, miroc3_2_hi, pcm1.

In addition, we chose two GCMs from the ensemble members as bracketing models based primarily on summer precipitation and temperature deltas, which have consequences for forest ecosystems in the region (Littell et al. 2010). These bracketing GCMs are pcm1 (wetter summers: +10% by 2040s, +4% by 2080s; less temperature increase: +1.6C by 2040s, +2.9C by 2080s) and miroc_3.2 (drier summers: -12% by 2040s, -28% by 2080s; more temperature increase: 3.1C by 2040s, 5.8C by 2080s). The ensemble (referred to as “ensemble A1B”) average and the two bracketing scenarios were then used as regional deltas in delta method downscaling and hydrologic modeling. For bias of the ensemble A1B and an ensemble of all evaluated GCMs, see Figures 2.14 – 2.18. The ensemble means do not change appreciably (Table 2.3) when the full GCM ensemble from all models is compared to the ensemble A1B.

To understand the consequences of this narrowing of the possible ensemble, we evaluated the ensemble that would result with no bias evaluation and selection and compared it to the narrowed ensemble of 10 GCMs used in the regional downscaling and hydrologic analyses. The average deltas expected from the full pool of GCMs (19 for A1B, 18 for B1, 15 for A2) taken over the regional domains in Figure 2.1 would be the full ensemble mean. It is also useful to evaluate the distribution of individual GCM estimates around the ensemble mean to understand the variability associated with different GCMs and the selection process.

Table 2.4. GCM rankings for temperature, precipitation, seasonal cycle of precipitation, 20th century trend, and combined North Pacific conditions.

GCM	Average Annual Temperature			Average Annual Precipitation			Seasonal Precipitation**			20th Century trend			North Pacific***
	Upper Misso.	PNW	Upper Color.	Up. Misso.	PNW	Upper Color.	Up. Misso.	PNW	Upper Color.	Up. Misso.	PNW	Upper Color.	
*echam5	1	7	1	5	6	7	13	11	7	5	2	3	4
*bccr	15	16	12	12	2	3	8	4	12	3	1	6	10
*hadcm	11	12	7	10	5	9	4	8	11	2	7	7	15
*miroc_3.2	3	5	2	14	16	12	3	12	18	8	5	5	8
*hadgem1	9	11	9	4	7	6	5	18	13	10	10	4	9
*echo_g	13	17	10	9	10	5	10	1	14	6	9	11	3
*pcm1	12	14	14	13	3	15	1	7	17	4	6	8	14
*cnrm_cm3	8	3	5	16	8	11	16	3	19	16	16	18	7
*csiro_3_5	16	10	13	7	15	10	6	19	8	11	11	12	11
*miroc3_2_hi	2	1	16	15	17	17	11	13	15	13	14	14	5
giss_er	4	2	3	6	1	13	12	6	10	7	4	1	19
inmcm3_0	7	6	11	17	4	16	2	2	16	9	13	2	13
cgcm3.1_t47	17	18	15	3	9	1	9	5	4	19	19	19	1
ccsm3	6	8	6	2	11	4	18	17	6	18	18	17	16
fgoals1_0_g	10	13	4	18	18	18	19	16	1	1	3	9	17
cgcm3.1_t63	19	19	19	1	12	2	15	9	3	15	17	16	2
giss_aom	5	4	8	19	19	19	14	14	9	14	8	10	12
gfdl_cm2_1	18	15	18	11	14	14	7	15	2	12	12	15	6
ipsl_cm4	14	9	17	8	13	8	17	10	5	17	15	13	18

* GCMs used in this study for A1B ensemble

** Ratio of months of maximum precipitation to months of minimum precipitation: NDJ/JAS - PNW; JJAS / NDJF –upper CO; MJ / ONDJ - upper Missouri.

*** North Pacific / North America combine temperature, precipitation, and sea-level pressure analysis from Mote and Salathé 2010

To inform such comparisons, and to enable users of these datasets to evaluate how individual model projections used in impacts studies would compare to the ensemble mean results, we analyzed the regional ensembles and developed seasonal deltas (Tables 2.5-2.7, Figures 2.19 – 2.22) and annual and seasonal scatterplots (Figures 2.23 – 2.25) that help put the models and the ensembles in context. The ensemble deltas differ slightly from those described in the WACCIA as summarized by Littell et al. (2009) from data in Mote and Salathé (2010) because the historical comparison in Mote and Salathé (2010) was weighted by performance of GCMs during the historical period – the values presented here are not weighted. This analysis also does not include the gfdl_2.0 model, only the gfdl_2.1 model, while both models were included in WACCIA.

2.6.2 *Performance of Ensemble A1B sub-sample*

The Ensemble A1B (10 models) mean annual deltas for temperature and precipitation are comparable (Table 2.3) to the full ensemble A1B of all (19 models), with the Ensemble A1B subset being slightly warmer in the 2080s (~ 0.3 C) in all three basins and slightly wetter in the Upper Colorado Basin (by 1% in the 2040s and 2% in the 2080s).

There are seasonal differences between the subset Ensemble A1B and the A1B estimate from all GCMs. Figures 2.19 – 2.22 show the seasonal range, median, and mean of the projected changes in temperature and precipitation by the GCMs for each region and SRES scenario for the 2040s and 2080s. The most noticeable effect of the selecting the Ensemble A1B on the range of seasonal future climate projections is the removal of models that are depicted as outliers beyond the 10%/90% whiskers in the full A1B distribution (e.g., 2040s JJA and SON temperature in the Columbia, or 2040s JJA precipitation in the upper Missouri), but this is not necessarily true in all cases – some models that rank reasonably well still produce projections far from the ensemble mean.

Ensemble A1B subset scatterplots are in Figures 2.23 to 2.25 and show the range of future projections associated with the highest ranking GCMs retained in the Ensemble A1B for each basin domain, Columbia, upper Missouri, and upper Colorado, respectively. Tables 2.5 to 2.7 show all seasonal and annual values for the basin domains.

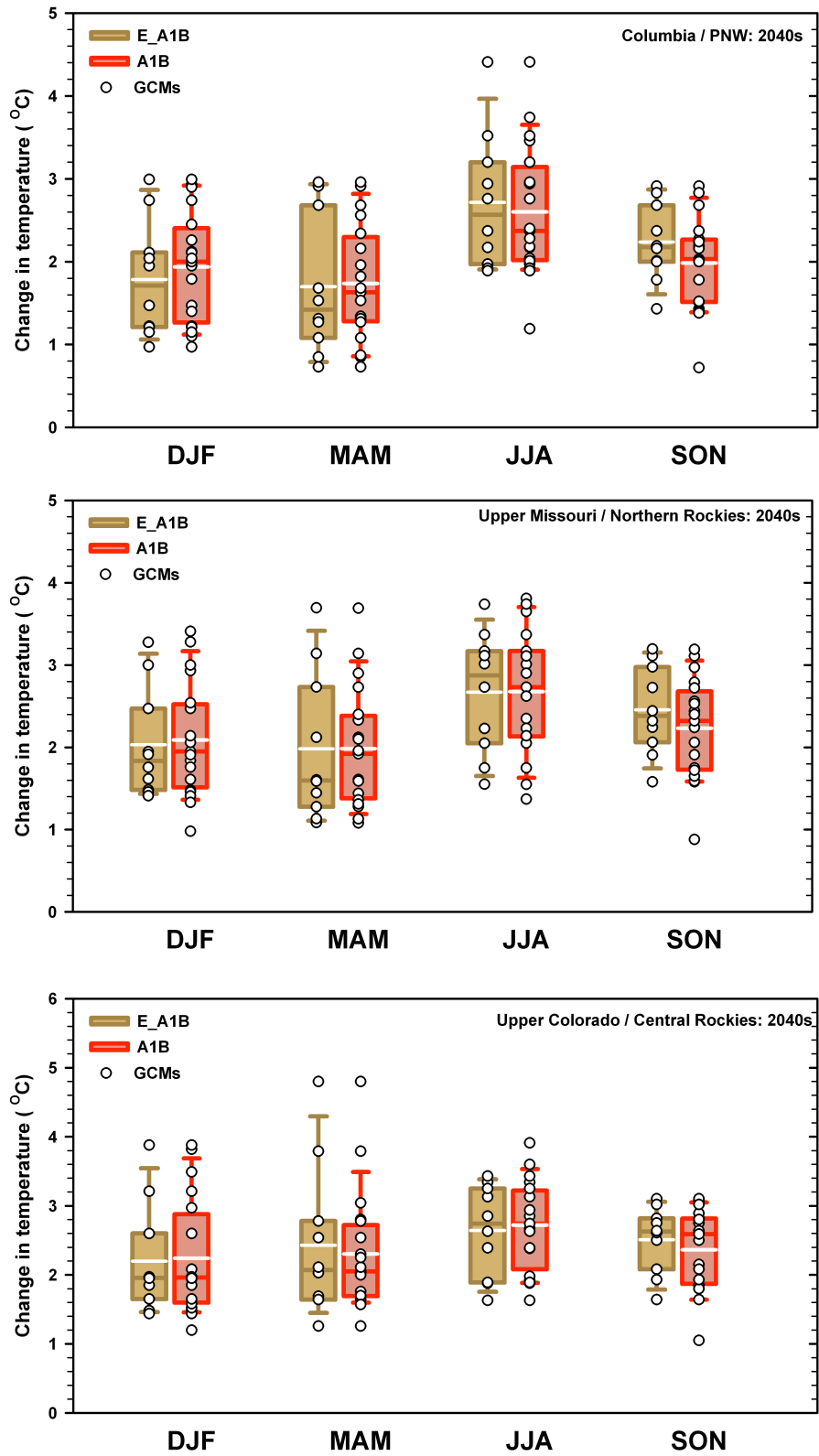


Figure 2.19. Comparison of regionally averaged 2040s temperature projections for Ensemble A1B (10 GCMs) and A1B across all available models (19 GCMs). Interpretation as in Figure 2.9.

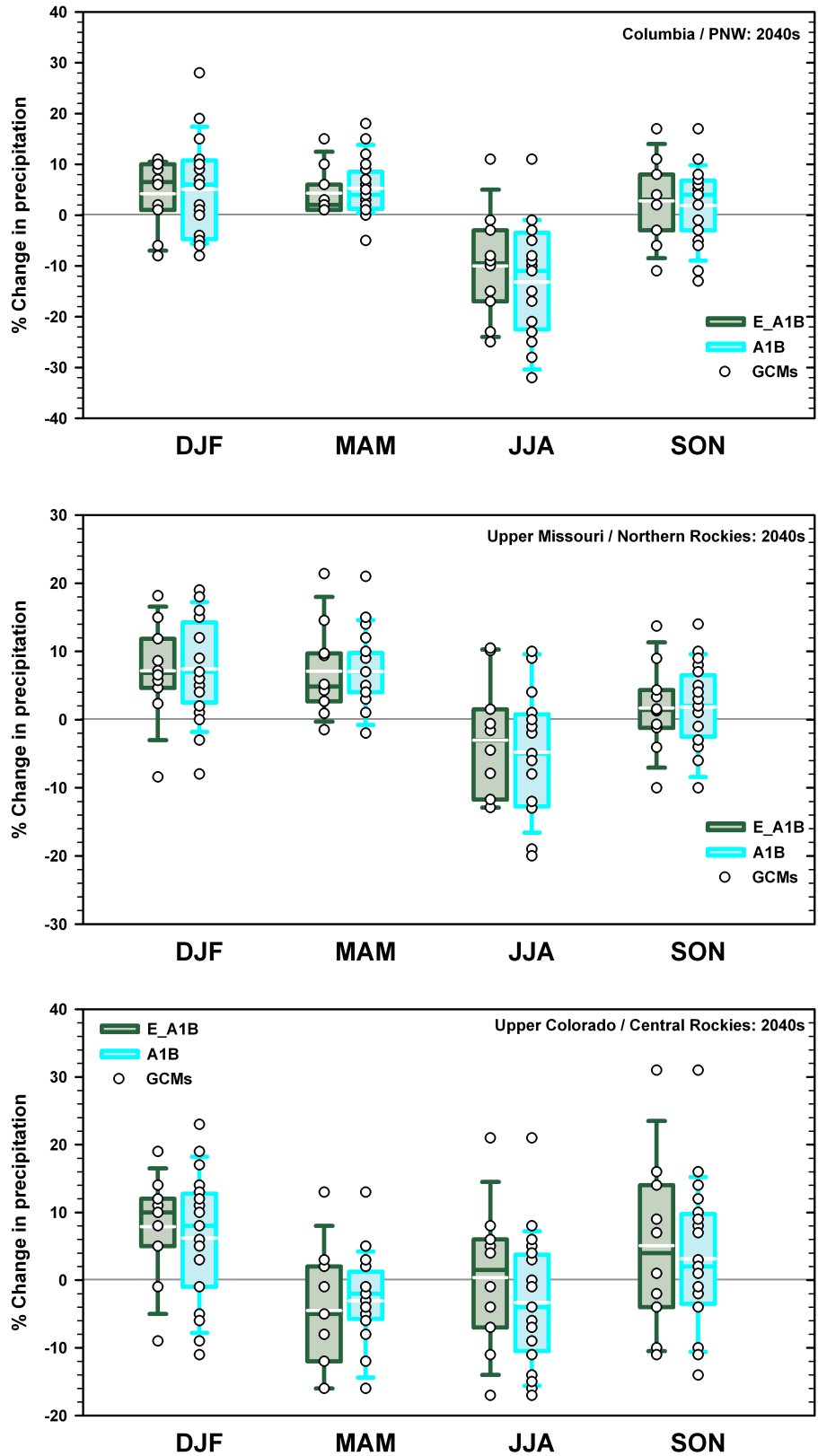


Figure 2.20. Comparison of regionally averaged 2040s precipitation projections for Ensemble A1B (10 GCMs) and A1B across all available models (19 GCMs). Interpretation as in Figure 2.9.

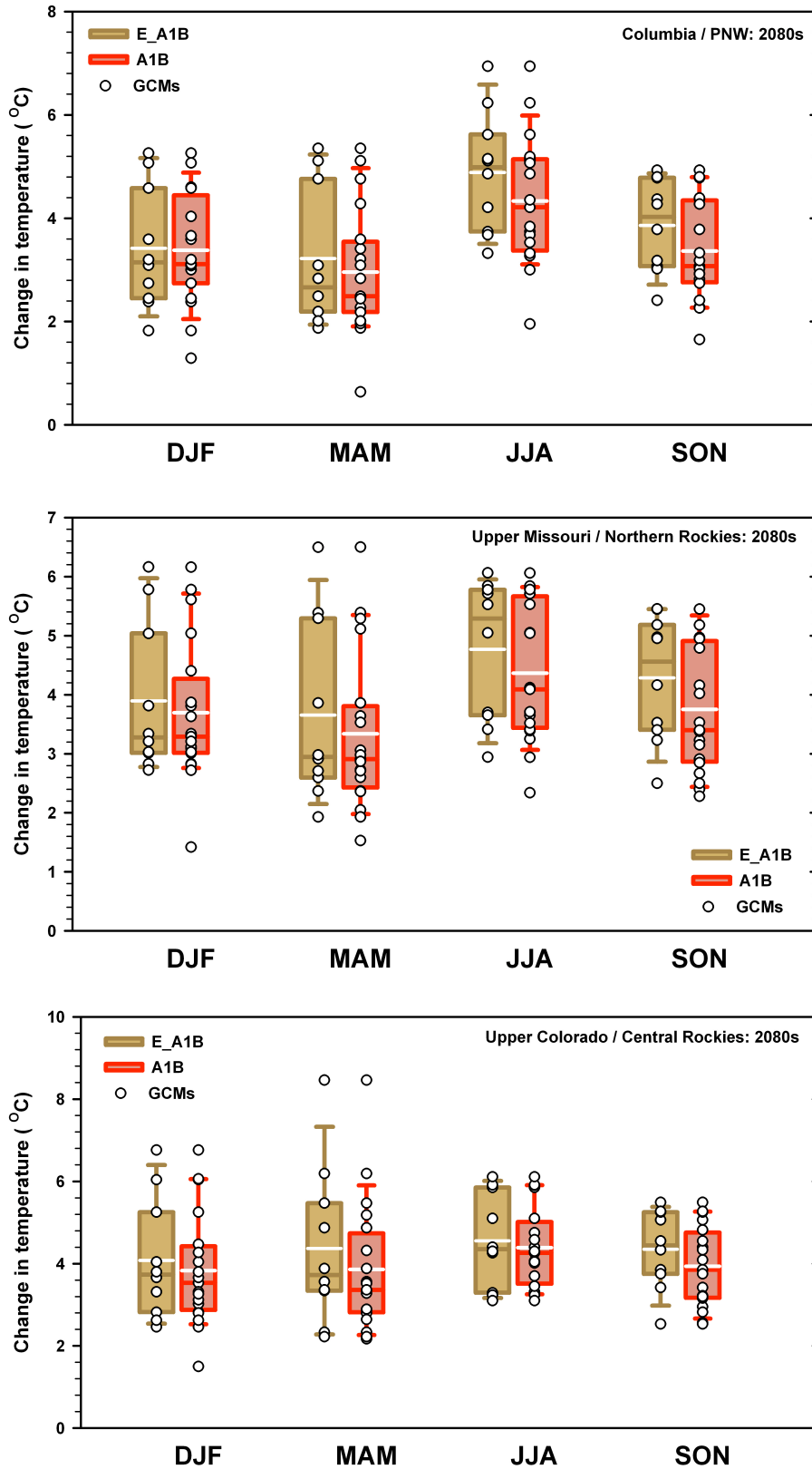


Figure 2.21. Comparison of regionally averaged 2080s temperature projections for Ensemble A1B (10 GCMs) and A1B across all available models (19 GCMs). Interpretation as in Figure 2.9.

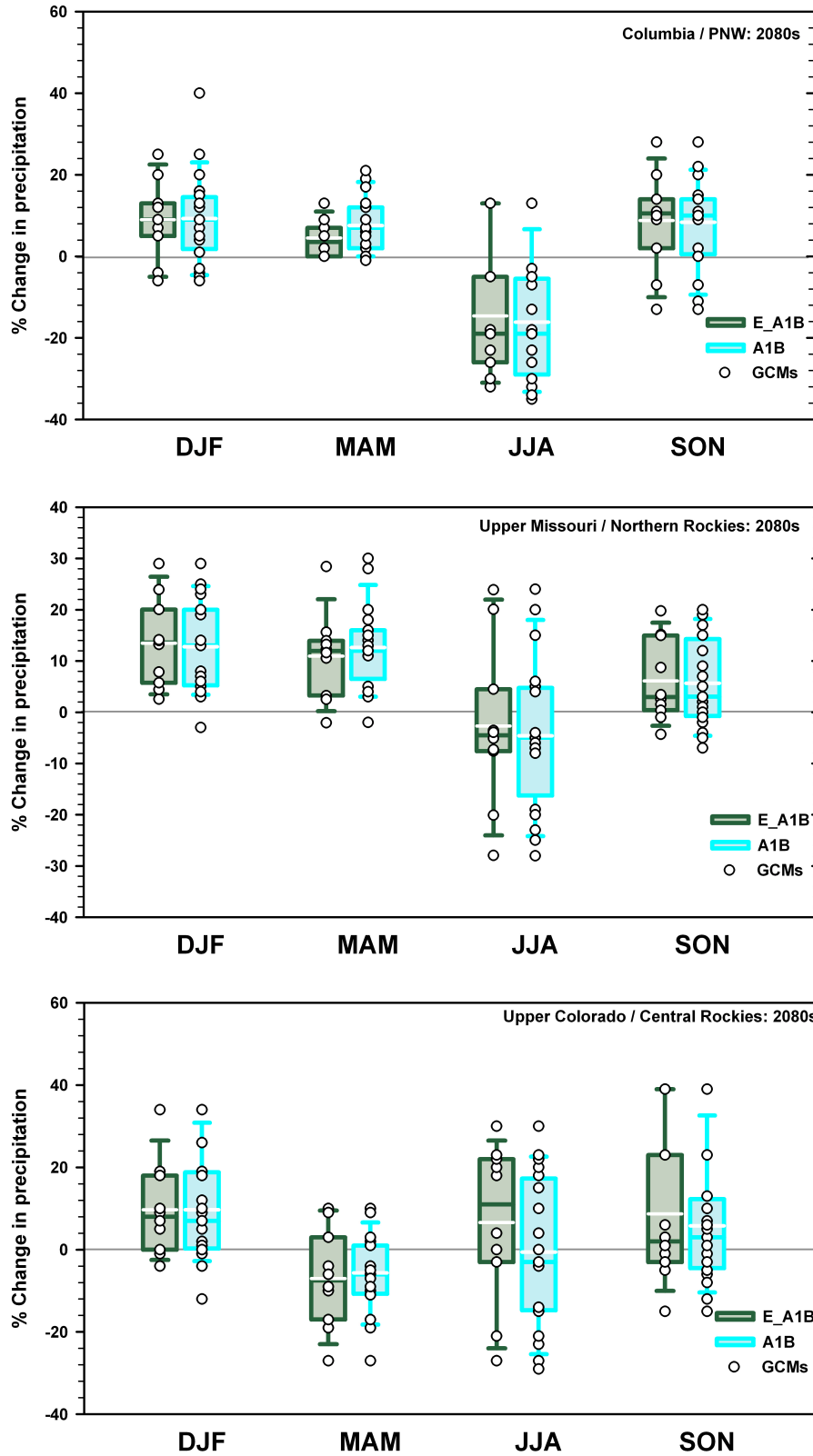


Figure 2.22. Comparison of regionally averaged 2080s precipitation projections for Ensemble A1B (10 GCMs) and A1B across all available models (19 GCMs). Interpretation as in Figure 2.9.

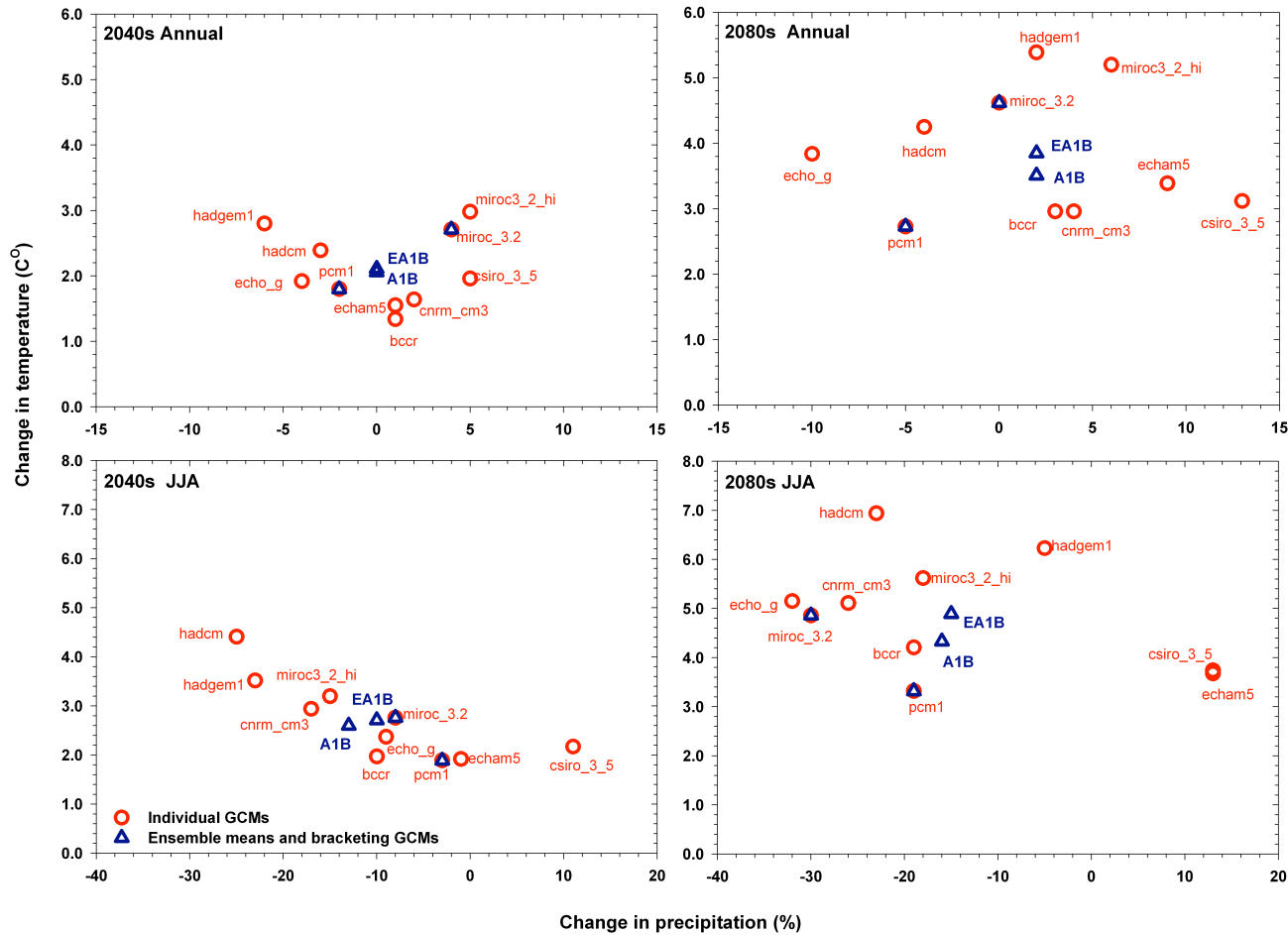


Figure 2.23. Scatterplots of Columbia Basin / PNW deltas for GCMs used in the Ensemble A1B and comparison with full A1B mean. Deltas are annual (top) and summer (JJA, bottom) for the 2040s (left) and 2080s (right). Blue triangles indicate Ensemble means (EA1B = Ensemble A1B of 10GCMs selected based on rankings in section 4; A1B = ensemble of 19 AR4 GCMs described in sections 2 and 3) and bracketing scenarios selected for the Upper Missouri Basin (GCMs PCM1 and MIROC 3.2).

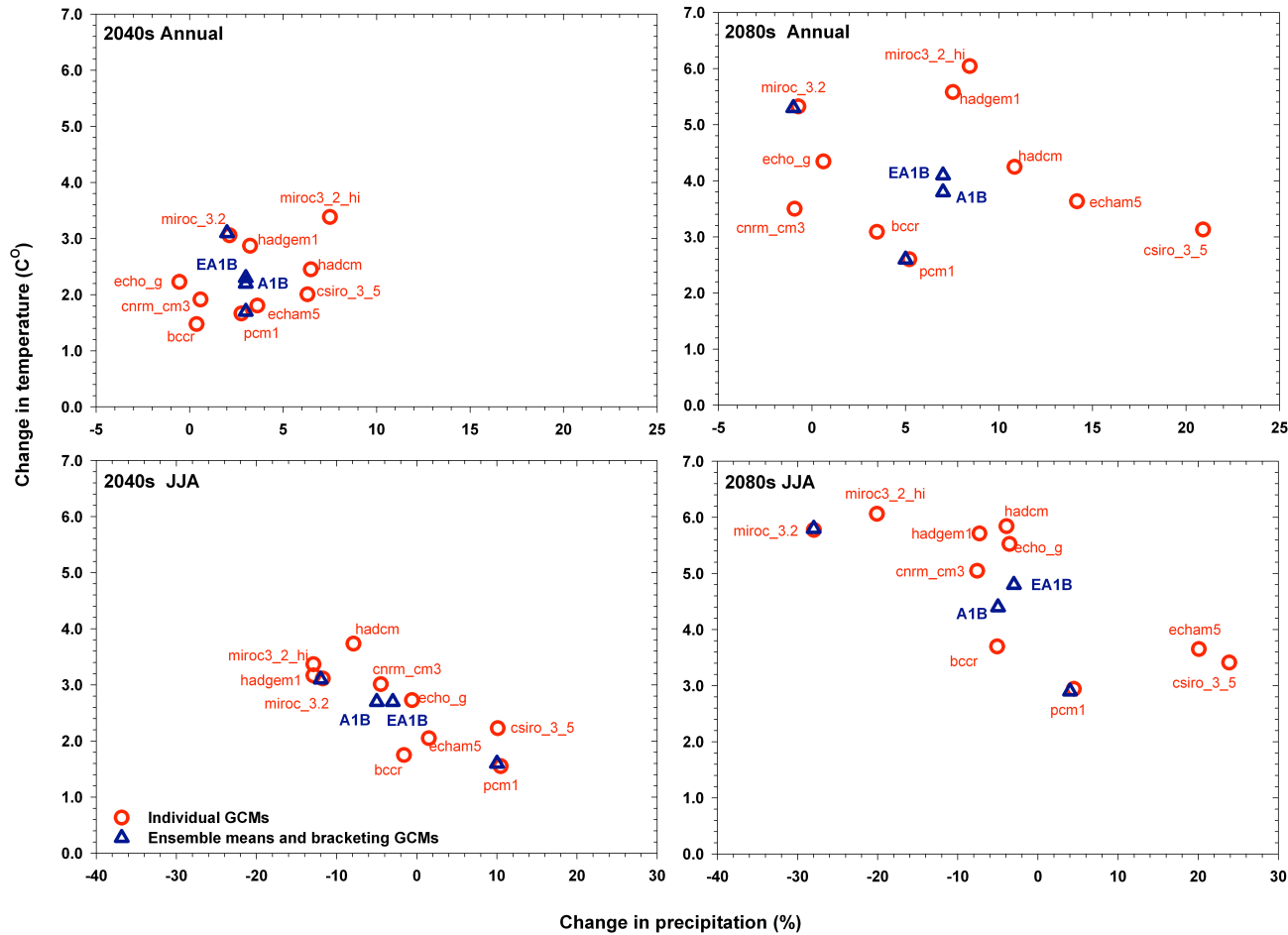


Figure 2.24. Scatterplots of Upper Missouri Basin / Northern Rockies deltas for GCMs used in the Ensemble A1B and comparison with full A1B mean. Deltas are annual (top) and summer (JJA, bottom) for the 2040s (left) and 2080s (right). Blue triangles indicate Ensemble means (EA1B = Ensemble A1B of 10GCMs selected based on rankings in section 4; A1B = ensemble of 19 AR4 GCMs described in sections 2 and 3) and bracketing scenarios selected for the Upper Missouri Basin (GCMs PCM1 and MIROC 3.2).

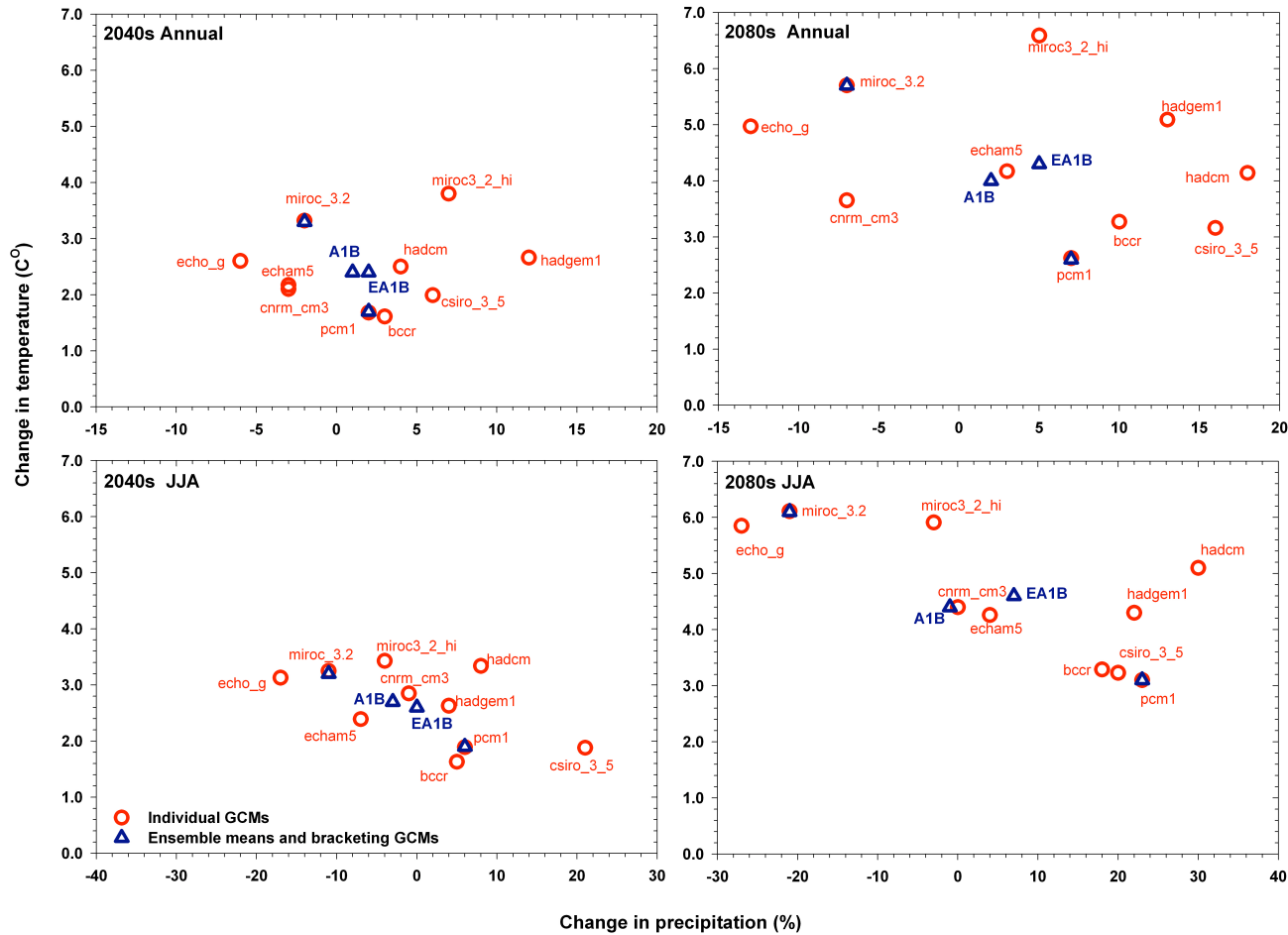


Figure 2.25. Scatterplots of Upper Colorado Basin / Central Rockies deltas for GCMs used in the Ensemble A1B and comparison with full A1B mean. Deltas are annual (top) and summer (JJA, bottom) for the 2040s (left) and 2080s (right). Blue triangles indicate Ensemble means (EA1B = Ensemble A1B of 10GCMs selected based on rankings in section 4; A1B = ensemble of 19 AR4 GCMs described in sections 2 and 3) and bracketing scenarios selected for the Upper Missouri Basin (GCMs PCM1 and MIROC 3.2).

Table 2.5. Columbia River Basin / Pacific Northwest seasonal and annual deltas for A1B (19 models) and EA1B (10 models) ensembles and bracketing scenarios for the MIROC 3.2 and PCM1 GCMs.

	Temperature (C)				Precipitation (%)					
	Months	A1B all models mean	EA1B Ensemble A1B mean	MIROC 3.2	PCM1	Months	A1B all models mean	EA1B Ensemble A1B mean	MIROC 3.2	PCM1
2040s	DJF	1.9	1.8	2.7	2.0	DJF	5	4	6	-8
	MAM	1.7	1.7	3.0	1.3	MAM	5	4	1	10
	JJA	2.6	2.7	2.8	1.9	JJA	-13	-10	-8	-3
	SON	2.0	2.2	2.4	2.0	SON	2	3	17	-6
	ONDJFM	1.8	1.8	2.5	1.8	ONDJFM	7	7	14	-1
	AMJJAS	2.3	2.4	2.9	1.8	AMJJAS	-7	-7	-6	-2
	ANNUAL	2.1	2.1	2.7	1.8	ANNUAL	0	0	4	-2
2080s	DJF	3.4	3.4	4.6	3.2	DJF	9	9	9	9
	MAM	3.0	3.2	4.8	2.0	MAM	8	5	9	5
	JJA	4.3	4.9	4.9	3.3	JJA	-16	-15	-30	-19
	SON	3.4	3.9	4.3	2.4	SON	8	9	14	-13
	ONDJFM	3.2	3.4	4.3	2.5	ONDJFM	12	12	16	4
	AMJJAS	3.8	4.3	5.0	3.0	AMJJAS	-7	-8	-15	-13
	ANNUAL	3.5	3.8	4.6	2.7	ANNUAL	2	2	0	-5

Table 2.6. Upper Missouri / Northern Rockies seasonal and annual deltas for A1B (19 models) and EA1B (10 models) ensembles and bracketing scenarios for the MIROC 3.2 and PCM1 GCMs.

	Temperature (C)				Precipitation (%)					
	Months	A1B all models mean	EA1B Ensemble A1B mean	MIROC 3.2	PCM1	Months	A1B all models mean	EA1B Ensemble A1B mean	MIROC 3.2	PCM1
2040s	DJF	2.1	2.0	3.0	1.9	DJF	7	7	7	-8
	MAM	2.0	2.0	3.1	1.1	MAM	7	7	9	10
	JJA	2.7	2.7	3.1	1.6	JJA	-5	-3	-12	10
	SON	2.2	2.5	3.0	2.1	SON	2	2	4	-1
	ONDJFM	2.1	2.1	2.9	1.8	ONDJFM	7	6	8	-3
	AMJJAS	2.4	2.5	3.2	1.6	AMJJAS	-1	0	-4	8
	ANNUAL	2.2	2.3	3.1	1.7	ANNUAL	3	3	2	3
2080s	DJF	3.7	3.9	5.0	3.0	DJF	13	13	14	6
	MAM	3.3	3.7	5.3	1.9	MAM	13	11	11	12
	JJA	4.4	4.8	5.8	2.9	JJA	-5	-3	-28	4
	SON	3.8	4.3	5.2	2.5	SON	6	6	0	-1
	ONDJFM	3.6	3.9	4.9	2.4	ONDJFM	12	13	14	6
	AMJJAS	4.0	4.4	5.7	2.8	AMJJAS	1	1	-16	5
	ANNUAL	3.8	4.1	5.3	2.6	ANNUAL	7	7	-1	5

Table 2.7. Upper Colorado/ Central Rockies seasonal and annual deltas for A1B (19 models) and EA1B (10 models) ensembles and bracketing scenarios for the MIROC 3.2 and PCM1 GCMs.

		Temperature (C)				Precipitation (%)				
	Months	A1B all models mean	EA1B Ensemble A1B mean	MIROC 3.2	PCM1	Months	A1B all models mean	EA1B Ensemble A1B mean	MIROC 3.2	PCM1
2040s	DJF	2.2	2.2	3.2	1.7	DJF	6	8	-1	-9
	MAM	2.3	2.4	3.8	1.3	MAM	-3	-4	-1	3
	JJA	2.7	2.6	3.2	1.9	JJA	-3	0	-11	6
	SON	2.4	2.5	3.0	1.9	SON	3	5	7	9
	ONDJFM	2.2	2.3	3.2	1.6	ONDJFM	4	4	2	-1
	AMJJAS	2.6	2.6	3.4	1.8	AMJJAS	-3	0	-5	5
	ANNUAL	2.4	2.4	3.3	1.7	ANNUAL	1	2	-2	2
2080s	DJF	3.8	4.1	5.2	2.6	DJF	10	10	-4	0
	MAM	3.9	4.4	6.2	2.2	MAM	-6	-7	-9	3
	JJA	4.4	4.6	6.1	3.1	JJA	-1	7	-21	23
	SON	3.9	4.3	5.3	2.5	SON	6	9	6	1
	ONDJFM	3.8	4.1	5.4	2.2	ONDJFM	7	6	1	3
	AMJJAS	4.2	4.6	6.0	3.0	AMJJAS	-3	3	-15	11
	ANNUAL	4.0	4.3	5.7	2.6	ANNUAL	2	5	-7	7

3. Downscaling from regional projections to 6km projections: delta method and modified delta downscaling approaches

The so called “delta method” is conceptually very simple and has been widely applied in water planning studies, particularly in earlier studies (prior to about 2000) when GCM resolution was typically very coarse and the models were only capable of simulating regional-scale changes in T and P (e.g., Lettenmaier et al. 1999). Although some variations have been developed, a common application of the delta method applies monthly changes in temperature and precipitation from a GCM, calculated at the regional scale, to an observed set of station or gridded temperature and precipitation records that are the inputs to a hydrologic model. The meteorological variables from the GCM simulation are typically averaged over an historical period from a control simulation and a future period from a scenario simulation to estimate the changes. Mote and Salathé (2010), for example, compared simulations from twenty GCMs, averaged over the entire PNW, for a 30-year window centered on the 1980s (1970-1999) to three future 30-year windows centered on the 2020s (2010-2039), 2040s (2030-2059), and 2080s (2070-2099). A subsequent study of the Columbia River basin (see Hamlet et al. and Climate Impacts Group 2010, Columbia Basin Climate Change Scenarios Project) used the same gridded historical meteorological dataset described in Elsner et al. 2010. However, simulations from the 10 best performing GCMs (as opposed to all nineteen) were used to derive average projected changes in climate for the same 30-year time windows listed above, and Hamlet et al. and Climate Impacts Group 2010 performed multiple downscaling methods.

In this study, we performed hydrological simulations using a modified delta method approach for the Columbia, upper Missouri (east to -104 longitude), and upper Colorado watersheds (Figure 2.1). Similarly to the Hamlet et al. 2010 Columbia basin study, we developed ensemble projections for the 2040s and 2080s future time windows (same as above) using simulations from the 10 best performing GCMs for these basins (see section 2.6). However, instead of applying the *same* average projected change in temperature and precipitation to all model grid cells within the watershed, we calculated a unique projected monthly change for each model grid cell to reflect projected spatial patterns simulated by the GCMs. To distinguish this method from the traditional delta method, we herein call it the modified delta method. Changes in mean climate,

calculated for each calendar month, are applied at daily time scale for each 1/16th (~6km) degree grid cell, as follows:

For all grid cells in the domain:

$$P_{new} = P_{obs} * P_{fact} \quad (1)$$

Where P_{fact} is the ratio of the CGM simulated mean precipitation from the future time period relative to the historical period (1970-1999), for each grid cell in a simulated region, in this case, the upper Missouri and upper Colorado watersheds:

$$T_{new} = T_{obs} + T_{delta} \quad (2)$$

Where T_{delta} is the difference in the CGM simulated mean temperature from the future time period relative to the historic period, again for each VIC model grid cell.

Note that multiplicative perturbations are used for precipitation to avoid potential sign problems (i.e. the potential to calculate negative precipitation using an additive approach), and additive perturbations are used with T to avoid problems with T not being a relative scale (i.e. the centigrade scale is zero at the freezing point of water at standard pressure, not at absolute zero).

Many features of the original time series and spatial variability of the gridded observations are preserved by the delta method, and any bias in the mean in the GCM simulations is automatically removed during the process. Changes in the seasonality of temperature and precipitation are captured, as well as how the changes vary spatially. The only fine-scale temporal information comes from the observed dataset.

3.1 Advantages and Limitations of the Modified Delta Method

A key advantage of the modified delta method is that observed patterns of temporal variability from the gridded observations are preserved, and comparison between future scenarios and observations is straight-forward and easily interpreted. The time sequence of events matches the historical record in the gridded data sets, facilitating direct comparison between the observations

and future scenarios. For example, particular drought years in the historical record can be directly compared in the historic and future simulations. Another advantage of this form of delta method experiment is that it captures the change in future spatial variability of temperature and precipitation projected by the GCMs for selected future time windows. Bias from the GCMs temporal sequencing is not introduced; however, the spatial resolution of the GCM (which is different for different GCMs) may introduce some spatial bias since they cannot resolve finescale geographic features. This slightly modified version of the traditional delta method (where temporally averaged and spatially averaged changes are applied to an entire region) facilitates a direct comparison of different GCMs with different error characteristics, different patterns of spatial and temporal variability, etc. As an example in the PNW, which is strongly affected by the El Niño Southern Oscillation (ENSO), the ability of a particular GCM to simulate the variability of tropical sea surface temperatures (and the large-scale teleconnections to the PNW associated with these variations) is an important element of the time series behavior of the scenario. By discarding the temporal information from the GCM and forcing the behavior of T and P in the future scenario to match observed patterns associated with ENSO, the delta method facilitates the comparison of changes in T and P from GCMs with potentially very different performance in this regard.

One of the strengths of the modified delta method is also its key limitation, because, by design, no information about possibly altered temporal information is extracted from the GCM simulations. So, for example, while some monthly information about the regional-scale intensity of climatic extremes from the GCM simulation is captured by the delta method, no information from the GCM about potentially changing *interarrival time*, or *duration* of climatic extremes (e.g. droughts and floods) is captured by the delta method. Likewise, only changes in monthly means are captured, and other potential changes in the probability distributions of T and P are ignored. Thus a key limitation of the delta method is that potential changes in the temporal variability or time series behavior of T and P are not captured by the approach.

3.2 Applications of the Modified Delta Method

The delta method (traditional or modified) is often applied in the context of an easily interpreted sensitivity analysis, or when a few model runs are intended to capture the consensus of a suite of T and P changes from a group of climate model simulations. In applications where the time

series behavior of T and P is a key driver of outcomes (e.g. in the case of estimating drought statistics) and is not necessarily simulated well (or equally well) for different GCMs, the choice of the delta method may avoid these difficulties. In applications where a large number of realizations of variability for a consistent level of systematic change is desirable (e.g. for testing a water supply system for reliability), the delta method provides a very straight-forward framework for the analysis. Delta method experiments are also a good framework for sensitivity analysis of changes in flood and low flow risks associated with systematic warming and changes in mean monthly precipitation statistics (see for example Mantua et al. 2010).

3.3 Modified Delta Method Runs for the Columbia, Colorado and Upper Missouri Watersheds

For the Columbia, upper Missouri, and upper Colorado watersheds, we used 91 years of observed climate (1916-2006, see Deems and Hamlet 2010, Elsner et al. 2010 for details), to which a number of delta method perturbations can be applied. This can be accomplished either in an ensemble mode where the ensemble is calculated AFTER the delta method downscaling (i.e., one run per individual GCM), or in a consensus mode where the ensemble is calculated BEFORE the delta method downscaling (i.e. average changes in T and P from all GCMs encompassed in a single run). For this study, we performed the latter approach and provide six delta method runs that represent the consensus of changes in T and P for the 10 best climate models (discussed above) for two future time periods and the A1B emissions scenario. Figures 3.1 and 3.2 illustrate the spatial variability in 2040s temperature and precipitation that form the input into the hydrologic modeling below. We also provide delta method runs for two bracketing scenarios (miroc_3.2 A1B – warm, and pcm1 A1B – cool) for two of the future time periods (2030-2059 and 2070-2099) and A1B emissions scenario.

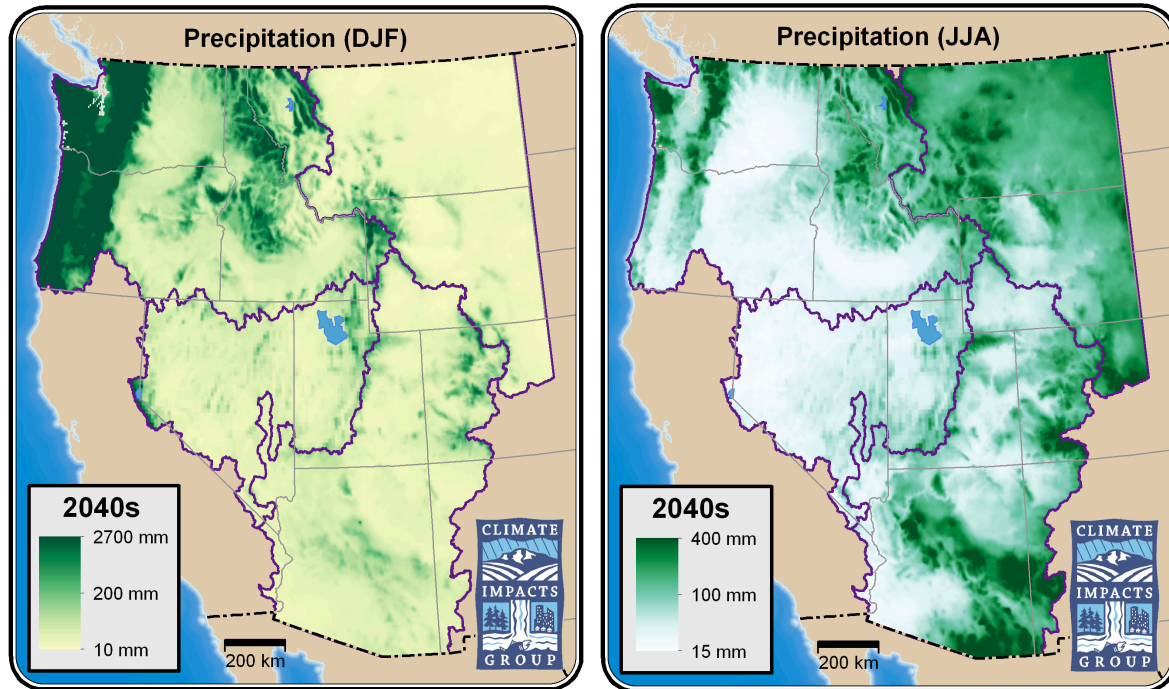


Figure 3.1. Downscaled 2040s total precipitation (DJF, left and JJA, right) for the full analysis domain. Ensemble of 10 GCMs, A1B emissions.

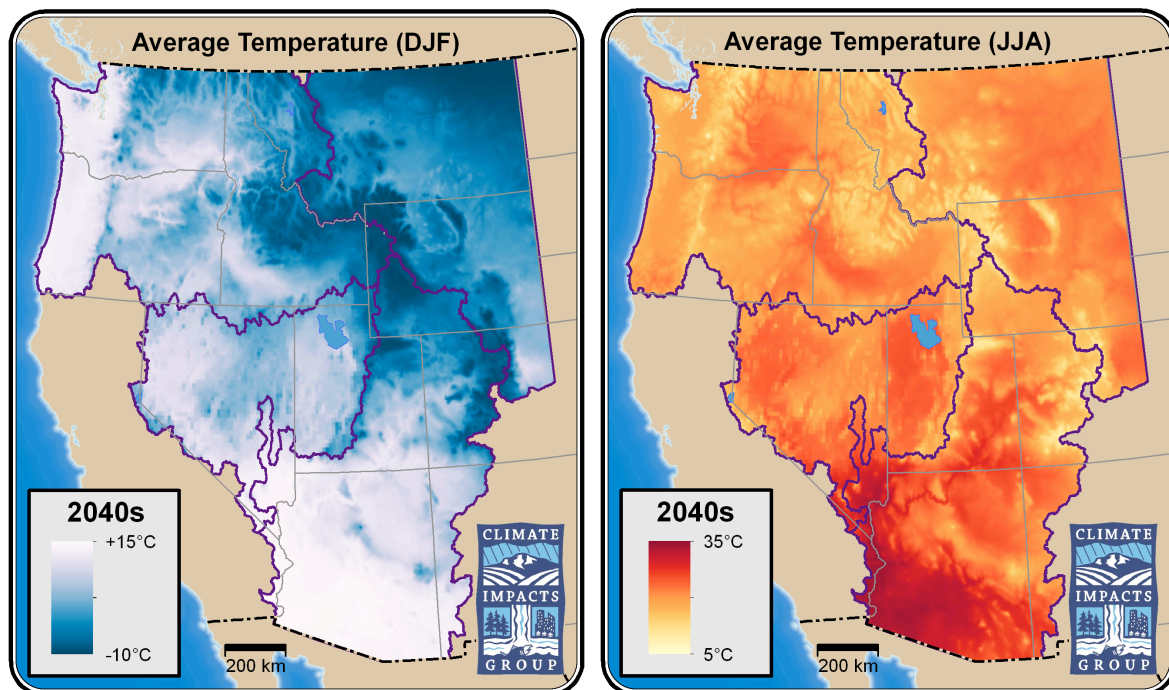


Figure 3.2. Downscaled 2040s average temperature (DJF, left and JJA, right) for the full analysis domain. Ensemble of 10 GCMs, A1B emissions.

4. Using modified delta method downscaled climate projections as inputs for hydrologic modeling in the Variable Infiltration Capacity model

This section parallels Elsner et al. 2010 extensively; the approaches outlined in that paper were followed nearly exactly in this work.

4.1 Primary Macro-Scale Hydrologic Products

The Variable Infiltration Capacity (VIC) macro-scale hydrologic model can be configured to archive a number of hydrologic variables that are produced at daily time step during the simulations. In the present study, specific output variables were selected to be consistent with previous studies in the Pacific Northwest (e.g., Elsner et al. 2010) and selected because of the usefulness of these hydrologic variables in past water planning and climate impacts case studies incorporating climate change. Appendix 1 Table 1.1 lists the variables that are archived in the present study, as well as notes regarding the definition of each variable, its units, and the method used for computing the monthly summary of each.

Results are archived for the historical as well as each of the 7 VIC runs for each basin (Historical 1916-2006; Ensemble A1B, Miroc 3.2, PCM1 2040s and 2080s). The raw VIC output is stored in a separate file for each grid cell. These raw daily output files are referred to as “flux” files and are available in the online directories described in Appendix 1. The meteorological input data for each simulation can also be made available. Each flux file contains one row for each day of the 92-year simulations (a total of 33,603 rows). The first 3 columns in each row record the date (year month day), while the following 21 columns record the value of each variable for that day, following the order provided in Appendix 1 Table 1.1. This raw output from VIC forms the basis for all of the products described below. Figures 4.1 through 4.5 show example maps of domain-wide climate and hydrologic variables that can be developed from the “wus” gridded data described in Appendix 1.

4.2 VIC model implementation

We applied the climate change projections from section 3 to generate hydrologic model simulations and to evaluate the impact of climate change on the hydrology of the basins of interest (Figure 2.1). We performed the hydrologic simulations using the VIC macroscale

hydrology model (Liang et al. 1994; Nijssen et al. 1997) at 1/16th degree latitude by longitude spatial resolution over the greater Columbia River watershed (approximately 5 by 6 km grid cells).

Studies of climate change impacts on regional hydrology are becoming increasingly common (Maurer 2007; Maurer and Duffy 2005; Hayhoe et al. 2007; Christensen and Lettenmaier 2007; Christensen et al. 2004; Payne et al. 2004; Van Rheezen et al. 2004; Miller et al. 2003; among others). Many of these studies use a scenario approach which evaluates projections of hydrological variables, like streamflow, using a hydrology model forced with downscaled ensembles of projected climate from global climate models (GCMs). These future climate simulations are then compared with a baseline hydrological simulation using historical climate (see e.g. Christensen and Lettenmaier 2007; Maurer 2007; Hayhoe et al. 2007; among others). This approach is sometimes termed “off-line” forcing of a hydrological model, because it does not directly represent feedbacks between the land surface and climate system. An alternative approach, based on regional climate models (see section 5), represents land atmosphere feedbacks; however, complications arise due to bias in the climate model simulations (see Wood et al. 2004 for a detailed discussion), and computational requirements that generally preclude the use of multi-model ensemble methods. For this reason, we used the off-line simulation approach.

The VIC model is a macroscale model, meaning it is intended for application to relatively large areas, typically ranging from 10,000 km² or so, up to continental and even global scales. A key underlying model assumption is that sub-grid scale variability (in vegetation, topography, soil properties, etc.) can be parameterized, rather than represented explicitly. The VIC model (Liang et al. 1994, 1996; Nijssen et al. 1997) has been used to assess the impact of climate change on U.S. hydrology in a number of previous studies. Hamlet and Lettenmaier (1999) studied the implications of GCM projections from the second IPCC assessment (1995) over the Columbia River watershed. Following the third IPCC Assessment Report (2001), Payne et al. (2004) studied climate change effects on the Columbia River, Christensen et al. (2004) studied effects on the Colorado River, and Van Rheezen et al. (2004) studied effects on California. Similarly, several recent studies involved implementation of the VIC model to analyze the effects of IPCC AR4 projections on hydrologic systems: Vicuna et al. (2007) and Maurer (2007) in California, Christensen and Lettenmaier (2007) on the Colorado River, and Hayhoe et al. (2007) on the

northeastern U.S. Most previous assessments have projected warmer temperatures leading to projections of reduced snowpack, and hence a transition from spring to winter runoff (Hamlet and Lettenmaier 1999; Payne et al. 2004). Other impacts common to previous studies of hydrological impacts of climate change in the PNW include earlier spring peak flow and lower summer flows.

4.2.1 *General VIC implementation*

Following Eslner et al. 2010, in this analysis, we increased the spatial resolution of the hydrological model over the PNW from 1/8th degree (used in all previous studies cited above) to 1/16th degree. An historical input data set including daily precipitation, maximum and minimum daily temperature, and windspeed was developed for this study at 1/16th degree spatial resolution and its unique features are described in Section 4.2.2.

Variables other than streamflow (e.g. simulated SWE or soil moisture) were not used to constrain model parameters, so the resulting projections are not calibrated. However, previous studies indicate that the model successfully simulates grid level processes. Mote et al. (2005) validated the sensitivity of the VIC snow model to changing temperature and precipitation in historical records, while Andreadis et al. (2009) compared VIC-simulated SWE with observations to show that the model captures observed snow accumulation and ablation reasonably well in varied forested terrain. Maurer et al. (2002) showed that VIC-simulated historical soil moisture was comparable to available observations. Hamlet and Lettenmaier (2007) showed that despite considerable bias in simulated absolute values, the persistent relationships between the mean annual flood and the extremes (e.g. 100-year flood) across a wide range of climatic conditions indicate the model's ability to capture the effects of observed changes in climate. In addition to increasing the VIC model resolution for this study, the number of GCMs from which the ensembles are formed was increased substantially relative to previous studies. We also adapted the model to allow output of potential evapotranspiration (PET) for each model grid cell. PET is the amount of water that would be transpired by vegetation, provided unlimited water supply, and is often used as a reference value of land surface water stress in characterizations of climate interactions with forest processes (e.g., Littell et al. 2010). PET is calculated in the VIC model using the Penman–Montieth approach (Liang et al. 1996) and the user may choose to output

PET of natural vegetation, open water PET, as well as PET of certain reference

4.2.2 *Development of historical gridded climate forcing for VIC*

VIC requires as forcing variables precipitation (Prcp) and temperature at a sub-daily time step, as well as downward solar and longwave radiation, surface wind, and vapor pressure deficit. All simulations described in this paper are based on a 1/16th degree spatial resolution data set of daily historical Prcp and daily temperature maxima and minima (Tmax, Tmin) developed from observations following methods described in Maurer et al. (2002) and Hamlet and Lettenmaier (2005), adapted as described below. Forcing variables other than daily precipitation and temperature maxima and minima are derived from the daily temperature range or mean temperature following methods outlined in Maurer et al. (2002). One exception is surface wind. Daily wind speed values for 1949–2006 were downscaled from National Centers for Environmental Prediction-National Center for Atmospheric Research (NCEP-NCAR) reanalysis products (Kalanay et al. 1996). For years prior to 1949, daily wind speed climatology was derived from the 1949–2006 reanalysis. We used the National Climatic Data Center Cooperative Observer (Co-Op) network and Environment Canada (EC) daily station data as the primary sources for precipitation and temperature values. We used a method described by Hamlet and Lettenmaier (2005) that corrects for temporal inhomogeneities in the raw gridded data using a set of temporally consistent and quality controlled index stations from the US Historical Climatology Network (HCN) and the Adjusted Historical Canadian Climate Database (AHCCD) data. This approach assures that no spurious trends are introduced into the gridded historical data as a result of inclusion of stations with records shorter than the length of the gridded data set. The data are adjusted for orographic effects using the PRISM (Daly et al. 1994, 2002) climatology (1971–2001) following methods outlined in Maurer et al. (2002).

Daily station data from 1915 to 2006 were processed as in Hamlet and Lettenmaier (2005), but using only Co-Op, EC, HCN, and AHCCD stations within a 100 km buffer of the domain. Quality control flags included in the raw Co-Op data set for each recorded value were used to ensure accuracy and to temporally redistribute “accumulated” Prcp values. We used the Symap algorithm (Shepard 1984; as per Maurer et al. 2002) to interpolate Co-Op/EC station data to a 1/16th degree. We then adjusted the daily Prcp, Tmax, and Tmin values for topographic influences by scaling the monthly means to match the monthly PRISM climate normals from

1970–2000. In the temperature rescaling method used for this study, Tmax and Tmin were adjusted by the same amount to avoid introducing a bias into daily mean temperatures and the daily temperature range. First, the average of the Tmax and Tmin values were computed for each of the monthly PRISM and monthly mean Co-Op time series. The difference between these values was applied as an offset to the average of the daily Tmax and Tmin in the appropriate month, thereby explicitly preserving the daily temperature range. For days where Tmin exceeds Tmax due to interpolation errors in the initial regridding step, we offset the average of these inverted Tmax and Tmin values and applied a climatological daily range from PRISM Tmax and Tmin.

The historical datasets developed for this study extend from January 1915 to December 2006. Results from historical simulations presented in this study and the period to which projected hydrologic scenarios are compared extend from October 1916 to September 2006 (water years 1917 to 2006) to allow for sufficient hydrologic model spinup.

4.3 Projections of future hydrologic conditions

The VIC model gridded outputs were summarized into monthly and seasonal variables to calculate projected hydrologic changes for the Columbia, Missouri, and Colorado basins (Tables 4.1 and 4.2, Figures 4.1 – 4.4). Based on ensemble means and bracketing models, by the 2040s, April 1 SWE is projected to decline ~22 -35% in the Columbia Basin, ~ 18 – 33% in the Missouri Basin, and 25 to 46% in the Colorado Basin (Table 4.1).

Table 4.1. 2040s changes (compared to 1916-2006) in selected seasonal snow water equivalent, potential evapotranspiration, actual evapotranspiration, soil moisture, and combined flow (runoff + baseflow) for the Columbia, Missouri, and Colorado Basins.

	Columbia			2040s Missouri			Colorado		
	PCM1	Ensemble A1B	Miroc 3.2	PCM1	Ensemble A1B	Miroc 3.2	PCM1	Ensemble A1B	Miroc 3.2
APR 1 SWE (%)	-35.1	-21.8	-26.0	-29.9	-18.1	-33.5	-25.3	-27.6	-46.0
DJF_AET (%)	8.1	7.4	11.8	-0.8	-0.3	-0.9	9.4	16.0	14.9
DJF_PET1 (%)	29.0	22.8	36.0	23.8	29.5	50.1	11.5	19.0	32.0
JJA_AET (%)	-1.1	0.4	1.9	7.7	-0.7	-5.6	4.6	-4.6	-14.6
JJA_PET1 (%)	5.3	8.0	7.6	2.6	6.1	7.2	0.5	0.7	0.6
MAM_AET (%)	9.6	12.4	22.3	7.1	10.1	13.2	8.5	8.4	2.8
MAM_PET1 (%)	9.7	12.2	21.3	8.2	13.3	19.7	7.2	12.3	17.3
SON_AET (%)	-1.5	-0.1	0.5	10.6	5.0	-1.2	18.9	16.5	11.3
SON_PET1 (%)	14.2	15.1	14.9	12.4	16.5	21.2	6.2	9.1	11.3
JUL 1 SM (%ile)	37.1	36.5	41.1	57.1	41.1	35.9	45.1	37.8	21.8
DJF_C.FLOW (%)	9.1	19.6	45.3	14.4	23.1	40.2	15.2	22.2	-1.3
MAM_C.FLOW (%)	0.7	8.9	14.5	6.2	15.4	19.5	2.0	1.3	-7.8
JJA_C.FLOW (%)	-26.5	-23.2	-26.2	-11.0	-25.8	-38.2	-11.8	-29.6	-41.7
SON_C.FLOW (%)	-3.4	7.4	42.0	0.0	-2.2	-5.9	15.3	7.9	-1.9

Table 4.2. 2080s changes (compared to 1916-2006) in selected seasonal snow water equivalent, potential evapotranspiration, actual evapotranspiration, soil moisture, and combined flow (runoff + baseflow) for the Columbia, Missouri, and Colorado Basins.

	Columbia			2080s Missouri			Colorado		
	PCM1	Ensemble A1B	Miroc 3.2	PCM1	Ensemble A1B	Miroc 3.2	PCM1	Ensemble A1B	Miroc 3.2
APR 1 SWE (%)	-42.4	-42.1	-45.6	-28.5	-39.9	-58.4	-27.8	-51.0	-70.9
DJF_AET (%)	15.2	16.0	22.4	1.0	1.2	0.6	15.7	29.5	21.2
DJF_PET1 (%)	47.5	48.2	67.8	44.6	68.3	100.9	21.3	37.3	54.7
JJA_AET (%)	-3.0	-0.9	-2.0	4.2	-1.6	-17.0	8.7	-5.9	-29.8
JJA_PET1 (%)	9.7	13.2	12.6	6.1	10.0	11.7	0.2	0.0	-2.4
MAM_AET (%)	14.2	23.1	36.0	13.4	18.8	18.5	11.2	12.7	-0.8
MAM_PET1 (%)	14.4	22.2	32.9	13.8	24.2	34.5	12.5	20.9	27.6
SON_AET (%)	-6.7	1.5	-2.5	7.0	9.7	-6.8	20.2	29.2	5.1
SON_PET1 (%)	18.5	24.8	29.2	17.6	28.0	37.5	9.3	14.9	19.1
JUL 1 SM (%ile)	29.1	28.7	34.2	47.2	34.6	22.4	42.4	30.0	9.1
DJF_C.FLOW (%)	19.7	39.7	7.3	35.0	64.5	91.3	26.5	37.7	67.5
MAM_C.FLOW (%)	1.8	9.8	16.4	14.2	20.6	13.9	4.6	-4.5	-26.0
JJA_C.FLOW (%)	-34.7	-39.3	-44.9	-24.6	-40.2	-55.9	-10.6	-41.8	-59.7
SON_C.FLOW (%)	-16.4	13.4	39.5	-3.1	1.0	-12.3	7.0	12.7	-13.8

By the 2080s, basin average April 1 SWE is projected to decline ~42 -46% in the Columbia Basin, ~ 29 – 58% in the Missouri Basin, and 28 to 71% in the Colorado Basin (Table 4.2). However, some locations have small projected increases in April 1 SWE, and the basin average change does not apply equally to all places in the basins – there is significant spatial variability in the nature of change in April 1 SWE depending on location (Figure 4.1). Particularly in the high Cascades, Greater Yellowstone area, and some of the high southern Rockies, smaller changes in SWE are projected.

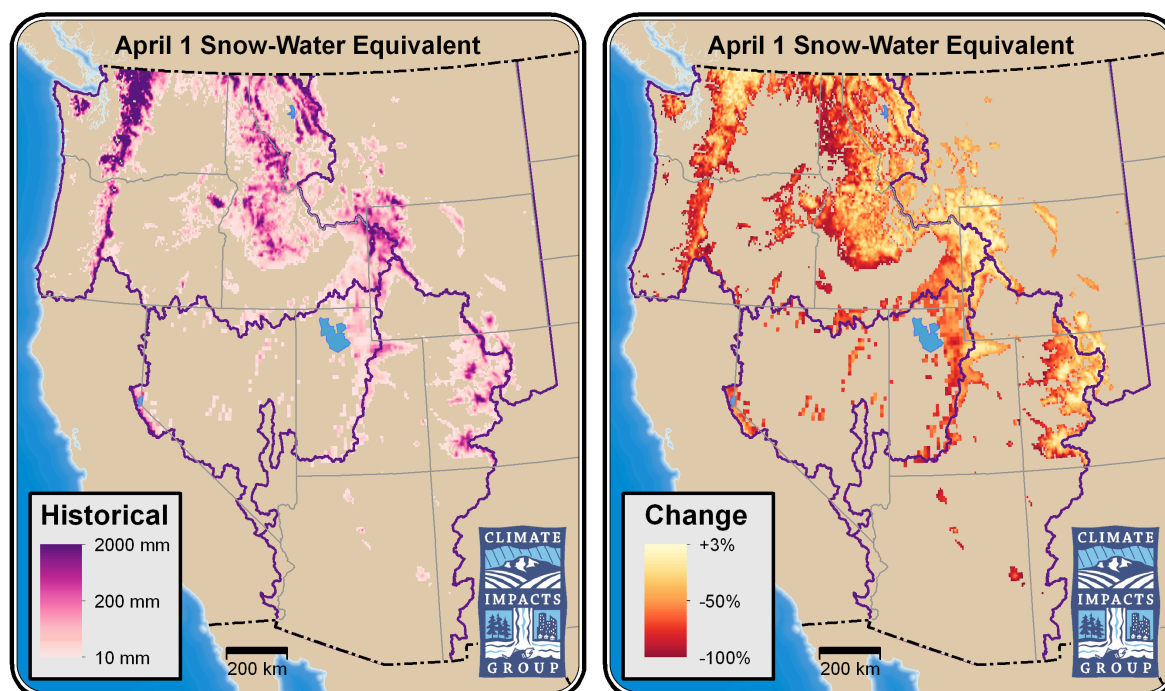


Figure 4.1. Snow water equivalent (SWE, April 1 historical, left and April 1 percent change 2040s) for the full analysis domain.

Potential evapotranspiration increases in all seasons in all basins except in the Colorado Basin in summer in the 2080s; the largest increases are in DJF (from 12% to over 100% increase depending on basin and time frame), but increases in all seasons are noteworthy (Tables 4.1 and 4.2). The percent increases in PET are largest in mountainous and historically wetter regions, and there is an important decline in PET in the lower Colorado River basin that contrasts with the higher elevations, bringing the basin average change close to zero when two very different responses appear to be occurring (Figure 4.2).

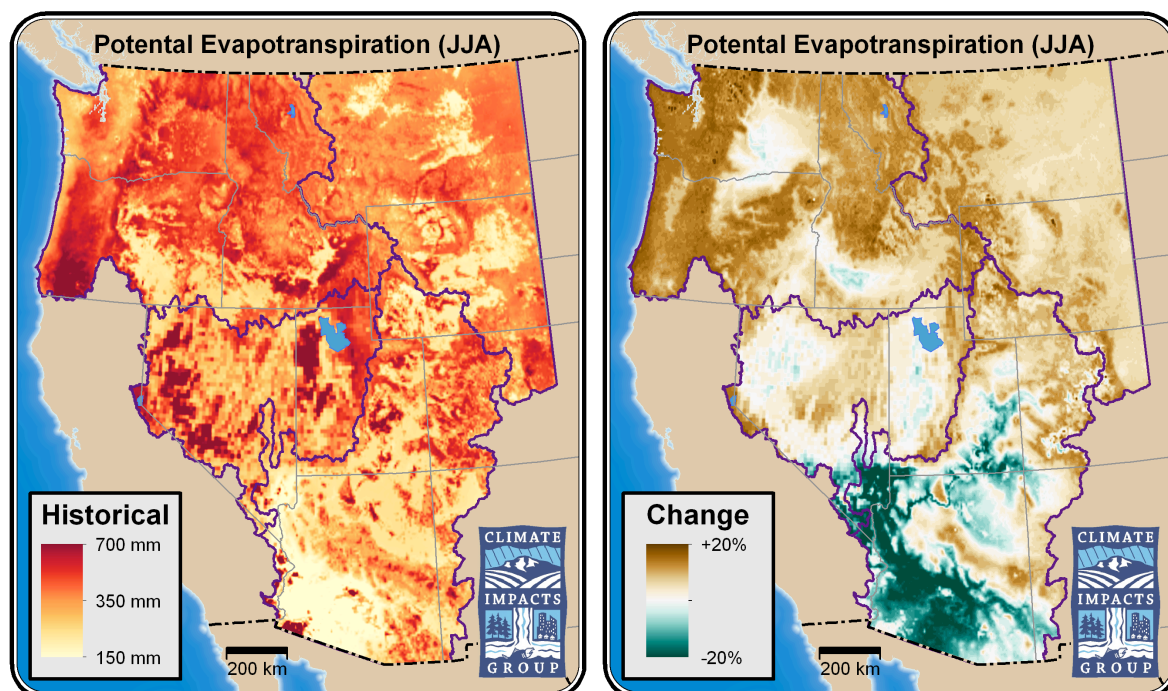


Figure 4.2. Total potential evapotranspiration (JJA historical, left and JJA, percent change in 2040s, right) for the full analysis domain.

Actual evapotranspiration responses are mixed, and probably reflect model disagreement on precipitation and regional differences in the timing and amount of projected precipitation change. July 1 soil moisture percentiles decline in all basins in all seasons except PCM1 in the Missouri Basin, which increases slightly.

The resulting relationship between PET and AET results in projected increases in water balance deficit ($PET - AET$) over much of the western US. Areas with higher historical deficit frequently increase the most (e.g., interior Columbia Basin, Snake River Plain, Great Basin increase by $> 150\text{mm}$, Figure 4.3).

July 1 soil moisture percentiles uniformly decrease except for small changes in the wetter PCM1 scenario for the Missouri Basin (Tables 4.1 and 4.2). Expressed as percent changes, decreases appear especially strong over mountainous areas and there are some small increases in more arid portions of the basins (Figure 4.4).

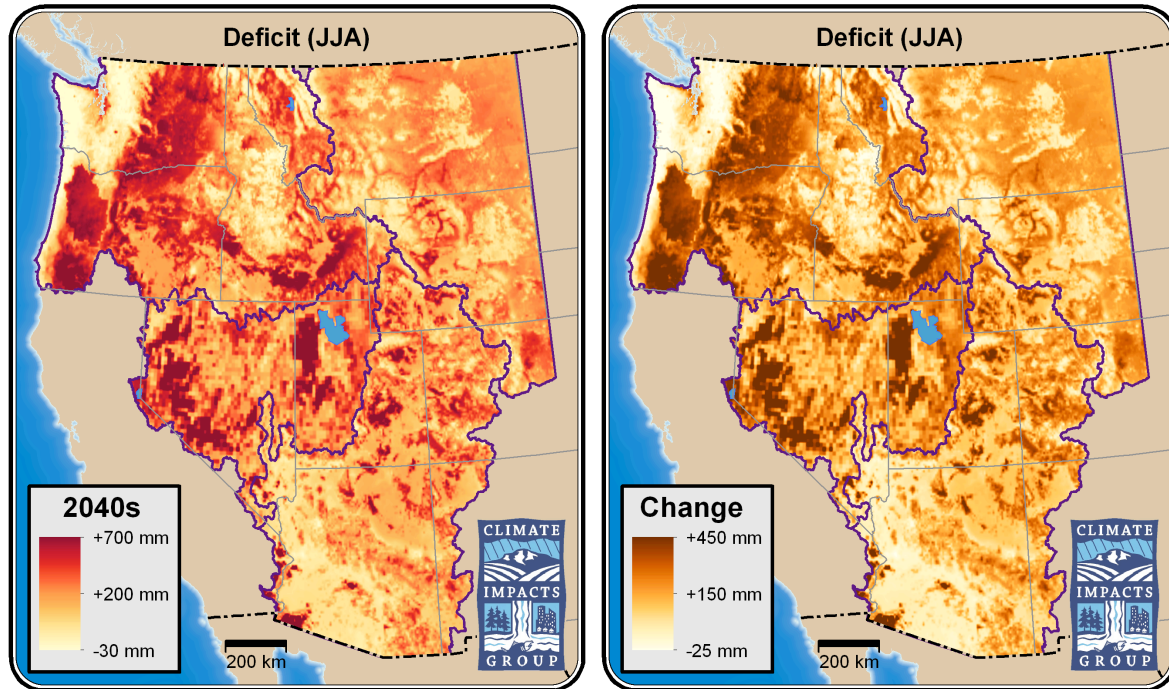


Figure 4.3. Total water balance deficit (JJA historical, left and JJA, change in 2040s) for the full analysis domain.

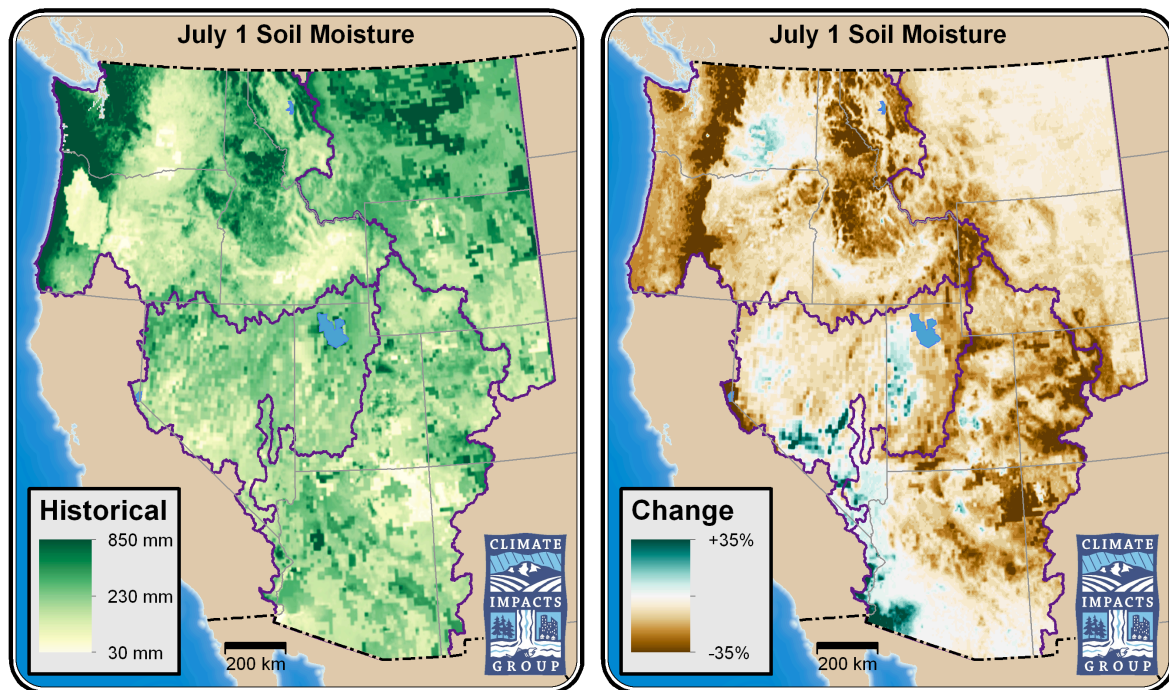


Figure 4.4. Total column soil moisture, (JJA, historical, left and JJA, percent change in 2040s) for the full analysis domain.

Mantua et al. (2010) calculated an index of snowpack vulnerability (April 1 SWE / ONDJFM Precipitation) that illustrates how much of the winter precipitation is entrained in spring snowpack. They defined “rain dominated” basins as those with < 10% of their winter precipitation entrained in April 1 snowpack, “transitional” or “transient” basins as those with between 10% and 40% of their winter precipitation entrained in April 1 snowpack, and “snow dominated” basins as those with greater than 40% of their winter precipitation entrained in snowpack. Shifts from transitional to rain dominated or from snow dominated to transitional can cause large changes in the timing and magnitude of seasonal hydrographs (Elsner et al. 2010) and water availability resulting from snowmelt. We developed snowpack vulnerability estimates at the HUC 5 level (Figure 4.5) from the VIC hydrologic output products. Historically snow dominated basins become transitional and transitional basins become rain dominated by the 2040s (Figure 4.5). Large declines appear to be concentrated in headwater systems (high North Cascades, Crown of the Continent, Greater Yellowstone, Uintas, Colorado Rockies) under the ensemble mean, with larger declines evident in the Miroc 3.2 scenario.

The resulting consequences for 2040s Ensemble A1B mean combined flow (runoff + baseflow) are similar for the Columbia, Missouri, and Colorado basins in winter (DJF: +20%, +23%, +22%, respectively) and summer (JJA: -23%, -26%, -30%, respectively). Spring (MAM) combined flow increases 9% in the Columbia, 15% in the Missouri, and 1.3% in the Colorado (Table 4.1). Autumn (SON) combined flow increases 7% in the Columbia and 8% in the Colorado, but declines 2% in the Missouri. The signs of these changes are similar for DJF, MAM and JJA in the bracketing models (except Miroc 3.2 in the Colorado, which projects -1.3% combined flow for DJF and -7.8 for MAM), but SON signs and magnitudes vary substantially. The sign of combined flow in DJF and JJA trends continue in the 2080s, with winter increases in the Columbia, Missouri, and Colorado basins (DJF: +40%, +65%, +38%, respectively) and summer decreases (JJA: -39%, -40%, -42%, respectively). Trends in MAM and SON are similar in sign and rate to the 2040s.

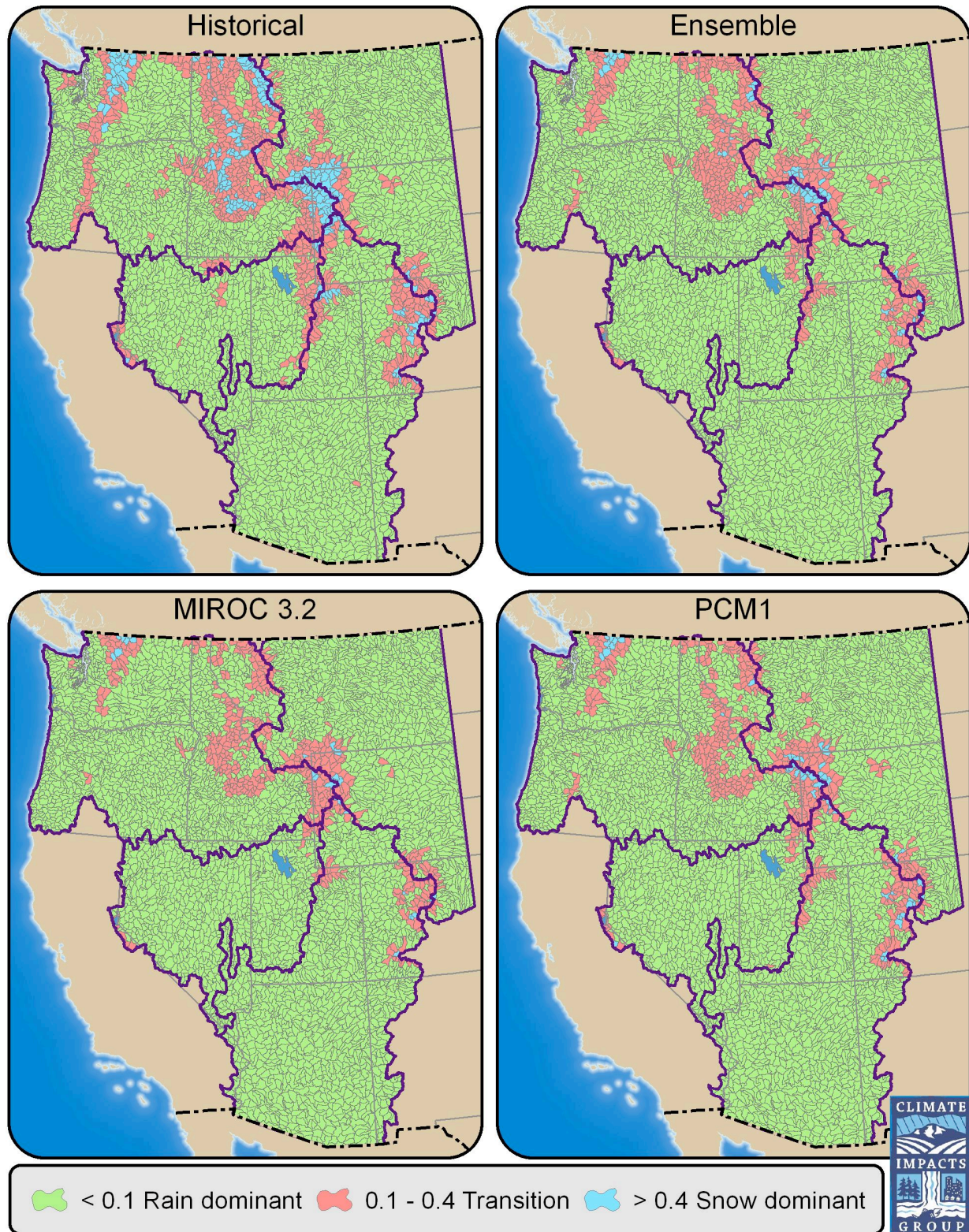


Figure 4.5. Ratio of April 1 SWE to cool season (ONDJFM) precipitation (historical, upper left, and ensemble, Miroc 3.2, and PCM1 2040s projections for the full analysis domain. Note the transition from snow dominated basins to transitional basins and from transitional basins to rain dominated basins in the Cascades, Northern Rockies, and Yellowstone areas but less so in the central Rockies.

5. Regional climate modeling

Regional climate models provide an alternative approach to downscaling GCM output. Statistical downscaling has advantages (processing speed, comparatively simple approach to climate) and disadvantages (difficulty in modeling local to sub-regional feedbacks, difficulty modeling fine-scale atmospheric and topographic interactions). Regional climate modeling, while more computationally intensive, has the potential to address the main disadvantages of statistical downscaling.

5.1 Regional climate modeling and models used in this study

The following is largely excerpted from Salathé et al. (2010) describing the rationale and basis for the study.

Global climate models do not have sufficient spatial resolution to represent the atmospheric and land surface processes that determine the unique regional climate of the Western US. Regional climate models explicitly simulate the interactions between the large-scale weather patterns simulated by a global model and the local terrain. We have performed two 100-year regional climate simulations using the Weather Research and Forecasting (WRF) model developed at the National Center for Atmospheric Research (NCAR). One simulation is forced by the NCAR Community Climate System Model version 3 (CCSM3) and the second is forced by a simulation of the Max Plank Institute, Hamburg, global model (ECHAM5). The mesoscale simulations produce regional changes in snow cover, cloudiness, and circulation patterns associated with interactions between the largescale climate change and the regional topography and land-water contrasts. These changes substantially alter the temperature and precipitation trends over the region relative to the global model result or statistical downscaling. To illustrate this effect, we analyze the changes from the current climate (1970–1999) to the mid twenty-first century (2030–2059). Changes in seasonal-mean temperature and precipitation are presented.

Global climate models do not account for the atmospheric processes that determine the unique spatially heterogeneous climatic features of the western U.S. For example, in Elsner et al. (2010) climate datasets with high spatial resolution (on a 0.0625° grid) are produced using a combination of global climate simulations and gridded observations by way of statistical downscaling methods (Mote and Salathé 2010). Statistical methods have been successfully employed in the Pacific Northwest (Salathé 2003, 2005; Widmann et al. 2003; Wood et al. 2004) and other regions (Giorgi and Mearns 1999). Statistical downscaling is based on fine-scale data derived using assumptions about how temperature and precipitation vary over complex terrain in order to interpolate the sparse station network (about 50-km or 31-mi spacing) to a 0.0625° grid. Information simulated by the coarse-resolution global models (with output on a 100-to-300 km or 62-to-124 mi grid) is then used to project the future climate. This approach represents the mean climate and local regimes quite well but does not take into account how the terrain influences individual weather systems. Mesoscale process involving land and water surface characteristics, such as orographic precipitation, convergence zones, snow-albedo feedbacks, and cold air drainage, are likely to respond to the changing large-scale climate (see, for example, Leung et al. 2004 and Salathé et al. 2008). Since mesoscale processes are not explicitly represented in global models and statistical downscaling, their role in determining regional climate change is not fully accounted for with these methods. The motivation for applying regional climate models, therefore, is to simulate these processes and to understand their role in regional climate change. In the typical regional climate modeling design, as used here, mesoscale processes do not feedback onto the global climate simulation, and large-scale features that depend on these feedbacks cannot be properly represented. However, many important feedbacks operate at the local scale, such as snow-albedo feedback, and these can substantially modify the regional climate projection.

A regional climate model is similar to a global climate model in that it simulates the physical processes in the climate system. Regional climate models cover a limited area of the globe and are run at much finer spatial resolution and can simulate the interactions between large-scale weather patterns and local terrain features not

resolved by global models. Global model output data are used to force the regional model at its boundaries and the regional model downscales the global model by producing fine-scale weather patterns consistent with the coarse-resolution features in the global model. The disadvantages of a regional climate model are that it is computationally expensive and cannot explicitly remove systematic differences (biases) between the global model and observations as statistical methods can. Thus, for many applications, some bias correction must be applied to the results, to remove the combined biases of the global and regional model. This approach is used in Rosenberg et al. (2010) using data from the WRF simulations presented here. Furthermore, due to the computational demands of regional models, there is a trade-off in using them for impacts studies between long simulations at high model resolution, to better simulate local effects, and a large ensemble of simulations using multiple regional and global models, to better represent the range of uncertainty. In this study, we have used only two regional simulations, but these have been performed for very long time periods and at relatively high resolution. While this approach limits our ability to understand the effects of inter-model differences, such effects are explored in Mote and Salathé (2010), Elsner et al. (2010), and Vano et al. (2010). As such, this paper complements the wider range of climate projections presented in those papers.

Salathé et al. (2010) reported results from two 100-year simulations with a regional climate model using two different global models to provide forcing at the boundaries. Both regional simulations use the Weather Research and Forecasting (WRF) model developed at the National Center for Atmospheric Research (NCAR). This model includes advanced representations of cloud microphysics and land-surface dynamics to simulate the complex interactions between atmospheric processes like precipitation and land surface characteristics such as snow cover and soil moisture. One simulation is forced by the NCAR Community Climate System Model version 3 (CCSM3) and will be referred to as CCSM3–WRF and the second is forced by a simulation of the Max Planck Institute, Hamburg, global model (ECHAM5), referred to as ECHAM5–WRF. The WRF model configuration is very similar for both simulations, with modifications described in Salathé et al. (2010). The ECHAM5–WRF simulation was performed on a 36-km grid while

the CCSM3–WRF simulation was on a 20-km grid. Thus, differences between the two simulations are primarily attributable to the forcing models and the grid spacing used. The ECHAM5–WRF grid encompasses the continental US while the CCSM3–WRF grid covers the western US. Here we present results for the western US, focusing on sub-regional results in the Columbia, Missouri, and Colorado basins. We base our analysis on differences in the regional simulations for the present climate, defined as the 30-year period 1970 to 1999, and the mid twenty-first century, the 30-year period 2030–2059.

5.2 Regional climate modeling: historical modeling

To establish whether the regional climate simulations can reproduce the observed climate of the Pacific Northwest, we compared the two simulations for the winter (December–January–February, DJF) and summer (June–July–August, JJA) to gridded observations averaged for the period 1970–1999, in a similar manner to Leung et al. (2003a, b). The gridded data consist of station observations interpolated to a 1/16-degree grid using an empirical model for the effects of terrain on temperature and precipitation (Daly et al. 1994; Elsner et al. 2010). Since the CCSM3 and ECHAM5 simulations are from free-running climate models, the observed temporal sequence (i.e. at daily to interannual time scales) is not reproduced. However, for averages over a period of 30 years, most natural and internal model variability should be removed and we expect any differences among the simulations and gridded observations to be the result of model deficiencies and, to some degree, differences in grid resolutions.

It is important to note that a regional model does not explicitly remove any bias in the forcing model, except where such bias is due to unresolved processes, and may introduce additional biases. This comparison, therefore, evaluates both the regional model and the global forcing model. Some uncertainty in the evaluation is introduced in using gridded observations as opposed to station observations since the gridding procedure interpolates between the sparse station network based on a simple terrain model for temperature and precipitation.

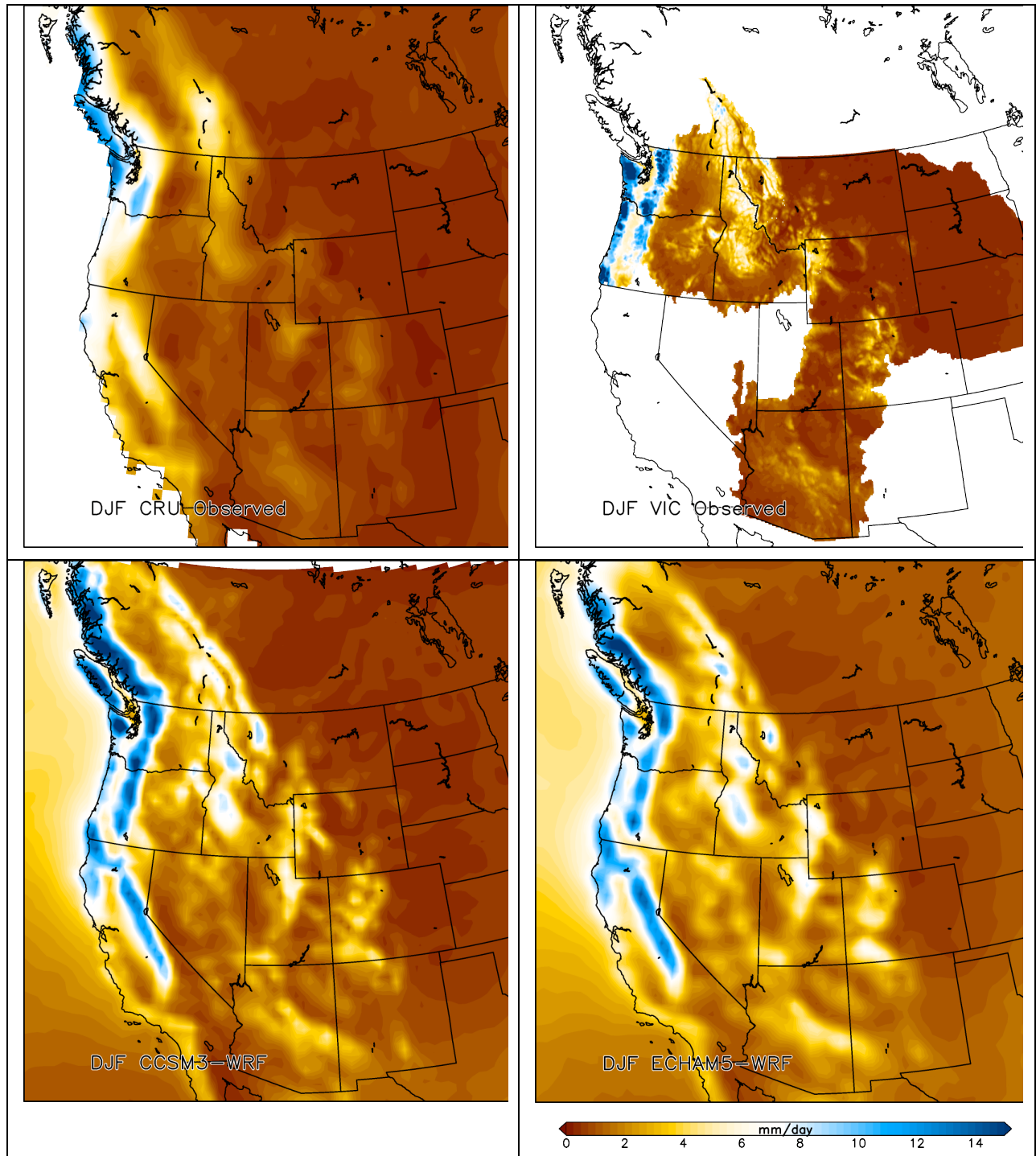


Figure 5.1. Seasonal mean precipitation (millimeters/day) in 1970–1999 for DJF from gridded CRU (top left), gridded VIC (top right), CCSM3–WRF (lower left), ECHAM5–WRF (lower right).

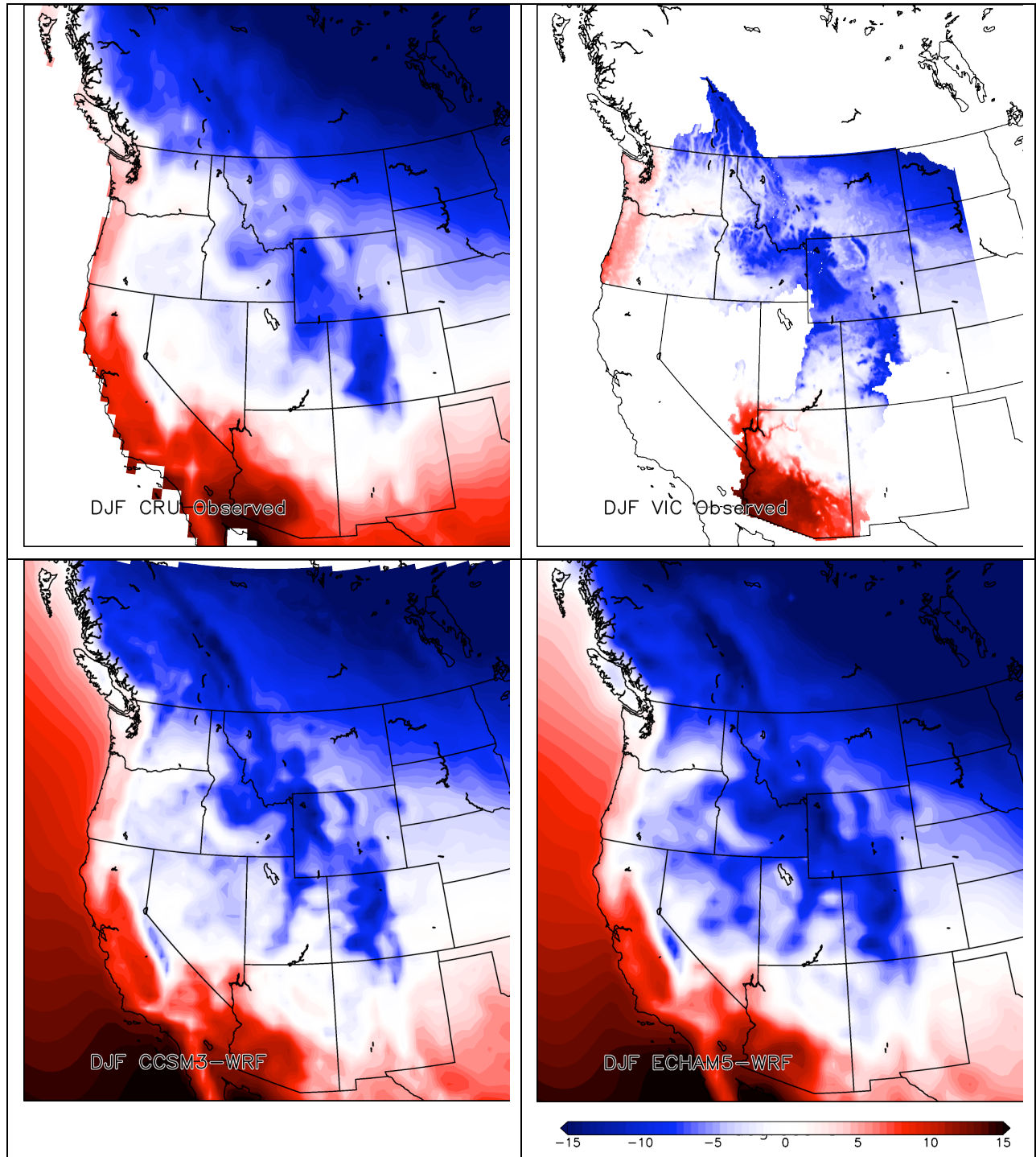


Figure 5.2. Seasonal mean temperature (in C) 1970–1999 for DJF from gridded CRU (top left), gridded VIC (top right), CCSM3–WRF (lower left), ECHAM5–WRF (lower right).

There is fairly good correspondence between observed (gridded CRU or gridded VIC model) winter precipitation and RCM modeled precipitation for both models (Figure 5.1), though RCM precipitation for both CCSM3 and ECHAM5 driven WRF runs appears to be about 30 cm higher than observed in the Sierra Nevada and some other mountainous regions of the west. Modeled temperature appears to be similar, with slight cool bias in the RCMs, particularly in the Sierra (Figure 5.2).

5.3 Regional climate modeling: future projections

Both the RCMs appear too wet (~3cm) in summer along the British Columbia coast, and CCSM3-WRF appears to be drier than observed over much of the west (Figure 5.3). The temperature fidelity appears similar to winter, with the cool and warm biases primarily centered over smaller mountain ranges or more isolated mountains (Figure 5.4).

Future changes in precipitation (Figure 5.5) and temperature (Figure 5.6) show considerably more spatial detail than would be evident in the individual GCMs used to constrain the WRF model. For example, the influence of sub-regional topography is evident in decreases in spring (MAM) precipitation in the higher elevations of the Cascades, Coast Ranges, and Sierra Nevada as well as the increases in autumn (SON) precipitation in the Pacific Northwest and inland Northwest (northern Idaho, western Montana). Sub-regional texture is also evident in temperature changes, particularly the greater warming expected in mountainous regions in winter (DJF) and spring (MAM) in the CCSM3-WRF model (Figure 5.6).

These results illustrate the potential of RCMs, but it is worth noting that some of the main uncertainties evident in the GCMs are necessarily translated to the RCM – only those uncertainties deriving from the GCMs inability to resolve more local features and feedbacks are mitigated, and thus the difference across GCMs is still a key source of variability in future projections. The ability to resolve sub-regional (and, eventually, landscape level) sensitivity to such feedbacks is a key feature of RCMs, and this represents one of the best places to advance research in interpreting global-to-regional climate change influences on resource dynamics.

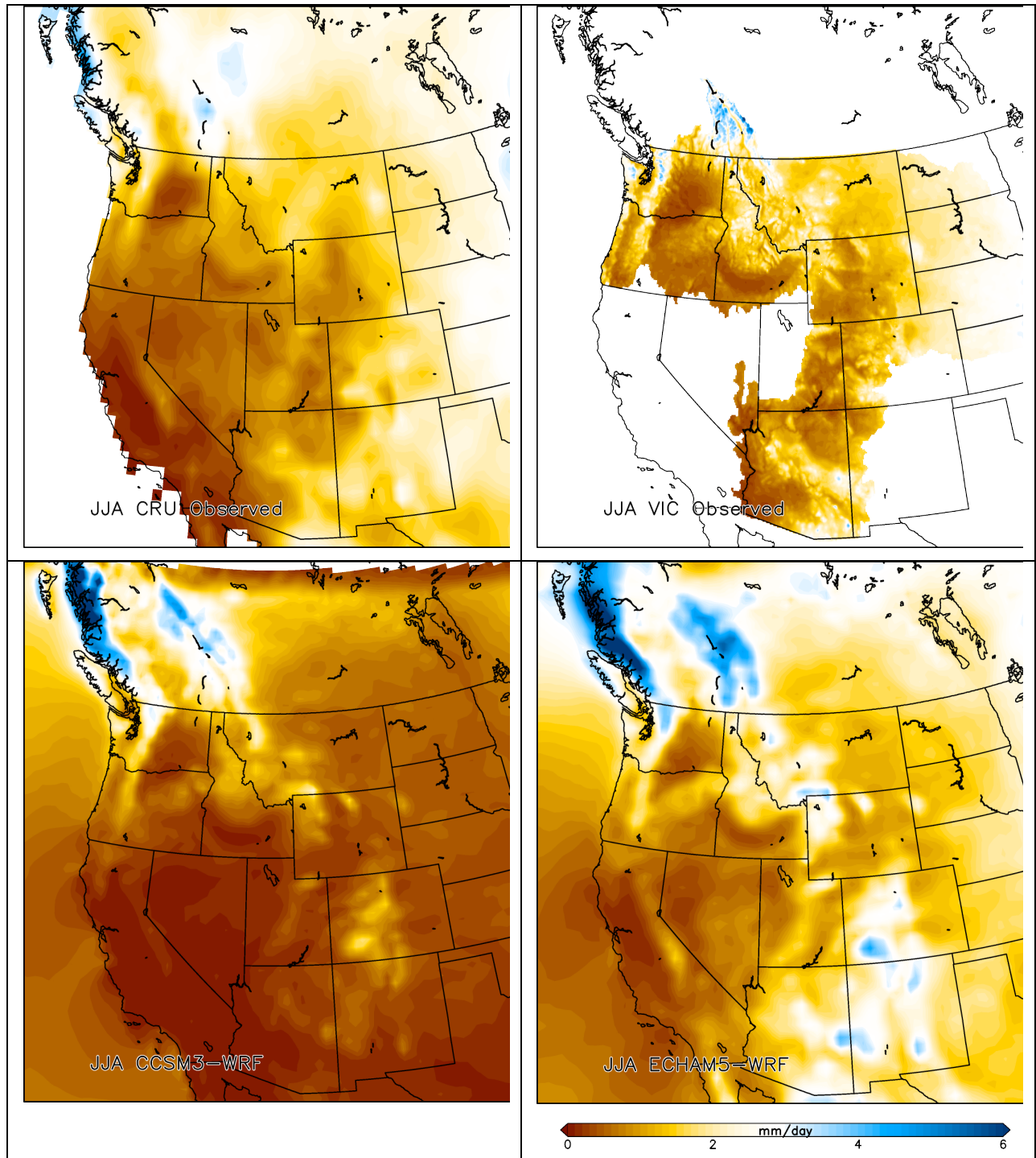


Figure 5.3. Seasonal mean precipitation (millimeters/day) in 1970–1999 for JJA from gridded CRU (top left), gridded VIC (top right), CCSM3–WRF (lower left), ECHAM5–WRF (lower right).

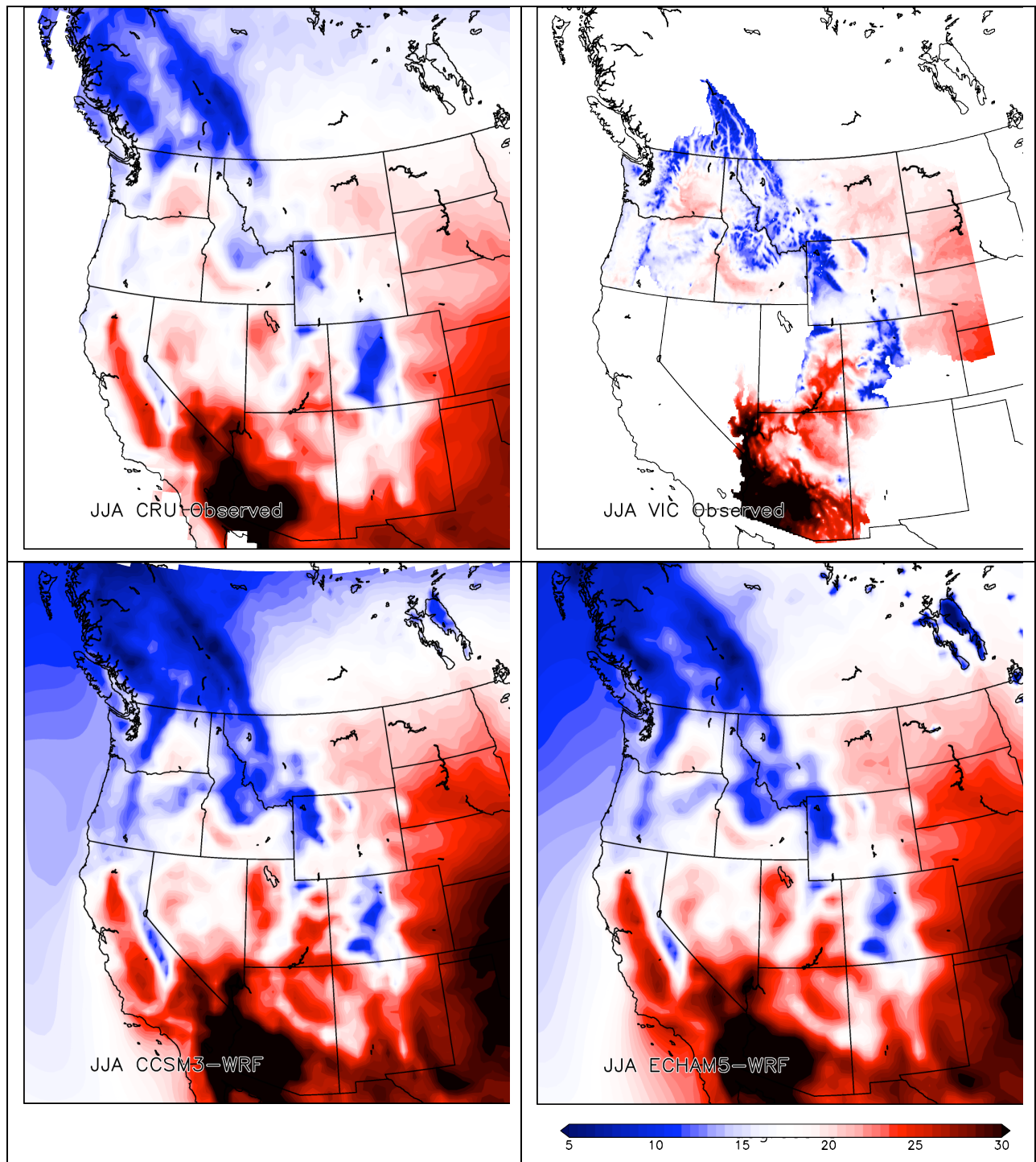


Figure 5.4. Seasonal mean temperature (in C) 1970–1999 for JJA from gridded CRU (top left), gridded VIC (top right), CCSM3–WRF (lower left), ECHAM5–WRF (lower right).

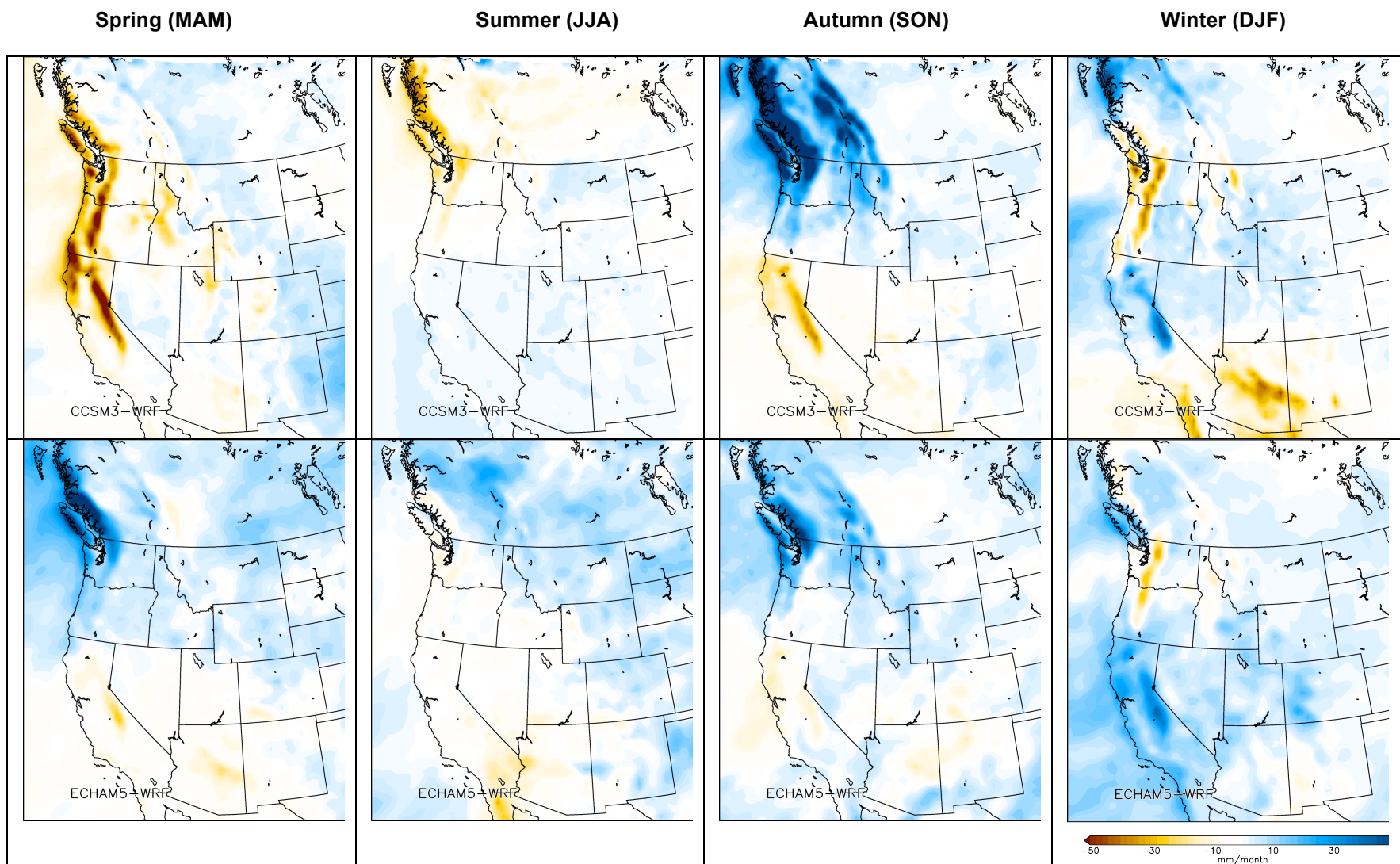


Figure 5.5. Change in precipitation (millimeters/month) from 1970–1999 to 2030–2059 for CCSM3–WRF (top row) and ECHAM5–WRF (bottom row) for the four seasons

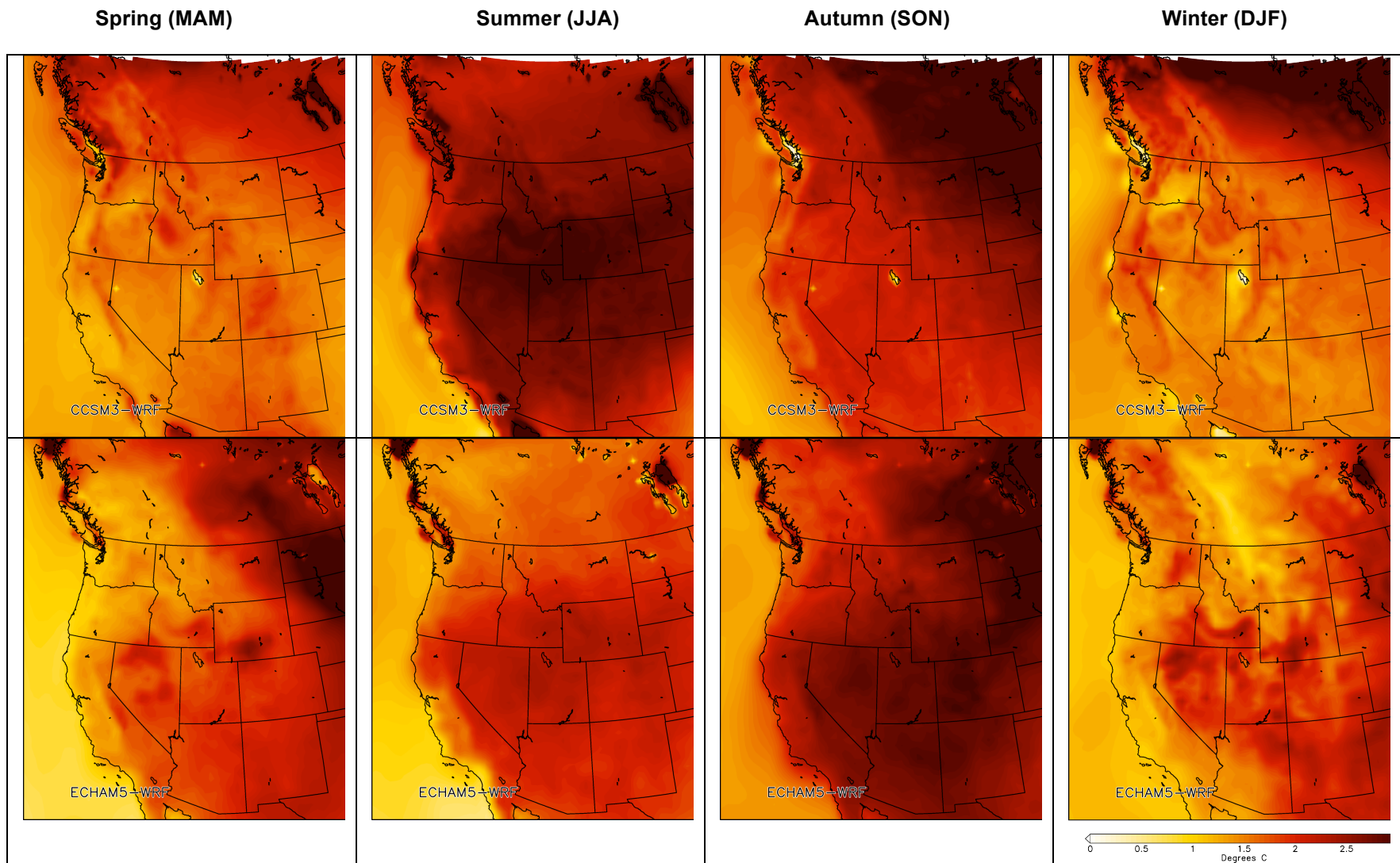


Figure 5.6. Change in temperature (C) from 1970–1999 to 2030–2059 for CCSM3–WRF (top row) and ECHAM5–WRF (bottom row) for the four seasons

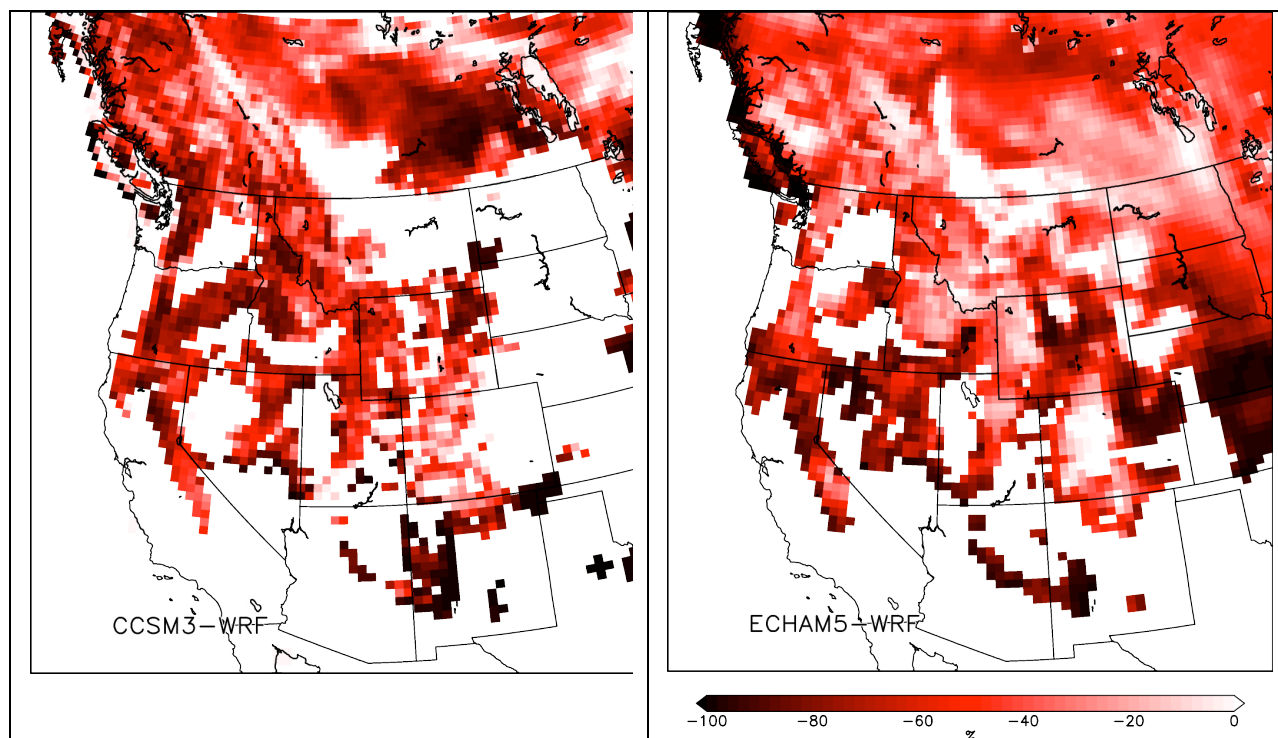


Figure 5.7. Percent change in April 1 SWE from 1970–1999 to 2030–2059 for CCSM3–WRF (left) and ECHAM5–WRF (right).

The RCM implementation described in Salathé et al. (2010) also includes April 1 snow water equivalent projections (Figure 5.7), which project declines larger for CCSM3-WRF than for ECHAM5-WRF, and which are spatially variable and roughly equivalent in magnitude to the changes projected in the hydrologic modeling section above.

The longitudinal and seasonal differences in temperature and precipitation in the RCM implementation and the GCMs illustrates one of the chief advantages in using the RCM approach, which is that the interactions between topography and weather that, over time, define the spatial expression of climate are modeled more explicitly. Figures 5.8 and 5.9 show comparisons of the precipitation and temperature (respectively) for GCMs and their RCM implementations against observed climate and known topography. Note the smoothly responding climate of the GCMs relative to topography and the improvement of the fit between observed and modeled climate in the RCM. However, it is also clear, particularly from the precipitation traces, that RCMs still do not necessarily capture the highly localized topography and its

influence on climate; below a certain scale, the model as implemented has trouble resolving the topographic features. Current work on refining the scale of WRF to 6km does exist, however, and that work might demonstrate improvement.

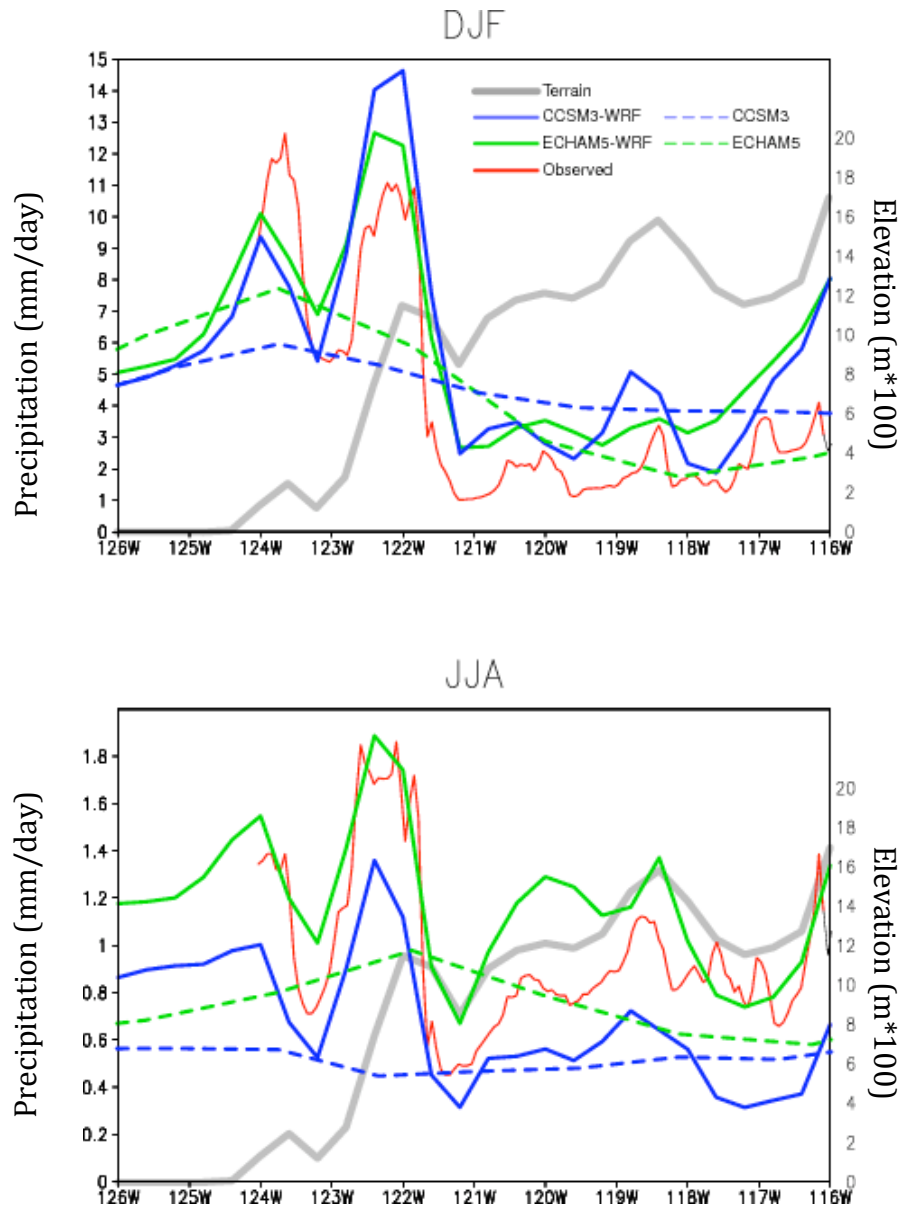


Figure 5.8. Historical precipitation for each winter (DJF, top) and summer (JJA, bottom) as simulated by the regional models and forcing global models along a West–East transect of at 47.8°N latitude. Terrain height is indicated by the thick grey line. The solid blue and green lines are for CCSM3-WRF and ECHAM5-WRF respectively, while the dashed blue and green lines are for CCSM3 and ECHAM5 GCMs.

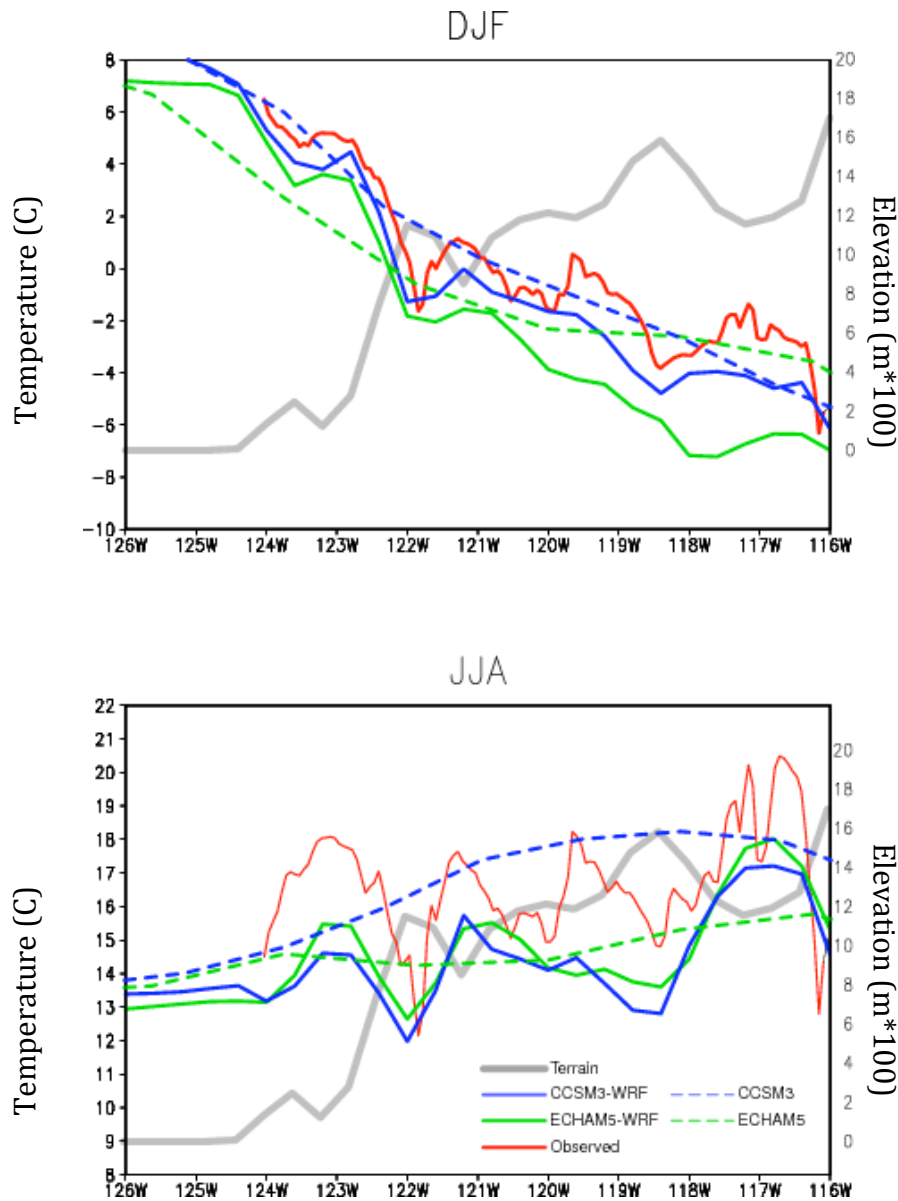


Figure 5.9. Historical temperature for each winter (DJF, top) and summer (JJA, bottom) as simulated by the regional models and forcing global models along a West–East transect of at 47.8°N latitude. Terrain height is indicated by the thick grey line. The solid blue and green lines are for CCSM3-WRF and ECHAM5-WRF respectively, while the dashed blue and green lines are for CCSM3 and ECHAM5 GCMs.

6. Acknowledgements

We acknowledge the modeling groups, the Program for Climate Model Diagnosis and Intercomparison (PCMDI) and the WCRP's Working Group on Coupled Modelling (WGCM) for their roles in making available the WCRP CMIP3 multi-model dataset. Support of this dataset is provided by the Office of Science, U.S. Department of Energy. We would also like to thank James Morrison, USFS Region 1, and Becky Kerns, USFS Region 6, for assistance with securing agency funding. We acknowledge Robert Norheim for producing all maps except those in the HCN and RCM sections.

7. References

- Climate Impacts Group. 2009. The Washington Climate Change Impacts Assessment: Evaluating Washington's Future in a Changing Climate. Executive Summary: Littell, J.S., M. McGuire Elsner, L.C. Whitely Binder, and A.K. Snover (eds). 2009. Available at: www.cses.washington.edu/db/pdf/wacciaexecsummary638.pdf
- Deems, J. and A. F. Hamlet. 2010. Historical Meteorological Driving Data Set. Online: http://www.hydro.washington.edu/2860/products/sites/r7climate/study_report/CBCCSP_chap3_metdata_draft_20091210.pdf
- Easterling, D. R., T. R. Karl, E.H. Mason, P. Y. Hughes, and D. P. Bowman. 1996. United States Historical Climatology Network (U.S. HCN) Monthly Temperature and Precipitation Data. ORNL/CDIAC-87, NDP-019/R3. Carbon Dioxide Information Analysis Center, Oak Ridge National Laboratory, U.S. Department of Energy, Oak Ridge, Tennessee.
- Elsner, M.M., L. Cuo, N. Voisin, J. Deems, A.F. Hamlet, J.A. Vano, K.E.B. Mickelson, S.Y. Lee, and D.P. Lettenmaier. 2010. Implications of 21st century climate change for the hydrology of Washington State. *Climatic Change* 102(1-2): 225-260, doi: 10.1007/s10584-010-9855-0.
- Hamlet, A.F., E.P. Salathé, and P. Carrasco. 2010. Statistical Downscaling Techniques for Global Climate Model Simulations of Temperature and Precipitation with Application to Water Resources Planning Studies. Online: http://www.hydro.washington.edu/2860/products/sites/r7climate/study_report/CBCCSP_chap4_gcm_draft_20100111.pdf
- Hamlet, A.F., et al. and Climate Impacts Group. 2010. Hydrologic Climate Change Scenarios for the Pacific Northwest Columbia River Basin and Coastal Drainages. Online: <http://www.hydro.washington.edu/2860/>
- Lettenmaier, D.P., Wood, A.W, Palmer, R.N., Wood, E.F. and E.Z. Stakhiv, 1999. Water resources implications of global warming: a U.S. regional perspective. *Climatic Change* vol. 43, no.3, November, 537-79

- Kalnay, E., M. Kanamitsu, R. Kistler, W. Collins, D. Deaven, L. Gandin, M. Iredell, S. Saha, G. White, J. Woollen, Y. Zhu, M. Chelliah, W. Ebisuzaki, W. Higgins, J. Janowiak, K. C. Mo, C. Ropelewski, J. Wang, A. Leetmaa, R. Reynolds, Roy Jenne, Dennis Joseph (1996). The NCEP/NCAR 40-Year Reanalysis Project. *Bulletin of the American Meteorological Society* 77 (3): 437–471.
- Littell, J.S., M. McGuire Elsner, L.C. Whitely Binder, A. Snover (eds). 2009. The Washington Climate Change Impacts Assessment: Evaluating Washington's Future in a Changing Climate - Executive Summary. In *The Washington Climate Change Impacts Assessment: Evaluating Washington's Future in a Changing Climate*, Climate Impacts Group, University of Washington, Seattle, Washington.
- Littell, J.S., E.E. Oneil, D. McKenzie, J.A. Hicke, J.A. Lutz, R.A. Norheim, and M.M. Elsner. 2010. Forest ecosystems, disturbance, and climatic change in Washington State, USA. *Climatic Change* 102(1-2): 129-158, doi: 10.1007/s10584-010-9858-x.
- Mantua, N.J., I. Tohver, and A.F. Hamlet. 2010. Climate change impacts on streamflow extremes and summertime stream temperature and their possible consequences for freshwater salmon habitat in Washington State.. *Climatic Change* 102(1-2): 187-223, doi: 10.1007/s10584-010-9845-2.
- Meehl, G. A., C. Covey, T. Delworth, M. Latif, B. McAvaney, J. F. B. Mitchell, R. J. Stouffer, and K. E. Taylor, 2007a. The WCRP CMIP3 multi-model dataset: A new era in climate change research, *Bulletin of the American Meteorological Society*, 88, 1383-1394.
- Meehl, GA, Stocker TF, Collins WD, Friedlingstein P, Gaye AT, Gregory JM, Kitoh A, Knutti R, Murphy JM, Noda A, Raper SCB, Watterson IG, Weaver AJ, and Zhao Z-C 2007b. Global climate projections. in *Climate change 2007: The Physical science basis. Contribution of working group I to the fourth assessment report of the Intergovernmental Panel on Climate Change* [Solomon, S, et al., (eds)]. Cambridge University Press, Cambridge, United Kingdom and New York, NY, USA
- Menne, M.J., C.N. Williams, and R.S. Vose, 2009: The United States Historical Climatology Network Monthly Temperature Data - Version 2. *Bull. Amer. Meteor. Soc.*, 90, 993-1007, doi: 10.1175/2008BAMS2613.1
- Mitchell TD, Carter TR, Jones PD, Hulme M, New M (2004) A comprehensive set of climate scenarios for Europe and the globe: the observed record (1901–2000) and 16 scenarios (2001–2100). Tyndall Centre Working Paper No 55, University of East Anglia, Norwich, UK
- Mote, P.W., and E.P. Salathé. 2010. Future climate in the Pacific Northwest. *Climatic Change* 102(1-2): 29-50, doi: 10.1007/s10584-010-9848-z.
- Nakićenović N, Swart R (eds.) (2000) Special report on emissions scenarios. A special report

of working group III of the Intergovernmental Panel on Climate Change. Cambridge University Press, Cambridge, United Kingdom and New York, NY, USA, 599 pp

Overland, J.E. and Wang, M.: 2007, 'Future regional Arctic sea ice declines', *Geophys. Res. Lett.* 34.

Raupach MR, Marland G, Ciais P, Le Quéré C, Canadell JG, Klepper G, Field CB (2007) Global and regional drivers of accelerating CO2 emissions. *Proc Natl Acad Sci* doi 10.1073/pnas.0700609104

Salathé, E.P., L.R. Leung, Y. Qian, and Y. Zhang. 2010. Regional climate model projections for the State of Washington. *Climatic Change* 102(1-2): 51-75, doi: 10.1007/s10584-010-9849-y.

Appendix 1

Meta-data and file structure for:

Bailey ecosection summaries

Omernik Ecoregion summaries

HUC 4 summaries

VIC combined basins gridded output

VIC regional / basin gridded output

Appendix 1: Key climatic and hydrologic products for USFS Regions 1 and 6

Home directory for all project data: <http://ces.washington.edu/picea/USFS/pub/>

This directory contains summaries from Historical Climate Network (HCN) trend analysis; historical and future VIC runs performed for the PNW, upper and lower CO, upper MO, and Great Basin domains (Fig. 2). A total of 7 runs were performed for each domain: one historical, and 6 future climate scenarios. The 6 future runs stem from one emissions scenario (A1B), two thirty-year time windows (2040s = 2030-2059, and 2080s = 2040-2069, and projected, downscaled temp/precip changes from: Miroc_3.2, pcm1, and a composite of the 10 GCMs that best represent the climate of the region (see Sections 3 and 4 in the full report).

Following is a description of what can be found in each directory.

Subdirectories and contents:

1.1) "summaries/" -- directory containing monthly summaries for all VIC output variables, by basin, both in tabular, time-series format, and the 92-year means in Grid-ASCII format, compatible with Arc-GIS.

The different historical and future (GCM runs) grids are in subfolders (example here for wus, or western US – all regions follow the same convention):

wus_A1B_2030-2059_comp/: 2040s composite (ensemble A1B)
 wus_A1B_2030-2059_miroc_3.2/: 2040s miroc_3.2 (warmer, drier summers)
 wus_A1B_2030-2059_pcm1/: 2040s pcm1 (less warming, wetter summers)
 wus_A1B_2070-2099_comp/: 2080s composite (ensemble A1B)
 wus_A1B_2070-2099_miroc_3.2/: 2048s miroc_3.2 (warmer, drier summers)
 wus_A1B_2070-2099_pcm1/: 2080s pcm1 (less warming, wetter summers)
 wus_hist/: 1916-2006 historical

Within each of the subfolders, there is a folder called **monthly_summaries/**. Inside are monthly ascii grid files for the 21 VIC output variables in Appendix Table 1.1 (below). See Section 2 below for more information on gridded datasets.

There are also two tar.gz files, which allow the entire folder's compressed contents to be downloaded. Each zipped file is a directory that contains two types of text files: **monthly summaries**, which are ASCII grid files that can be imported into a GIS (Geographic Information System) and **fluxes**, which are text files that contain monthly values for each simulated month and year for each hydrologic model grid cell and output variable.

1.2) "subrgn_summaries/" -- directory containing summaries for the Omernik, Bailey, and 4th-level-HUC sub-regions, with summary tables and plots for a number of ecologically-relevant variables

Each folder contains summaries (graphical and tabular) of historical and future climate and hydrologic variables by Omernik's level III ecoregions, Bailey's ecosections, and HUC 4 (8 digit) for the Colorado, Columbia, Great Basin, and upper Missouri Basin.

Each subfolder is a detailed summary of historical and future climate and hydrology for each unit. There are 54 files in each subfolder, representing different summaries by variable and time period. A Key to the file structure is in Table 1.2 below, which is an example file for huc4_17070204. Wherever huc4_17070204 appears in a file name, the unit name would be substituted in other folders. Otherwise, the file names and column headers would be the same.

1.3) "summary tables/" -- directory containing summaries for all of the above subregions in space-delimited table format, with one row for each subregion, and one column for each scenario.

"varname_" "month".dat, jd*.dat, max_swe.dat:

summary tables for bailey, 4th-level-HUC ("huc4"), and omernik

"HUC5_apr01swe_to_ONDJFMprecip_ratio_wus.dat":

summary table listing the mean Apr01 SWE for historical and future scenarios for each of the 5th-level-HUCs ("huc5") in our domains

These folders contain summary tables listing the monthly historical and 2040s and 2080s A1B emissions scenario projected change in 16 VIC derived variables averaged over each unit (Bailey ecoregion, Omernik ecoregion, HUC_4). These variables also include the ratio of mean Apr01 SWE to total ONDJFM precipitation for historical and future scenarios for each of the 5th-level-HUCs ("huc5") in the domains, essentially the western US (minus California and drainages to CA coast) ratio of April 1 snow water equivalent to cool season (October – March) precipitation, by HUC5.

1.4) "HCN/" -- directory containing trend plots for Precip, Tmin, and Tmax for all HCN stations located in each of the domains.

These are plots of trends (1915-2006, 1950-2006, 1970-2006) , by basin (CO = Colorado, GB = Great Basin, MB = Northern Rockies / Upper Missouri, PNW = Pacific Northwest / Columbia) in maximum temperature (TMAX), minimum temperature (TMIN), and precipitation (PCP) by basin (CO = Colorado, GB = Great Basin, MB = Northern Rockies / Upper Missouri, PNW = Pacific Northwest / Columbia) with HCN StationID, LAT, LON, ELEV(m), Linear_Trend, 95pct_confidence_limits:(low, high). Trends are in mm/yr (PCP) and degrees C/yr (TMAX and TMIN)

1.5) "GCM_plots/" -- diagnostics for GCM comparison and evaluation

diagnostic tabular data (.dat files) and graphics (.eps files) for GCM evaluation

1.6) Other folders and files:

*.tar.gz: The root folder also contains downloadable, compressed .tar.gz files of each of the folders. Windows users will need third party software to un-tar these (e.g., WinZip or gzip).

Each zipped file may unzipped using software such as WinZip or may be unzipped in UNIX using the following command: `tar xzf <filename>`

VIC_code/ For the really adventurous, here is the code that was used to run the hydrologic model

Littell_etal_2010/ Folder for white paper and any corrections related to data products

x_subrgn_maps_ignore/ Locator maps for Omernik, Bailey, and HUC units.

xx_tst_plots_ignore/ Diagnostic maps for SWE and VIC analyses

Appendix 1, Table 1.1. VIC hydrologic model output variables. The variables are displayed in the order that they are archived in the raw VIC output files. Monthly summaries are archived for each of these variables, both in time series and gridded formats. The right-hand column shows the method used to aggregate monthly output for each variable.

ID	Abbrev.	Output Variable	Notes	Units	Summary Type
1	precip	Daily total precipitation		mm	Monthly total
2	tavg	Daily average temperature		°C	Monthly average
3	tmax	Daily maximum temperature		°C	Monthly average
4	tmin	Daily minimum temperature		°C	Monthly average
5	olr	Outgoing longwave radiation		W/m ²	Monthly average
6	isr	Incoming shortwave radiation	solar radiation	W/m ²	Monthly average
7	rh	Relative humidity		%	Monthly average
8	vpd	Vapor pressure deficit		Pa	Monthly average
9	et	Daily evapotranspiration		mm	Monthly total
10	runoff	Daily Runoff		mm	Monthly total
11	baseflow	Daily Baseflow		mm	Monthly total
12	soilm1	Soil Moisture, Layer 1		mm	1 st of month
13	soilm2	Soil Moisture, Layer 2		mm	1 st of month
14	soilm3	Soil Moisture, Layer 3		mm	1 st of month
15	swe	Snow water equivalent	total water content of the snowpack	mm	1 st of month
16	snodep	Snow depth		cm	1 st of month
17	pet1	Potential Evapotranspiration 1	natural vegetation, no water limit	mm	Monthly total
18	pet2	Potential Evapotranspiration 2	open water surface (fixed albedo)	mm	Monthly total
19	pet3	Potential Evapotranspiration 3	natural vegetation, no water limit, no vegetation resistance	mm	Monthly total
20	pet4	Potential Evapotranspiration 4	Tall reference crop (alfalfa)	mm	Monthly total
21	pet5	Potential Evapotranspiration 5	Short reference crop (short grass)	mm	Monthly total

File	Description	Time unit	Time frame	GCMs
SWEvTZ_A1B_2030_2059_com p.dat	Data for snow water equivalent vs. temperature by elevation within unit	April 1st	Projection: 2040s	Ensemble A1B
SWEvTZ_A1B_2030_2059_miro c_3.2.dat	Data for snow water equivalent vs. temperature by elevation within unit	April 1st	Projection: 2040s	miroc_3.2
SWEvTZ_A1B_2030_2059_pcm 1.dat	Data for snow water equivalent vs. temperature by elevation within unit	April 1st	Projection: 2040s	pcm1
SWEvTZ_A1B_2070_2099_com p.dat	Data for snow water equivalent vs. temperature by elevation within unit	April 1st	Projection: 2080s	Ensemble A1B
SWEvTZ_A1B_2070_2099_miro c_3.2.dat	Data for snow water equivalent vs. temperature by elevation within unit	April 1st	Projection: 2080s	miroc_3.2
SWEvTZ_A1B_2070_2099_pcm 1.dat	Data for snow water equivalent vs. temperature by elevation within unit	April 1st	Projection: 2080s	pcm1
SWEvTZ_hist.dat	Data for snow water equivalent vs. temperature by elevation within unit	April 1st	historical	none
combinedflow_monthly_tot_dm.d at	Tabular data for combined monthly flow	Monthly	historical, 2040s, 2080s	Ensemble A1B, miroc 3.2, pcm1
combinedflow_monthly_tot_dm.p ng	.png graphic for combined monthly flow - comparison	Monthly,	historical, 2040s, 2080s	Ensemble A1B, miroc 3.2, pcm1
et_monthly_tot_dm.dat	Tabular data for evapotranspiration (actual)	Monthly, DJF, MAM, JJA, SON, JJJA	historical, 2040s, 2080s	Ensemble A1B, miroc 3.2, pcm1
et_monthly_tot_dm.png	.png graphic for evapotranspiration (actual) - comparison	Monthly,	historical, 2040s, 2080s	Ensemble A1B, miroc 3.2, pcm1
pet1_monthly_tot_dm.dat	Tabular data for potential evapotranspiration (nat. veg., no h2o limit)	Monthly, DJF, MAM, JJA, SON, JJJA	historical, 2040s, 2080s	Ensemble A1B, miroc 3.2, pcm1
pet1_monthly_tot_dm.png	.png graphic for potential evapotranspiration (nat. veg., no h2o limit) - comparison	Monthly	historical, 2040s, 2080s	Ensemble A1B, miroc 3.2, pcm1
pet3_monthly_tot_dm.dat	Tabular data for potential evapotranspiration (nat. veg., no h2o limit, no veg aero resist.)	Monthly, DJF, MAM, JJA, SON, JJJA	historical, 2040s, 2080s	Ensemble A1B, miroc 3.2, pcm1
pet3_monthly_tot_dm.png	.png graphic for potential evapotranspiration (nat. veg., no h2o limit, no veg. aero resist) - comparison	Monthly	historical, 2040s, 2080s	Ensemble A1B, miroc 3.2, pcm1
precip_monthly_tot_dm.dat	Tabular data for total monthly precipitation	Monthly, DJF, MAM, JJA, SON	historical, 2040s, 2080s	Ensemble A1B, miroc 3.2, pcm1
precip_monthly_tot_dm.png	.png graphic for total monthly precipitation - comparison	Monthly, DJF, MAM, JJA, SON	historical, 2040s, 2080s	Ensemble A1B, miroc 3.2, pcm1

17 Apr 2011

Littell et al. 2011

rh_monthly_avg_dm.dat	Tabular data for average monthly relative humidity	Monthly, JJA	historical, 2040s, 2080s	Ensemble A1B, miroc 3.2, pcm1
rh_monthly_avg_dm.png	.png graphic for average monthly relative humidity - comparison	Monthly, JJA	historical, 2040s, 2080s	Ensemble A1B, miroc 3.2, pcm1
scatter_huc4_17070204_apr01S WEvT.png	.png graphic for scatter of change in pixel apr 1 snow water equivalent vs. temperature	April 1st	2040s, 2080s	Ensemble A1B
scatter_huc4_17070204_apr01S WEvZ.png	.png graphic for scatter of change in pixel apr 1 snow water equivalent vs. elevation	April 1st	2040s, 2080s	Ensemble A1B
scatter_huc4_17070204_maxSW EvT.png	.png graphic for scatter of change in pixel max snow water equivalent vs. temperature	Date of Max SWE	2040s, 2080s	Ensemble A1B
scatter_huc4_17070204_maxSW EvZ.png	.png graphic for scatter of change in pixel max snow water equivalent vs. elevation	Date of Max SWE	2040s, 2080s	Ensemble A1B
soilmoist_monthly_day1_dm.dat	Tabular data for first of month monthly soil moisture	Monthly	historical, 2040s, 2080s	Ensemble A1B, miroc 3.2, pcm1
soilmoist_monthly_day1_dm.png	.png graphic for first of month monthly soil moisture - comparison	Monthly	historical, 2040s, 2080s	Ensemble A1B, miroc 3.2, pcm1
swe_monthly_day1_dm.dat	Tabular data for total first of month snow water equivalent	Monthly, DJF, MAM, JJA, SON	historical, 2040s, 2080s	Ensemble A1B, miroc 3.2, pcm1
swe_monthly_day1_dm.png	.png graphic for first of month total snow water equivalent - comparison	Monthly	historical, 2040s, 2080s	Ensemble A1B, miroc 3.2, pcm1
tmax_monthly_avg_dm.dat	Tabular data for monthly average maximum temperature	Monthly, DJF, MAM, JJA, SON	historical, 2040s, 2080s	Ensemble A1B, miroc 3.2, pcm1
tmax_monthly_avg_dm.png	.png graphic for monthly average maximum temperature - comparison	Monthly	historical, 2040s, 2080s	Ensemble A1B, miroc 3.2, pcm1
tmin_monthly_avg_dm.dat	Tabular data for monthly average minimum temperature	Monthly, DJF, MAM, JJA, SON	historical, 2040s, 2080s	Ensemble A1B, miroc 3.2, pcm1
tmin_monthly_avg_dm.png	.png graphic for monthly average minimum temperature - comparison	Monthly	historical, 2040s, 2080s	Ensemble A1B, miroc 3.2, pcm1
tsrs_A1B_2030_2059_comp_tavg_monthly_avg.dat	Time series of composite average monthly average temperature	Monthly	2040s deltas + 91 yr, historical variability	Ensemble A1B
tsrs_A1B_2030_2059_miroc_3.2_tavg_monthly_avg.dat	Time series of composite average monthly average temperature	Monthly	2040s deltas + 91 yr, historical variability	miroc3.2
tsrs_A1B_2030_2059_pcm1_tavg_monthly_avg.dat	Time series of composite average monthly average temperature	Monthly	2040s deltas + 91 yr, historical variability	pcm1
tsrs_A1B_2070_2099_comp_tavg_monthly_avg.dat	Time series of composite average monthly average temperature	Monthly	2080s deltas + 91 yr, historical variability	Ensemble A1B
tsrs_A1B_2070_2099_miroc_3.2_tavg_monthly_avg.dat	Time series of composite average monthly average temperature	Monthly	2080s deltas + 91 yr, historical variability	miroc3.2

17 Apr 2011

Littell et al. 2011

tsrs_A1B_2070_2099_pcm1_tavg_monthly_avg.dat	Time series of composite average monthly average temperature	Monthly	2080s deltas + 91 yr, historical variability	pcm1
tsrs_hist_tavg_monthly_avg.dat	Time series of composite average monthly average temperature	Monthly	historical	none
tsrs_huc4_17070204_A1B_2030_2059_comp.dat	Time series of 11 monthly average or total hydrologic flux variables	Monthly	2040s deltas + 91 yr, historical variability	Ensemble A1B
tsrs_huc4_17070204_A1B_2030_2059_miroc_3.2.dat	Time series of 11 monthly average or total hydrologic flux variables	Monthly	2040s deltas + 91 yr, historical variability	miroc3.2
tsrs_huc4_17070204_A1B_2030_2059_pcm1.dat	Time series of 11 monthly average or total hydrologic flux variables	Monthly	2040s deltas + 91 yr, historical variability	pcm1
tsrs_huc4_17070204_A1B_2070_2099_comp.dat	Time series of 11 monthly average or total hydrologic flux variables	Monthly	2080s deltas + 91 yr, historical variability	Ensemble A1B
tsrs_huc4_17070204_A1B_2070_2099_miroc_3.2.dat	Time series of 11 monthly average or total hydrologic flux variables	Monthly	2080s deltas + 91 yr, historical variability	miroc3.2
tsrs_huc4_17070204_A1B_2070_2099_pcm1.dat	Time series of 11 monthly average or total hydrologic flux variables	Monthly	2080s deltas + 91 yr, historical variability	pcm1
tsrs_huc4_17070204_hist.dat	Time series of 11 monthly average or total hydrologic flux variables	Monthly	historical	none
tsrs_snostats_huc4_17070204_A1B_2030_2059_comp.dat	Time series of max SWE, julian day max swe, 10% accumulation, 90% melt, days between 10%/90%	Annual	2040s deltas + 91 yr, historical variability	Ensemble A1B
tsrs_snostats_huc4_17070204_A1B_2030_2059_miroc_3.2.dat	Time series of max SWE, julian day max swe, 10% accumulation, 90% melt, days between 10%/90%	Annual	2040s deltas + 91 yr, historical variability	miroc3.2
tsrs_snostats_huc4_17070204_A1B_2030_2059_pcm1.dat	Time series of max SWE, julian day max swe, 10% accumulation, 90% melt, days between 10%/90%	Annual	2040s deltas + 91 yr, historical variability	pcm1
tsrs_snostats_huc4_17070204_A1B_2070_2099_comp.dat	Time series of max SWE, julian day max swe, 10% accumulation, 90% melt, days between 10%/90%	Annual	2080s deltas + 91 yr, historical variability	Ensemble A1B
tsrs_snostats_huc4_17070204_A1B_2070_2099_miroc_3.2.dat	Time series of max SWE, julian day max swe, 10% accumulation, 90% melt, days between 10%/90%	Annual	2080s deltas + 91 yr, historical variability	miroc3.2
tsrs_snostats_huc4_17070204_A1B_2070_2099_pcm1.dat	Time series of max SWE, julian day max swe, 10% accumulation, 90% melt, days between 10%/90%	Annual	2080s deltas + 91 yr, historical variability	pcm1
tsrs_snostats_huc4_17070204_hist.dat	Time series of max SWE, julian day max swe, 10% accumulation, 90% melt, days between 10%/90%	Annual	historical	none
vpd_monthly_avg_dm.dat	Tabular data for average monthly and average JJA vapor pressure deficit	Monthly, JJA	historical, 2040s, 2080s	Ensemble A1B, miroc 3.2, pcm1
vpd_monthly_avg_dm.png	,png graphic for average monthly and average JJA vapor pressure deficit	Monthly	historical, 2040s, 2080s	Ensemble A1B, miroc 3.2, pcm2

Appendix 2: Gridded Regional Datasets

There are two types of gridded files provided for each variable (for example in /summaries/colo_A1B_2030-2059_comp/monthly_summaries/), including gridded summary tables (no extension) and GIS ascii grids (.asc extension). Gridded summary tables provide full spatial coverage (i.e., all grid cells in the model domain), at monthly time scale, of the key hydrologic variables using the monthly aggregation scheme listed in Table 1. Each product is provided as a gridded file (one file for each variable and calendar month) in ASCII format. The rows of these files are water years (e.g., WY 1916-2006), and the columns contain the unique values for each grid cell in the model (i.e. a latitude/longitude position for each grid cell in the domain – 16,595 columns for the upper Missouri and 17,995 columns for the Colorado). The first two rows of the files give the latitude and longitude, respectively, of each grid cell location and the rows below are populated with the monthly data for each year from 1916 to 2006. By way of an example, gridded snow water equivalent (SWE) is summarized by taking data from the first day of each month (Table 2, example file name: “swe_monthly_day1_apr”). As a consequence, the April 1 summary file for SWE for the upper Missouri basin will have 93 rows (one each for latitude and longitude followed by one for each water year) and 16,595 columns (one for each grid cell). There will be a total of 12 such files that provide the summary for SWE for each of the simulations listed in Table 1.

In addition to the monthly summary tables, the long-term monthly mean data of each hydrologic variable is provided in GridASCII format, compatible with ArcGIS. Although GridASCII format is a standard developed for use with ArcInfo, the format is quite simple and other data processing software can easily be adapted to read in this file format. GridASCII files store regularly gridded latitude/longitude data based on the descriptors defined in the header for each file. The data are gridded so that the top row corresponds to the northernmost latitude, decreasing to the southernmost latitude in the final row. Columns thus correspond to variations in longitude, where the leftmost column corresponds to the western extent, and the rightmost column the eastern extent of the

domain. The header in each GridASCII file describes the position and spacing of the grid as well as the format of the data. A description of the GridASCII header is given in Table 2, and further information can be obtained from the ESRI help website (<http://webhelp.esri.com>, search for: "ESRI ASCII Raster format").

Table Appendix 1.3 – Description of GridASCII file format.

<i>Row number</i>	<i>Contents in file</i>	<i>Description</i>
row 1:	ncols xxx	integer number of columns
row 2:	nrows xxx	integer number of rows
row 3:	xllcorner xxx	longitude of the lower-left corner (lower-left corner of grid cell)
row 4:	yllcorner xxx	latitude of the lower-left corner (lower-left corner of grid cell)
row 5:	cellsize xxx	cell spacing
row 6:	NODATA_value xxx	default is -9999
row 7-end:	regularly gridded data	space-delimited, floating point.

Appendix 2

**Look-up codes for USFS units by
Omernik, Bailey, and HUC classification**

Clearwater National Forest	Cleveland National Forest	Coconino National Forest	Coeur d'Alene National Forest	Columbia River Gorge National Scenic Area	Colville National Forest	Comanche National Grassland	Coronado National Forest
17010205	18070202	15010004	17010204	17070105	17010215	11020005	15040003
17010304	18070203	15020008	17010213	17070106	17010216	11020007	15040005
17060302	18070301	15020015	17010214	17070306	17020001	11020010	15040006
17060303	18070302	15020016	17010303	17080001	17020002	11020013	15050201
17060304	18070303	15060202	17010304		17020003	11040001	15050202
17060306	18070304	15060203	17010305		17020004	11040002	15050203
17060307	18070305					11040003	15050301
17060308	18100200					11040004	15050302
						11040005	15050304
							15080200
							15080301
							15080302
							15080303
Crooked River National Grassland	Curlew National Grassland	Custer National Forest	Deerlodge National Forest	Deschutes National Forest	Desert Range Experimental Station	Dixie National Forest	Eastman Lake
17070301	16020309	10070001	10020003	17070301	16020301	14070003	18040007
17070305	17040209	10070002	10020004	17070302	16020302	14070005	
17070306		10070005	10020005	17070305		14070006	
17070307		10070006	10020006	17090001		14070007	
		10080010	10030101	17090004		15010003	
		10080014	17010201	17100301		15010008	
		10090101	17010202	17120005		15010010	
		10090102	17010205	18010201		15010013	
		10090207				16030001	
		10090209				16030002	
		10110201				16030006	
		10110202					

Eldorado National Forest	Fishlake National Forest	Flathead National Forest	Fort Bliss McGregor Range	Fremont National Forest	Gallatin National Forest	Gifford Pinchot National Forest	Gila National Forest
16050101	14070002	10030104	13050003	17070302	10020007	17030002	13020208
16050201	14070003	10030201	13050004	17120005	10020008	17070105	13020211
18020128	16030001	10030205		17120006	10030101	17070106	13030101
18020129	16030002	17010101		17120007	10040201	17080001	13030102
18040012	16030003	17010102		18010201	10070001	17080002	13030202
18040013	16030004	17010203		18010202	10070002	17080003	15040001
	16030005	17010206		18010204	10070003	17080004	15040002
	16030006	17010207		18020001	10070005	17080005	15040003
	16030007	17010208			10070006	17100103	15040004
	16030008	17010209			17040202	17110015	
		17010210				17110016	
		17010211					
		17010212					
Grand Mesa National Forest	Gunnison National Forest	Helena National Forest	Hensley Lake	Humboldt National Forest	Inyo National Forest	Jemez National Recreation Area	Kaibab National Forest
14010005	11020001	10020006	18040007	15010011	16050301	13020201	14070007
14020004	13010001	10030101		16020301	16060010	13020202	15010001
14020005	13010004	10030102		16040101	18030001		15010002
14030001	14010004	10030103		16040102	18030002		15010003
14030004	14010005	17010201		16040103	18030010		15010004
	14020001	17010203		16040109	18040006		15020016
	14020002			16040201	18040009		15060201
	14020003			16060006	18090101		15060202
	14020004			16060007	18090102		
				16060008	18090103		
				16060012	18090201		
				16060014	18090205		
				17040213			
				17050102			
				17050104			
				17050105			
				17050106			

San Bernardino National Forest	San Isabel National Forest	San Juan National Forest	Santa Fe National Forest	Sawtooth National Forest	Sequoia National Forest	Sequoia National Monument	Shasta National Forest
18070106	10190001	13010001	11080004	16020308	18030001	18030006	18010204
18070202	11020001	13010002	13020101	16020309	18030002	18030010	18010205
18070203	11020002	13010005	13020102	17040209	18030003		18010207
18070302	11020006	14020006	13020201	17040210	18030004		18010208
18090208	11020007	14030002	13020202	17040211	18030005		18010210
18100100	11020010	14030003	13020204	17040212	18030006		18010211
18100200	13010002	14080101	13060001	17040213	18030007		18020002
	13010003	14080102	14080103	17040218	18030008		18020003
	14010003	14080104		17040219	18030010		18020004
	14010004	14080105		17040220	18090205		18020005
	14020001	14080107		17040221	18090206		18020101
	14020003	14080202		17050111			18020112
				17050113			18020118
				17050120			
				17060201			
Shoshone National Forest	Sierra National Forest	Silver Peak Wilderness	Siskiyou National Forest	Sitgreaves National Forest	Siuslaw National Forest	Six Rivers National Forest	Snoqualmie National Forest
10070001	18030009	18060006	17100302	15020002	17090003	17100311	17020011
10070006	18030010		17100305	15020005	17090007	17100312	17030001
10080001	18040006		17100306	15020008	17090008	18010101	17030002
10080002	18040007		17100309	15020010	17100203	18010102	17030003
10080003	18040008		17100310	15060102	17100204	18010104	17070106
10080007	18090101		17100311	15060103	17100205	18010105	17080004
10080009	18090102		17100312	15060104	17100206	18010209	17110006
10080012			18010101	15060105	17100207	18010210	17110009
10080013			18010209		17100303	18010211	17110010
10080014						18010212	17110012
10180006							17110013
14040101							17110014
14040102							17110015
14040104							
17040101							
17040102							

Stanislaus National Forest	Tahoe National Forest	Targhee National Forest	Teton National Forest	Thunder Basin National Grassland	Toiyabe National Forest	Tonto National Forest	Trinity National Forest
16050201	16050101	10020001	10070001	10090208	15010015	15020008	18010102
16050302	16050102	10020007	10080001	10110201	16040107	15020010	18010104
18040008	18020123	17040101	10080012	10120101	16050101	15040007	18010209
18040009	18020125	17040103	10080013	10120102	16050102	15050100	18010210
18040010	18020126	17040104	14040101	10120103	16050201	15060103	18010211
18040011	18020128	17040201	17040101	10120104	16050301	15060105	18010212
18040012	18080003	17040202	17040102	10120105	16050302	15060106	18020112
		17040203	17040103	10120106	16050303	15060203	18020113
		17040204	17040104	10120107	16050304	15070102	
		17040215	17040204	10120201	16060002		
		17040216			16060003		
		17040217			16060004		
		17060204			16060005		
					16060010		
					16060011		
					16060012		
					16060014		
					16060015		
					18020123		
					18020129		
					18040009		
					18040010		
					18040012		
					18080003		
					18090101		
					18090102		
					18090202		

Uinta National Forest	Umatilla National Forest	Umpqua National Forest	Uncompahgre National Forest	Wallowa National Forest	Wasatch National Forest	Wenatchee National Forest	White River National Forest
14060003	17050202	17070302	14020002	17050201	14040106	17020005	11020001
14060004	17060103	17090001	14020005	17050203	14040107	17020008	14010001
14060007	17060104	17090002	14020006	17060101	14040108	17020009	14010002
16020201	17060106	17100301	14030002	17060102	14060003	17020010	14010003
16020202	17060107	17100302	14030003	17060103	16010101	17020011	14010004
16020203	17070102	17100307	14030004	17060105	16020101	17030001	14010005
16020204	17070103	17100308	14080104	17060106	16020102	17030002	14020001
16030004	17070104	18010201		17060209	16020201	17110005	14020004
16030005	17070202				16020203	17110006	14050001
	17070203				16020204	17110009	14050002
	17070204				16020304	17110010	14050005
					16020305	17110013	14050006
					16020306		
					16030005		
Whitman National Forest	Willamette National Forest	Winema National Forest					
17050116	17070301	17070302					
17050119	17070302	17100307					
17050201	17070306	17120005					
17050202	17090001	18010201					
17050203	17090002	18010202					
17060102	17090003	18010203					
17060104	17090004	18010204					
17060105	17090005	18010206					
17070103	17090006						
17070201	17090011						
17070202	17100301						
17070203							

Appendix 2. Table 2.2 Omernik Ecoregions by National Forest. This list does not account for area of forest in ecoregion.

USFS Unit	Omernik Ecoregions				
Angeles National Forest	6	8	14		
Apache National Forest	22	23	79		
Arapaho National Forest	21				
Ashley National Forest	18	19	20		
Beaverhead National Forest	16	17			
Bighorn National Forest	17	18	43		
Bitterroot National Forest	15	16	17		
Black Hills National Forest	17				
Blodgett Experimental Forest	5				
Boise National Forest	12	16			
Bridger National Forest	17	18			
Cache National Forest	13	18	19	80	
Caribou National Forest	13	17	18	19	80
Carson National Forest	21	22			
Challis National Forest	16	17			
Cibola National Forest	22	23	24		
Clearwater National Forest	15	16			
Cleveland National Forest	6	8			
Coconino National Forest	22	23			
Coeur d'Alene National Forest	15				
Columbia River Gorge National Scenic Area	3	4	9	10	
Colville National Forest	15				
Comanche National Grassland	25	26			
Coronado National Forest	79	81			
Crooked River National Grassland	9	11			
Curlew National Grassland	13	80			
Custer National Forest	17	18	43		
Deerlodge National Forest	16	17			
Deschutes National Forest	4	9	11	80	
Desert Range Experimental Station	13				
Dixie National Forest	13	14	19	20	
Eastman Lake	6				
Eldorado National Forest	5				
Fishlake National Forest	13	19	20		
Flathead National Forest	15	17	41		
Fort Bliss McGregor Range	23	24			
Fremont National Forest	9	80			
Gallatin National Forest	17	43			
Gifford Pinchot National Forest	4	9			
Gila National Forest	22	23	24		
Grand Mesa National Forest	20	21			
Gunnison National Forest	20	21			

Helena National Forest	17	41	43		
Hensley Lake	6				
Humboldt National Forest	13	80			
Inyo National Forest	5	13	14		
Jemez National Recreation Area	21	22			
Kaibab National Forest	20	22	23		
Kaniksu National Forest	15				
Kiowa National Grassland	25	26			
Klamath National Forest	4	9	78		
Kootenai National Forest	15	41			
Lassen National Forest	5	6	9	80	
Lewis and Clark National Forest	17	41	42	43	
Lincoln National Forest	22	23	24		
Lolo National Forest	15	16	17	41	
Los Padres National Forest	6	8			
Malheur National Forest	11				
Manti-La Sal National Forest	19	20	21		
Medicine Bow National Forest	18	21			
Mendocino National Forest	6	78			
Modoc National Forest	9	80			
Mount Baker National Forest	2	77			
Mount Hood National Forest	4	9			
Nez Perce National Forest	10	11	16		
Ochoco National Forest	11	80			
Okanogan National Forest	10	15	77		
Olympic National Forest	1	2	77		
Oregon Dunes National Recreation Area	1				
Pawnee National Grassland	25				
Payette National Forest	11	12	16		
Pike National Forest	21	26			
Plumas National Forest	5	6	13	80	
Prescott National Forest	22	23	81		
Rio Grande National Forest	21	22			
Rogue River National Forest	4	9	78		
Roosevelt National Forest	18	21			
Routt National Forest	21				
Saint Joe National Forest	10	15			
Salmon National Forest	16	17			
San Bernardino National Forest	6	8	14	81	
San Isabel National Forest	21	26			
San Juan National Forest	20	21			
Santa Fe National Forest	21	22			
Sawtooth National Forest	12	13	16	17	80
Sequoia National Forest	5	6	8	14	
Sequoia National Monument	5				
Shasta National Forest	4	5	6	9	78

Shoshone National Forest	17	18			
Sierra National Forest	5	6			
Silver Peak Wilderness	6				
Siskiyou National Forest	1	78			
Sitgreaves National Forest	22	23			
Siuslaw National Forest	1	3			
Six Rivers National Forest	1	78			
Snoqualmie National Forest	2	4	9	10	77
Stanislaus National Forest	5	6			
Tahoe National Forest	5	13			
Targhee National Forest	12	17			
Teton National Forest	17				
Thunder Basin National Grassland	17	43			
Toiyabe National Forest	5	13	14		
Tonto National Forest	23	79	81		
Trinity National Forest	6	78			
Uinta National Forest	13	19	20		
Umatilla National Forest	10	11			
Umpqua National Forest	4	78			
Uncompahgre National Forest	20	21			
Wallowa National Forest	11				
Wasatch National Forest	13	18	19		
Wenatchee National Forest	4	9	10	77	
White River National Forest	20	21			
Whitman National Forest	11				
Willamette National Forest	4				
Winema National Forest	4	9			

Appendix 2. Table 2.3. Bailey's ecosections by National Forest

National Forest	Bailey's Ecosection					
Angeles National Forest	M262B					
Apache National Forest	-313C	-321A	M313A			
Arapaho National Forest	M331H	M331I				
Ashley National Forest	-341C	-342G	M331D	M331E		
Beaverhead National Forest	M332A	M332B	M332E			
Bighorn National Forest	-342A	M331B				
Bitterroot National Forest	M332A	M332B	M332E			
Black Hills National Forest	-331F	M334A				
Blodgett Experimental Forest	M261E					
Boise National Forest	-342C	M332A	M332F			
Bridger National Forest	-342E	-342G	M331D	M331J		
Cache National Forest	-341A	-342B	M331D			
Caribou National Forest	-342B	-342E	M331D			
Carson National Forest	-313B	-331J	M313A	M331F	M331G	
Challis National Forest	M332A	M332E	M332F			
Cibola National Forest	-313E	-321A	M313A	M313B		
Clearwater National Forest	M332A	M333D				
Cleveland National Forest	-261B	M262B				
Coconino National Forest	-313C	-313D	M313A			
Coeur d'Alene National Forest	M333A	M333D				
Columbia River Gorge National Scenic Area	-242A	M242B	M242C			
Colville National Forest	M333A					
Comanche National Grassland	-331B	-331I				
Coronado National Forest	-321A	-322B				
Crooked River National Grassland	-342H	M242C				
Curlew National Grassland	-342B					
Custer National Forest	-331F	-331G	-342A	M331A	M331B	
Deerlodge National Forest	M332B	M332D	M332E			
Deschutes National Forest	-342B	-342H	M242B	M242C		
Desert Range Experimental Station	-341A					
Dixie National Forest	-313A	-341F	M341C			
Eastman Lake	-262A	M261F				
Eldorado National Forest	M261E					
Fishlake National Forest	-341A	M341C				
Flathead National Forest	M332B	M333B	M333C	M333D		
Fort Bliss McGregor Range	-321A	M313B				
Fremont National Forest	-342B	M242C	M261G			
Gallatin National Forest	M331A	M332D	M332E			
Gifford Pinchot National Forest	-242A	M242B	M242C			

Gila National Forest	-321A	M313A					
Grand Mesa National Forest	-341B	M331G	M331H	M341B			
Gunnison National Forest	M331G	M331H					
Helena National Forest	M332B	M332D	M332E				
Hensley Lake	-262A						
Humboldt National Forest	-341A	-341E	-341F	-341G	-342B	-342C	M341A
Inyo National Forest	-322A	-341D	M261E				
Jemez National Recreation Area	M313A	M331G					
Kaibab National Forest	-313A	-313C	-313D	M313A			
Kaniksu National Forest	M333A	M333B	M333D				
Kiowa National Grassland	-315A	-315B					
Klamath National Forest	M261A	M261D	M261G				
Kootenai National Forest	M333B	M333C	M333D				
Lassen National Forest	-342B	M261D	M261E	M261F	M261G		
Lewis and Clark National Forest	-331D	M332B	M332C	M332D	M333C		
Lincoln National Forest	-315A	-321A	M313B				
Lolo National Forest	M332A	M332B	M333B	M333C	M333D		
Los Padres National Forest	-261A	-261B	M262A	M262B			
Malheur National Forest	-342B	-342C	M332G				
Manti-La Sal National Forest	-313A	-341A	-341B	M331D	M341C		
Medicine Bow National Forest	-342F	-342G	M331H	M331I			
Mendocino National Forest	M261A	M261B	M261C				
Modoc National Forest	-342B	M261D	M261G				
Mount Baker National Forest	-242A	M242B	M242C				
Mount Hood National Forest	M242B	M242C					
Nez Perce National Forest	-331A	M332A	M332G				
Ochoco National Forest	-342B	-342H	M332G				
Okanogan National Forest	M242B	M242C	M333A				
Olympic National Forest	-242A	M242A					
Oregon Dunes National Recreation Area	M242A						
Pawnee National Grassland	-331H						
Payette National Forest	-331A	-342C	M332A	M332G			
Pike National Forest	M331H	M331I					
Plumas National Forest	-342B	M261E	M261F				
Prescott National Forest	-313C	M313A					
Rio Grande National Forest	-331J	M331F	M331G				
Rogue River National Forest	M242B	M242C	M261A	M261D			
Roosevelt National Forest	M331I						
Routt National Forest	-342G	M331H	M331I				
Saint Joe National Forest	-331A	M333D					

Salmon National Forest	M332A	M332B	M332E			
San Bernardino National Forest	M262B					
San Isabel National Forest	-331J	M331F	M331G	M331H	M331I	
San Juan National Forest	-313A	-341B	M313A	M331G		
Santa Fe National Forest	-313B	-331J	M313A	M313B	M331F	M331G
Sawtooth National Forest	-342B	-342C	M332A	M332F		
Sequoia National Forest	-262A	M261E	M261F			
Sequoia National Monument	M261E					
Shasta National Forest	-262A	M261A	M261D	M261F	M261G	
Shoshone National Forest	-342G	M331A	M331D	M331J		
Sierra National Forest	M261E	M261F				
Silver Peak Wilderness	-261A					
Siskiyou National Forest	-263A	M261A				
Sitgreaves National Forest	M313A					
Siuslaw National Forest	M242A					
Six Rivers National Forest	-263A	M261A	M261B			
Snoqualmie National Forest	-242A	-342I	M242B	M242C		
Stanislaus National Forest	M261E	M261F				
Tahoe National Forest	M261E					
Targhee National Forest	-342B	-342D	M331A	M331D	M332E	
Teton National Forest	M331A	M331D	M331J			
Thunder Basin National Grassland	-331F	-331G				
Toiyabe National Forest	-322A	-341D	-341E	-342B	M261E	M341A
Tonto National Forest	-313C	-322B	M313A			
Trinity National Forest	M261A	M261B	M261C			
Uinta National Forest	-341A	M331D	M331E			
Umatilla National Forest	-342H	M332G				
Umpqua National Forest	M242B	M242C	M261A			
Uncompahgre National Forest	-341B	M331G				
Wallowa National Forest	M332G					
Wasatch National Forest	-341A	M331D	M331E			
Wenatchee National Forest	-342I	M242B	M242C			
White River National Forest	M331H	M331I	M341B			
Whitman National Forest	-342C	-342H	M332G			
Willamette National Forest	M242B	M242C				
Winema National Forest	M242C	M261D	M261G			



Figure Appendix 2.2. Omernik level III ecoregions in the model domain. Green polygons under transparent ecoregions indicated USFS lands.